The impact of diurnal photosynthetic and starch branching enzyme activity on the composition and fine structure of barley starch.

A DISSERTATION
SUBMITTED TO THE FACULTY OF
UNIVERSITY OF MINNESOTA
BY

Avi Goldstein

IN PARTIAL FULFILLMENT OF THE REQUIREMENTS
FOR THE DEGREE OF
DOCTOR OF PHILOSOPY

Alessandra Marti

September, 2015

Acknowledgements

I would like to express my sincerest gratitude to the late Dr. Koushik Seetharaman, for without your endless support, encouragement, advice, hospitality, and friendship I would have never embarked on this adventure. You have inspired me to grow not only as an academic, but even more so as a person, and I will remember fondly the good times we shared.

Thank you to Dr. Alessandra Marti, who took over as adviser following the passing of Dr. Koushik Seetharaman, for your assistance and friendship. It is imperative to acknowledge the enormous contribution provided by Dr. Eric Bertoft. Thank you so much for your support, patience, and mentorship throughout my studies. The project could not have been completed without your invaluable guidance. Thank you also to Dr. George Annor for your thoughtful input and contributions to the project. I would like to thank my graduate committee members Dr. Jim Anderson, Dr. Bill Atwell, Dr. Baljit Ghotra, and Dr. Kerry Huber. In no particular order I would like to thank Dr. Andreas Blennow, Dr. Jean-Luc Putaux, and Dr. Ian Tetlow for their collaboration.

Thank you to my lab mates Enoch Quayson, Varatharajan Vamadevan, Xiaxue Que, and Nesrin Hesso for making my time at the University of Minnesota so worthwhile and enjoyable.

Thank you to my mother Evelyn, my brothers Aaron and Neil, and my sister Alyssa for their constant love and encouragement during this process. I could not have completed this journey without your constant support.

Dedication

This thesis is dedicated in memory of Harry Goldstein (1952-2005) and Dr. Koushik Seetharaman (1966-2014).

Abstract

In this work, the roles of two universal features of starch biosynthesis were investigated to better understand their impact on starch molecular structure. To investigate the impact of diurnal photosynthetic activity on starch fine structure, normal and waxy barley were cultivated in a greenhouse under normal diurnal, or constant light photosynthetic conditions. The impact of starch branching enzymes on starch structure was investigated by studying the lintners of barley starch, which had all known genes coding for starch branching enzymes (SBE I, SBE IIa, SBE IIb) suppressed in the grain resulting in a novel amylose-only starch (AOS). The structure of AOS lintners was compared to lintners from normal barley starch (NBS) and waxy barley starch (WBS).

Unexpectedly, NBS and WBS displayed growth rings regardless of lighting regimes. It was observed that the molecular structure and composition of (NBS) was influenced by the diurnal lighting regime, as NBS contained lower quantities of amylose, and a lower ratio of long chain amylose:short chain amylose (determined by gel permeation chromatography) when cultivated under the diurnal lighting regime compared to the constant light regime. While the composition of WBS remained constant, higher relative crystallinity values (determined by X-ray diffraction), and greater crystalline quality (determined by differential scanning calorimetry) were observed when cultivated under the diurnal lighting regime. When considering the fine structure of amylopectin from NBS and WBS, differences in structure were observed when cultivated under the different lighting regimes. The structure of clusters and building blocks of amylopectin were investigated following their isolation by partial and complete hydrolysis with α-

amylase from *Bacillus amyloliquefaciens*. Clusters of amylopectin from NBS and WBS cultivated under diurnal photosynthetic conditions were larger, and contained a greater number of building blocks compared to their counterparts cultivated in constant light conditions.

AOS exhibited irregular morphological features and contained multi-lobed granules with a rough surface texture. When viewed by transmission electron microscopy (TEM), acid hydrolyzed components of AOS displayed strong textured aggregates with an organization not previous seen in other specimens, whereas NBS and WBS displayed expected stacks of elongated elements with a width of 5-7 nm, believed to represent crystalline amylopectin side chains viewed longitudinally. High performance anion-exchange chromatography of lintners at equivalent levels of acid hydrolysis (45 wt%) revealed that the average degree of polymerization of the AOS lintner was 21, substantially smaller than that of NBS and WBS (42). While NBS and WBS lintners displayed size distribution and chain length profiles expected of those from barley starch, the AOS lintner displayed a unique size distribution profile wherein a repeat-size of the molecules corresponding to 5-6 glucose residue was observed, which corresponds to the approximate number of residues required per turn of the helical structure of amylose. These data suggests that both diurnal photosynthetic activity, and the suppression of all genes coding for SBEs had significant impacts on the structure of barley starch granules.

Table of Contents

List of Tables

List of Figures

Chapter 1: Literature Review

Barley

Barley (*Hordeum vulgare)* is the fourth largest cereal crop in the world following wheat, corn, and rice in terms of production. Barley is a grass belonging to the family *Poaceae*, the tribe *Triticeae* and the genus *Hordeum* (Vasanthan and Hoover, 2009). Throughout history, barley has been utilized as a major food grain in many parts of the world, with documented use as early as 8000 BC. The global production of barley for 2015 is estimated to be 139 million tonnes, with the United States projected to produce ~4 million tonnes. In the United States, the majority of barley is used for livestock feed, with little utilization for foods or further value added processing. In other parts of the world, barley is utilized in soups, stews, bakery products and baby foods. Barley malt extracts and syrups are ingredients which are exploited to enhance the functional property of baked goods such as improved texture, loaf volume, flavor, and color.

Barley is a cereal crop with the widest range of production areas in the world (Kling et al., 2004). It is capable of being grown in the highest altitudes of the Himalayan Mountains, around certain deserts in Africa, and near the Arctic Circle in the northern areas of Asia, Europe, and North America (Horsley et al., 2009). Barley is considered by farmers to be the easiest and safest cool-season crop to cultivate (Horsley et al., 2009). Barley can be divided into two groups based on spike morphology, six-rowed and two-rowed barley. The difference between the two groups relates to the fertility of the spikelets. Six-rowed barley contains three fertile spikelets, which can develop into kernels, whereas in two-rowed barley only the central spikelet is fertile. Barley can also be

classified according to growing habits (i.e. winter or spring barley) or hull adherence (i.e. hulled or hulless) (Horsley et al., 2009).

The composition of barley grains vary depending on variety and genetic background, although they generally contain starch (~53% db.), cellulose (~4% db.), arabinoxylan (~6% db.), lignin (~2% db.), beta-glucan (~5% db.), lipid (~2% db.), protein (~16% db.), and ash (~3% db.) (Vasanthan and Hoover, 2009). Barley has recently been classified as a functional food. Consumption of dietary fibers and beta-glucan from barley has been associated with reduced risk of type II diabetes, cardiovascular disease, and colorectal cancer. The FDA currently approves a health claim for cell wall polysaccharides from barley grain.

Barley starch typically contains two clearly defined populations, A-type (large, lenticular) and B-type (small, irregularly shaped) granules. The main carbohydrate components of starch granules are amylose and amylopectin. Amylose is an essentially linear α-(1,4)-D-glucan chain with a degree of polymerization (DP) and molecular weight (MW) generally in the range of 700-5000 and 10^5-10^6 Da, respectively. The amylose content of barley starch is generally 0-46% (Vasanthan and Hoover, 2009), with some particularly large amylose molecules containing up to ten or more branches (Perez and Bertoft, 2010). Amylopectin is a relatively highly branched molecule containing an α-(1,4)-D-glucan backbone and approximately 5% α-(1,6)-D-glucan linkages. The average chain length and MW of amylopectin is generally 17-22 glucose units, and $7x10^7$-$5.7x10^9$ Da, respectively.

Starch structure

The molecular structure of starch components has been extensively described in the literature. When studying the molecular structure of starch, one can investigate the relative amount, size, and characteristics of the major starch components amylose and amylopectin. While information on the molecular structure is quite extensive, it does not provide guidance into how the chains are organized within the macromolecule (Bertoft, 2013). A common structural feature of starch granules is the presence of alternating amorphous and semi-crystalline layers, which are commonly referred to as growth rings (Figure 1.1). The semi-crystalline rings are composed of alternating crystalline and amorphous lamellae with a 9 nm repeat distance. The external chain segments of amylopectin are able to form double helices that form the crystalline lamellae. The internal chains of the amylopectin molecule containing the branch points contribute to the amorphous lamellae. Understanding the organization of the branched amylopectin component is important as the organization of chains on the backbone of the amorphous lamellae has a very strong effect on granular architecture (Jenkins and Donald, 1995). By characterizing both the molecular structure and granular architecture of starch components, one can attain key insights of the organization of the granule and its predicted functional attributes.

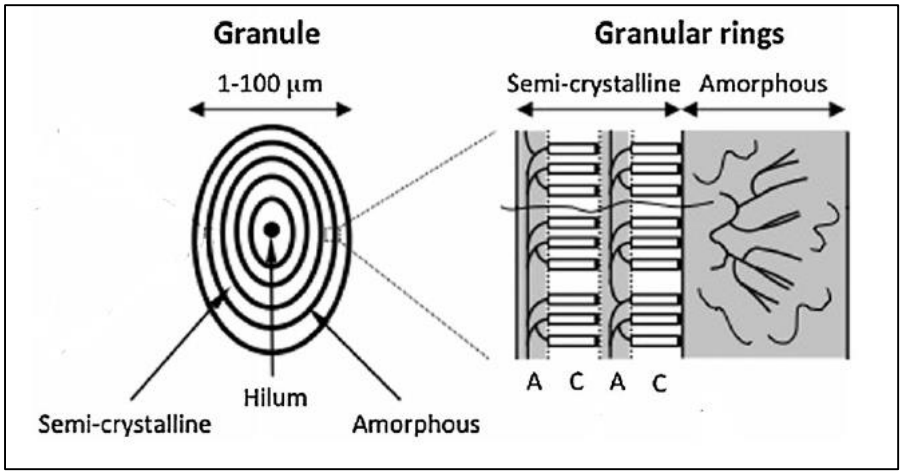

Figure 1.1: Depiction of starch granular growth rings. A represents amorphous components. C represents crystalline components. Adapted from Vamadevan and Bertoft (2015).

Amylose structure

When amylose is treated with β-amylase, an exo-acting enzyme, every second α-(1,4)-D-linkage from the non-reducing end of the polysaccharide chain is hydrolyzed until it reaches a branch point which cannot be bypassed. The treatment of amylose with β-amylase therefore completely hydrolyzes the linear (external) regions of amylose into maltose producing β-limit dextrins (β-LD), which contain all branch points and the residual internal chain segments (Chiba, 1988). The β-amylolysis limit of amylose is 70-90% (Hanashiro, 2015). The average chain length of the β-LD varies depending on source, and is reportedly between 50 and 160 residues (Takeda et al., 1987). Amylose contains a small number of long side chains with chain lengths ranging from several hundred DP's to a similar length of the main amylose chain (Hanashiro, 2015). The vast majority of side chains, however, are short chains on a molar basis, exhibiting chain length distribution

similar to those seen in amylopectin (Hanashiro, 2015). The side chains are not organized in a cluster fashion as is seen in amylopectin.

Amylopectin structure

Due to its greater degree of branching, amylopectin maintains a more complex molecular structure than that of amylose. Amylopectin is believed to be the component of starch which dictates the granule architecture. The botanical origin of starch influences the molecular size, shape, and structure of amylopectin. Amylopectin structure can be separated into distinct hierarchical levels. According to Peat et al., (1952) amylopectin contains three categories of chains; A-, B-, and C-chains. A-chains are not substituted by other chains and are connected via α-(1,6)-linkage to the rest of the amylopectin molecule. B-chains are substituted by one or several other chains (either A- or B-chains) via α-(1,6)-linkages. C-chains carry the sole reducing end-group of the amylopectin molecule, but are otherwise similar to B-chains. Each amylopectin molecule contains only a single C-chain.

The different hierarchical structure levels of amylopectin, (Figure 1.2) including the unit chain profile, internal chain profile, clusters, and building blocks, are reviewed below.

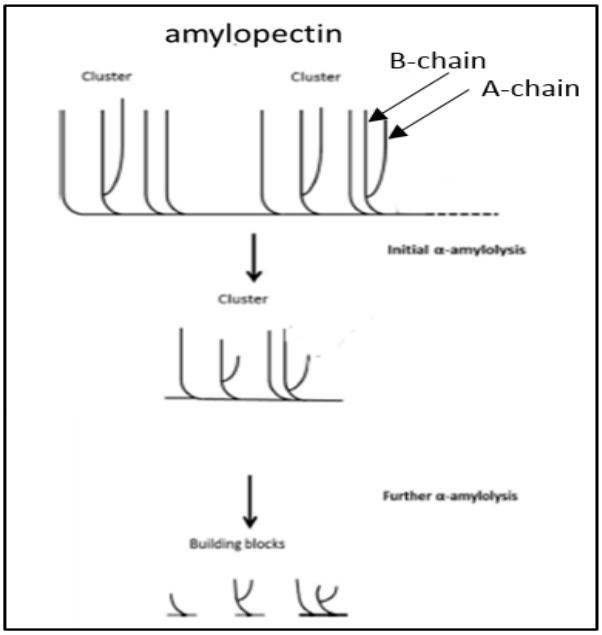

Figure 1.2: Schematic representation of different hierarchical levels of amylopectin structure. Adapted from Zhu et al. (2015).

Unit and internal chain profile of amylopectin

The most common structural element of amylopectin that has been analyzed is the unit chain profile (Bertoft, 2013). The distribution of chains can be determined by introducing enzymes (typically isoamylase and pullulanase) which specifically hydrolyze α-(1,6)-linkages in amylopectin. The distribution of linear chains can then be analyzed by a variety of chromatographic methods. The unit chain profile can be divided into two distinct categories, short chains (DP < 36) and long chains (DP > 36). It has been reported that the short chains help build up clusters (defined below), while the long chains serve to interconnect clusters (Bertoft, 2013).

In order to quantify the ratio of A- chains to B-chains in amylopectin one must introduce exo-acting enzymes to obtain a limit dextrin (LD). Two major types of exo-

acting enzymes are used to obtain LD's (Bertoft, 2013). When β-amylase attacks A-chains, they are reduced to into maltotriose or maltose stubs, whereas the external regions of B-chains are reduced to maltose or glucose stubs (Bertoft, 2013). The remaining components are referred to as the β-LD. The second type of exo-acting enzyme which is used (albeit much less frequently) is phosphorylase *a* from rabbit muscle. Phosphorylase *a* produces glucose-1-phosphate and reduces A-chains to maltotetraose stubs, whereas the external segments of B-chains are reduced to maltotriose stubs. The remaining component is referred to as the φ-limit dextrin (φ-LD). The structure of the φ-LD is not dependent on whether the original chains contained an odd or even amount of glucose residues (Bertoft, 1989). If one were to sequentially hydrolyze amylopectin with phosphorylase *a* followed by β-amylase, a φ,β-LD is obtained. In the resulting φ,β-LD, all external A-chains are reduced to maltose stubs, whereas the external components of B-chains are reduced to glucose stubs. If the φ,β-LD is debranched, one can quantify the chain length distribution of the internal B-chains. Within the literature two major groups of internal B-chains have been reported, short (DP < 27) and long (DP > 27) B-chains (Bertoft et al., 2008). The division (based on DP) is dependent on the sample. Further, the shortest B-chains can be subdivided into 'fingerprint' B_{fp}-chains (DP 3–7), and BS_{major}-chains (DP ≥ 8). With knowledge of the unit chain and internal unit chain distribution of amylopectin, a number of robust calculations can be completed to describe the structure of amylopectin including the average total internal chain length (TICL), average internal chain length (ICL), and average external chain length (ECL), wherein the TICL represents the whole internal B-chain lengths, and ICL represents the internal chain length between branches.

Cluster structure of amylopectin

Clusters of amylopectin are formed when branch points in amylopectin are situated within 9 glucose residues of each other (Bertoft, 2013). Clusters can be isolated and analyzed by utilizing an endo-acting enzyme, which can cleave internal chains releasing amylopectin clusters. Within the literature three different enzymes have been used to isolate clusters, although the α-amylase enzyme from *Bacillus amyloliquefaciens* has been reported to possess the most distinctive endo-action pattern (Bijttebier et al., 2010), and therefore is the best suited enzyme for the purpose of cluster isolation. Clusters are produced/isolated via a controlled hydrolysis reaction with the α-amylase from *B. amyloliquefaciens.* The enzyme contains 9 subsites in the area around the catalytically active site, allowing the enzyme to attack external chains (producing mostly maltohexaose), as well as attacking long internal chains which inter-connect clusters, thereby releasing the clusters (Bertoft, 1986). The hydrolysis reaction will proceed at a rapid rate when all 9 subsites of the enzyme are filled with D-glucosyl residues. Once the long glucose chains are hydrolyzed and only chains with less than 9 glucose units remain, the kinetics of hydrolysis will slow down considerably (Bertoft, 2013). Clusters are considered to be formed once the initial high rate of hydrolysis decreases. At this point clusters are precipitated with methanol and isolated. Just as with amylopectin, one can attain the φ,β-LD of clusters by removing the residual external chains that remain after the α-amylase attack, allowing for the characterization of the internal chains of clusters. Structural parameters identified in clusters include the average degree of polymerization of the cluster, number of chains, types of chains, degree of branching, and average chain length (CL) of the cluster.

Building block structure of amylopectin

Building blocks represent the smallest tightly branched units of amylopectin which can be isolated following the extensive hydrolysis of clusters at a greater enzyme concentration (compared to cluster hydrolysis conditions) with the α-amylase of *B. amyloliquefaciens.* The units are in practice α-LDs, which are produced by α-amylase (Bertoft et al., 1999). If the building blocks are treated with β-amylase, linear fragments of DP 4-6 will be shortened into DP 1-3, allowing for better separation of linear fragments from the smallest branched building blocks of DP 5 and greater (Bertoft, 2015). Building blocks can be divided into groups based on their size and number of chains. Group 1 consists of glucose, maltose, and maltotriose (and are derived from the linear fragments), whereas Group 2, 3, and 4 building blocks consist of branched dextrins with 2, 3, and 4 chains, respectively. Group 5 (DP 20-34) and 6 (DP > 35) building blocks appear in the lowest amounts compared to groups 1-4, and the number of chains they possess varies but is generally larger than four. Building blocks exhibit a much greater density than clusters, containing an internal chain length between 1-3 residues (Bertoft, 2013). The interblock chain length (IB-CL), or the number of glucose units between building blocks, can also be calculated. IB-CL can range from 5.5-8 glucose residues, depending on the source of starch (Bertoft et al., 2012a).

Structure–function relationship of starch

The functional properties of starch have been reported to directly stem from its structure (Vamadevan et al., 2015). The swelling behavior of starch, which is a critical functional

attribute, differs greatly depending on its genetic background (Tester and Morrison, 1990). More specifically, Tester and Morrison (1990) reported that the swelling behavior of starch was dictated by amylopectin following the analysis of the swelling properties of maize and amylose-free maize starches. Long (DP > 18) amylopectin chains have been reported to inhibit swelling, whereas short (DP < 14) amylopectin chains promote swelling (Gomand et al., 2010a). Vamadevan et al. (2013) postulated that starch swelling cannot be explained solely by the ratio of short:long amylopectin chains, and rather that other structural parameters such as the quantity of 'fingerprint' A_{fp}-chains (DP 6-8) unable to form double helices, the length of external amylopectin chains, and the organization of internal amylopectin segments (especially IB-CL) determine the crystal structure (and defects), which facilitate the entry of water into the starch granule and subsequent swelling. Vamadevan and Bertoft (2015) urged that significant consideration should be placed on understanding how different chain categories and their interactions influence crystalline stability and granule swelling.

The gelatinization of starch is an endothermic reaction requiring an aqueous medium (Vamadevan and Bertoft, 2015), which is typically water in food products. Starch heated in the presence of moisture typically undergoes a glass transition in the amorphous background prior to gelatinization, which is an irreversible phase transition (Vamadevan and Bertoft, 2015). A number of physical changes occur during gelatinization including granular swelling, loss of birefringence and crystallinity, leaching of polymers, and changes in viscosity (Svensson and Eliasson, 1995). The gelatinization of starch is strongly influenced by the concentration of starch, or conversely, the concentration of moisture in the starch-moisture system. The dynamic relationship was recently reviewed

elsewhere (Goldstein et al., 2010). The gelatinization behavior of starches is also influenced by their genetic backgrounds (Vamadevan et al., 2013). Numerous studies (Shi and Seib, 1992, Fredriksson et al., 1998, Gomand et al., 2010a) have reported on the relationship between the average chain length of amylopectin and gelatinization parameters, although it is unlikely that the average chain length values influence melting parameters as the average chain length of amylopectin does not reflect the stability of crystalline components (Vamadevan and Bertoft, 2015). Rather, just as with swelling behavior, gelatinization parameters are postulated to be influenced by the organization of chains in the crystalline lamellae, structural parameters such as IB-CL, ECL, amount of A_{fp}-chains, and the environmental conditions during the growth period (Alvani et al., 2012, Vamadevan et al., 2013). Starch containing short (DP < 6) IB-CL and high amounts of A_{fp}-chains have been reported to melt at lower temperatures, while starches with a long IB-CL (DP > 6) and fewer A_{fp}-chains melt at higher temperatures (Vamadevan et al., 2013). It should be noted that in other cereals (ex. wheat) the gelatinization properties and amylopectin structure have been shown to differ between A-type and B-type starch granules (Kim and Huber, 2010).

A multitude of other functional attributes of starch are governed by structure-function relationships, including starch pasting properties, retrogradation, and freeze-thaw stability, as discussed elsewhere (Vamadevan and Bertoft, 2015).

Photosynthesis and diurnal activity

Photosynthesis is a process that occurs in plants, algae, and some bacteria wherein light energy is utilized to convert carbon dioxide and water into carbohydrates and oxygen

(Rabinowitch and Govindjee, 1969). Briefly, the process of photosynthesis is carried out in a series of light dependent and light independent (dark) reactions (Rabinowitch and Govindjee, 1969). During the light reactions energy from light is used to form the energy molecules adenosine triphosphate (ATP) and reduced nicotinamide adenine dinucleotide phosphate (NADPH), which are subsequently used in a chain of dark reactions when carbon is fixed and synthesized into glucose and sucrose. Starch is subsequently formed from glucose through a complex interplay of starch synthases, and starch branching and debranching enzymes (Tetlow, 2011). The starch is commonly classified as storage or transient starch. Both transient and storage starch are used to fuel plant growth, although they influence growth in different manners. Storage starch is deposited in the amyloplasts of non-photosynthetic tissues of plants to serve as an energy source during germination and sprouting (Streb and Zeeman, 2012). Transient starch is produced in the chloroplasts of photosynthetic tissues during daylight and is used during the following night to supply the plant with carbohydrates and energy (Streb and Zeeman, 2012). Furthermore, transient starch acts as carbohydrate reservoir, which buffers the diurnal changes in the supply of photoassimilates (Streb and Zeeman, 2012).

As discussed earlier, the growth rings of starch granules consist of semi-crystalline and amorphous material, but the reason of their appearance has remained uncertain. The literature on the underlying mechanism of growth ring formation is scarce. In 1895, Meyer hypothesized that starch granules lay down one growth ring per day due to diurnal rhythms. A diurnal rhythm is characterized as a rhythm which follows a daily cycle. Fluctuations in the rate of photosynthesis will follow a daily cycle in part related to the level of environmental irradiance, with the highest levels of net photosynthesis, assimilate

export, and activity of sucrose phosphate synthase observed at midday, coinciding with the time of maximum irradiance (Kalt-Torres et al., 1987). In 1926, Van de Sande-Bakhuyzen reported that starch granules in wheat grown under constant light conditions displayed no growth rings. This finding was later supported by Buttrose (1960), who also found that rings were absent in barley starch samples grown under constant light. Buttrose (1960) mentioned that the disappearance of growth rings when grown under constant light conditions relates to the "classical idea that daylight photosynthesis provides an abundant supply of starch precursor, resulting in dense packing of starch molecules, followed by a fall-off in supply during darkness, with a consequent looser, more hydrated molecular packing". Wherein if no 'fall-off' in the supply of precursor would occur due to constant light growing conditions, there would be no change in the dense packing of starch molecules, resulting in no growth rings. However, potatoes grown under constant light conditions retained their growth ring patterns (Pilling and Smith, 2003). Thus, to date, there is conflicting information in the literature relating to the effect of constant light growing conditions and the presence of growth rings in starch granules. In addition, no attempts have been made to analyze the molecular structure in starch cultivated under constant light conditions.

Starch synthesis

As mentioned above, starch is produced as an end product of photosynthesis. The formation of glucose polymers in starch involves a complex interplay of starch biosynthetic enzymes, as depicted in Figure 1.3. The pathway of starch synthesis will differ depending on whether or not the tissues are photosynthetic or non-photosynthetic**.**

Throughout the pathways, a number of key enzymes are involved such as ADPglucose phosphorylase (AGPase), starch synthase (SS), starch branching enzyme (SBE), and starch debranching enzyme (DBE) (Comparot-Moss and Denyer, 2009). In the following paragraphs a cursory overview of starch synthesis is covered, highlighting major products and enzymes of starch synthesis.

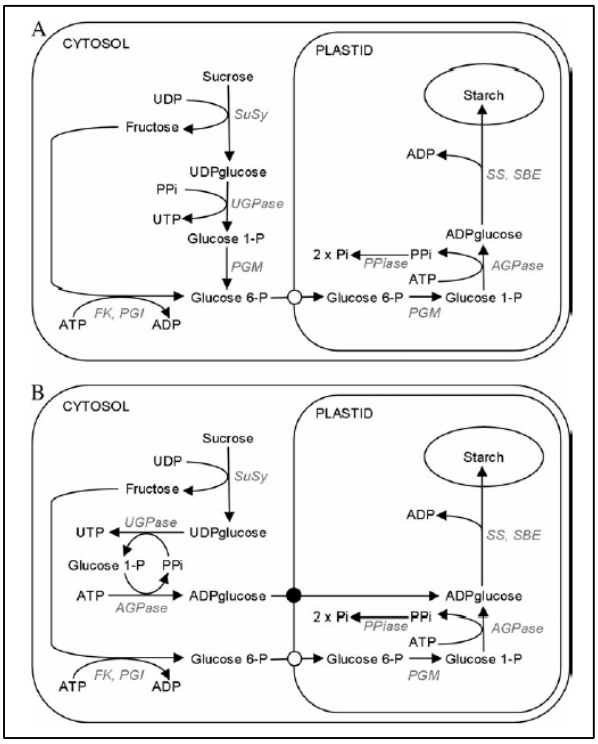

Figure 1.3: Pathways of starch synthesis in typical non-photosynthetic cell (A) and typical photosynthetic cell (B). Figure from Comparot-Moss and Denver (2009).

The pathway for the formation of starch polymers starts with sucrose, as sucrose catabolism in the cytosol and mitochondria produces the necessary substrates for starch synthesis, glucose 6-phosphate and ATP (Comparot-Moss and Denyer, 2009). These precursors are transported into the plastid via the specific translocators glucose 6-phosphate/phosphate transporter and the ATP/ADP transporter. Once inside the plastid, glucose 6-phosphate is converted to glucose 1-phosphate (via phosphoglucomutase).

Glucose 1-phosphate is subsequently converted to ADP-glucose by utilizing ATP and ADP-glucose pyrophosphorylase (Comparot-Moss and Denyer, 2009).

ADP-glucose is the primary sugar nucleotide donor of glucose during starch synthesis. A variety of different isoforms for starch synthase work to elongate glucose polymers by the formation of α-(1,4)- bonds. The different isoforms of starch synthase can be grouped into subfamilies including granule-bound starch synthase (GBSS), and soluble starch synthase (SS I-IV). GBSS primarily works to elongate amylose chains. Two isoforms of GBSS (GBSS I and GBSS II) have been identified in the literature. GBSS I has been reported to be active in storage tissues, whereas GBSS II synthesizes amylose in non-storage tissues where transient starch is produced (Vrinten and Nakamura, 2000).

SS I, II, III, and IV are responsible for the chain elongation of amylopectin. Each class of SS influences the elongation of amylopectin in different manners. SS I is responsible for the elongation of the shortest amylopectin chains, elongating from DP 6-7 to DP 8-12 (Commuri and Keeling, 2001). SS II elongates short amylopectin chains (DP < 10) to intermediate length chains (DP 12-24). The main role of SS III during amylopectin synthesis is the elongation of short chains to long chains (DP > 30). The production of long amylopectin chains which span through many clusters are governed by SS II and/or SS III (Commuri and Keeling, 2001). The role of SS IV is reported to influence the number of starch granules within the plastid of *Arabidopsis* leafs, although it is not certain if SS IV plays the same role in storage seed tissues (Tetlow, 2011).

SBE plays a very important role in the formation of the distinct fine structure of starch granules. SBE catalyzes the formation of the α-(1,6)-branch points. SBE achieves

branch point formation by cleaving an internal α-(1,4)-bond and transferring the released reducing end to a C6 hydroxyl group to form an α-(1,6)-branch point of amylopectin (James et al., 2003, Tetlow, 2011). Just as SS contains different isoforms with different roles of chain elongation, SBE can be divided into two major classes; SBE I and SBE II. SBE I and II differ in respect to the length of chain which is transferred. In an *in vitro* study, SBE II has been reported to transfer shorter chains than SBE I (Takeda et al., 1993). In addition, SBE I prefers to form branches for amylose like chains. On the other hand, SBE II preferentially branches amylopectin chains. SBE II exists in two different isoforms, SBE IIa and SBE IIb. Apparently, their levels of expression differ in different cereals (Morell et al., 1997). SBE IIa is expressed in every tissue, whereas SBE IIb is only expressed in the endosperm.

In addition to the role of SSs and SBEs, DBEs also play an important role in the formation of the amylopectin component (Tetlow, 2011), and work in conjunction with SSs and SBEs. Two groups are DBEs have been identified, specifically the isoamylase-type and the pullulanase-type. The isoamylase-type are likely involved in the trimming of inadequately spaced branches allowing for tighter packing of glucan chains, whereas the pullulanase-type reportedly work on tightly branched glucans and has a weak affinity for loosely spaced glucans (Tetlow, 2011). The debranching enzymes work to remove improperly spaced glucans at the surface of growing granules, which would prevent them from crystallization.

Reduction in the activity of specific starch synthesizing enzymes has been documented to influence the polymer structure and composition of starch granules. Pilling and Smith (2003) investigated starch from the tubers of transgenic potatoes with altered

activities of GBSS and SS III, the two isoforms with the highest activity levels. Plants with reduced activity of GBSS, which is responsible for the synthesis of amylose, exhibited 'normal' appearing growth rings in the periphery of the granule indicating that amylose is not necessary for the formation of growth rings, and that the presence of growth rings may be a function of changes in the amylopectin component (Pilling and Smith, 2003). Starch from potato tubers with reduced activity of SS III, the isoform with the highest activity related to amylopectin synthesis in tubers, did not exhibit normal growth rings. Reducing the activity of SS III resulted in amylopectin with altered size distribution of its short chain components, as well as a greater abundance of very long amylopectin chains and a greater proportion of amylose, resulting in a lack of distinct growth rings (Pilling and Smith, 2003). These results indicate that growth ring formation can be influenced by the structure of starch polymers, and can be disrupted by the presence of long amylopectin or long amylose chains.

Effect of altered supply of substrates for starch synthesis

The rate at which sucrose, the substrate required for starch synthesis, is supplied to a diurnal plant is greater during the day compared to at night (Pilling and Smith, 2003). As a result, the rate of starch synthesis (in tubers) at the end of the day is about twice the level of the rate recorded at the end of the night (Geigenberger and Stitt, 2000). Influencing the supply of substrate required for starch synthesis, through either altered environmental growing conditions, or transgenic means, may potentially impact the organization of starch granules in a variety of ways (Pilling and Smith, 2003). Changes in the concentration of ADP-glucose can influence the activity of different isoforms of starch

synthase, which can subsequently influence starch structure (Clarke et al., 1999). There is indirect evidence that the concentration of ADP-glucose may influence the composition and structure of starch from potato tubers (Geigenberger and Stitt, 2000). Altering the supply/availability of sucrose required for starch synthesis may also influence the concentrations of a wide range of metabolites and potentially the concentration of other cellular components. These changes in the chemical environment could influence the organization of newly formed amylopectin molecules (Pilling and Smith, 2003). In addition, Pilling and Smith (2003) reported that it is theoretically possible that the rate of amylopectin synthesis may influence the manner in which the granule is organized.

Acid hydrolysis

Native starches may not have properties which make them ideal for use in certain food applications, and therefore, starches may be modified to improve desired functionality (BeMiller and Huber, 2015). Chemical modification of starch has been extensively studied throughout the last century (Wang and Copeland, 2015). Chemical modification of starch can greatly improve functional limitations of native starches, such as low resistance to shear, poor thermal stability, or high tendency toward retrogradation (Wang and Copeland, 2015). The oldest, yet still commonly utilized chemical modification method is acid hydrolysis. Acid hydrolysis of starch was first reported by Nägeli in 1874 and Lintner in 1886, wherein native starch granules hydrolysis was conducted with sulphuric acid or hydrochloric acid, respectively. The overlying principle of acid hydrolysis is that the crystalline components of carbohydrate are more resistant to acid catalyzed hydrolysis than amorphous carbohydrate components (Robin, 1974). The residues, which remain

following acid hydrolysis, are commonly referred to as lintners (2.2 M HCl hydrolysis) or Nägeli dextrins (15% H_2SO_4 hydrolysis).

It has been reported that starch typically exhibits a two-stage hydrolysis pattern (Biliaderis et al., 1981). During the first stage, rapid hydrolysis occurs, followed by a second stage wherein the hydrolysis slows down. The rapid stage of hydrolysis corresponds to acid hydrolyzing the amorphous regions of the starch granule. During the second stage of hydrolysis, crystalline material is degraded at a slower rate. The molecular structure of the remaining lintner depends on the degree of acid hydrolysis, although generally two types of dextrins are present; linear dextrins and branched dextrins. The linear dextrins typically exhibit an average DP_n between 13-17 whereas single branched dextrins display an average DP_n between 24-30 (Watanabe and French, 1980). In addition, small amounts of double or multiple branched dextrins ($DP_n > 35$) and short stubs resistant to debranching have been reported (Umeki et al., 1981).

Amylose-only starch

Barley has long been viewed as an ideal system for genetic and breeding studies due to the relative simplicity of its genetic system and diversity of the species (Kling et al., 2004). *In planta* production of starches containing high proportions of resistant starch (RS) has received significant attention as increased RS generation can enhance the health profile of a crop. Resistant starch is well documented for its health promoting glycemic effects as it is resistant to enzymatic hydrolysis and escapes digestion in the stomach and small intestine (Englyst, 1982). The amount of amylose present in starch has been positively correlated to RS content, low digestibility, and low glycemic responses (Carciofi et al.,

2012). While the structure of resistant starch is complex and elusive (Carciofi et al., 2012), the amylose component of starch appears to decrease the substrate accessibility to amylases due to the tendency of amylose to retrograde/re-crystallize following processing. Bioengineering efforts have successfully provided increased amylose in a number of cereal crops (wheat, rice, corn, barley), although crop yields are significantly lower for these plants (Carciofi et al., 2012). Recently, a 100% amylose line of barley was achieved by silencing all SBE isoenzymes (SBE I, SBE IIa, SBE IIb) responsible for the production of amylopectin by utilizing a single RNAi hairpin. The 100% amylose barley retained high yields similar to other barley varieties. As expected, the 100% amylose barley line exhibited high contents of RS (65%) following gelatinization. The 100% amylose barley contained irregularly shaped granules, and unique thermal properties and crystallinity (Carciofi et al., 2012).

Research objectives and hypotheses

The objectives of this work project were to (i) gain a better understanding of the impact of diurnal photosynthetic activity on barley starch fine structure, and (ii) investigate the impact of altered expression of starch branching enzymes (SBE) on starch fine structure. To investigate the role of diurnal photosynthetic activity on starch fine structure, normal and waxy barley were cultivated under normal diurnal photosynthetic or constant light conditions, after which their starches were isolated, and fine structure analyzed. The influence of SBE expression on starch structure was investigated by comparing the profile of acid hydrolyzed normal and waxy barley starch to that of barley with silenced expression of genes coding for SBEs, yielding a novel amylose-only starch.

Specific Objectives:

1. Investigate presence of growth rings in barley starch cultivated under normal diurnal or constant light growing conditions.
2. Determine the effect of diurnal photosynthetic activity on the molecular composition of normal and waxy barley starch.
3. Determine the effect of diurnal photosynthetic activity on the fine structure of waxy barley starch and amylopectin from normal barley starch.
4. Determine the effect of altered expression of SBEs on starch structure by comparing the structure of acid hydrolyzed amylose-only starch to that of normal and waxy barley starch.

Hypotheses:

1. Diurnal photosynthetic activity will not influence the presence of growth rings in barley starch.
2. Diurnal photosynthetic activity will not influence the molecular composition of barley starch.
3. Diurnal photosynthetic activity will not influence the fine structure of amylopectin from barley starch.
4. The expression of starch branching enzymes will not influence the structure of acid hydrolyzed barley starch.

Chapter 2: The influence of diurnal photosynthetic activity on the morphology, structure, and thermal properties of normal and waxy barley starch.

Summary

This study investigated the influence of diurnal photosynthetic activity on the morphology, molecular composition, crystallinity, and gelatinization properties of normal barley starch (NBS) and waxy barley starch (WBS) granules. Normal and waxy barley cultivated in a greenhouse under normal diurnal or constant light photosynthetic conditions were investigated. Interestingly, growth rings were observed in all samples regardless of lighting conditions. The size distribution of whole and debranched WBS components analyzed by gel permeation chromatography did not appear to be influenced by the different lighting regimes, however, a greater relative crystallinity measured by wide-angle X-ray scattering and greater crystalline quality as judged by differential scanning calorimetry was observed under the diurnal lighting regime. NBS cultivated under the diurnal photosynthetic lighting regime displayed a lower amylose content, and lower ratio of long: short amylose chains than its counterpart grown under constant light. Although the relative crystallinity of NBS was not influenced by lighting conditions, lower onset, peak, and completion gelatinization temperatures were observed under diurnally grown NBS compared to constant light conditions. It is concluded that barley starch was influenced by the diurnal photosynthetic lighting regime resulting in altered structural and gelatinization parameters, although the differences vary depending on the enzyme composition of the barley studied.

Introduction

A common structural feature present in starch granules is the presence of alternating semi-crystalline and amorphous structures. The alternating structures, commonly referred to as 'growth rings', can sometimes be viewed in native starch, but are readily observed following treatment with dilute acid or enzymes using a variety of microscopic techniques such as light, scanning electron, and transmission electron microscopy. The growth rings represent alternating layers of increasing and decreasing levels of crystallinity, refractive index, density, and resistance to enzymatic attack. Although the presence of growth rings is a universal feature of starch granules, the underlying mechanisms responsible for their appearance are still uncertain. Prior investigations on the nature of growth rings suggested their occurrence may be the result of plants following either a diurnal or circadian rhythm. Meyer (1895) hypothesized that in starch granules one growth ring per day is formed due to the diurnal rhythm. In 1925, Bakhuyzen reported that wheat starch grown under constant light conditions did not display growth rings. A similar result was obtained by Buttrose (1960) wherein growth rings were not observed in barley starch when grown under constant light conditions. The underlying theory for the disappearance of growth rings according to Buttrose (1960) is that during sunlight, when the generation of precursor for starch synthesis is high, crystalline growth rings are synthesized. During the night, when essential precursors for starch synthesis cannot be produced via photosynthesis, the granule synthesizes the amorphous components. However, when potato (tuber) starch was grown in constant light conditions, growth rings were observed (Pilling and Smith, 2003). The growth rings found in starch from potato grown under constant light differed from those grown under

diurnal conditions, as prominent ‘major’ rings, in which the enzymatically digested amorphous zone was large, alternated with ‘minor’ rings with a narrower digested zone (Pilling and Smith, 2003). It should be noted that similar patterns of alternating ‘major’ and ‘minor’ rings were also observed in starch granules in other studies on potato starch grown under normal conditions (Frey-Wyssling and Buttrose, 1961).

To the author’s knowledge, the effect of diurnal photosynthetic activity on the physicochemical and molecular characteristics of starch has not been previously reported. This research therefore investigated the effect of diurnal and constant light growing conditions on selected physical, chemical, and morphological properties of normal and waxy barley starch through light and confocal microscopy, gel permeation chromatography, X-ray diffraction, and differential scanning calorimetry analysis. Barley was selected as a model cereal as this plant has previously been investigated in other studies on diurnal activity (Buttrose, 1960). Results from this research will allow for a greater understanding of the influence of diurnal activity on the physical and molecular characteristics of barley starch.

Materials and methods

Barleys

To investigate the role of diurnal photosynthetic activity, two varieties of barley, Cinnamon (waxy barley starch; WBS) and Golden Promise (normal barley starch; NBS) were cultivated under normal diurnal or constant light growing conditions in a greenhouse at the University of Copenhagen (Copenhagen, Denmark). The constant light

barley samples were shielded from natural sunlight and grown for three months from planting until maturation under constant artificial light using mercury lamps. Diurnal samples were grown under ambient conditions, with supporting illumination from 4 a.m.-8 p.m.

Enzymes

β-amylase (10,000 U/mL) from barley [(1,4)-α-D-glucan maltohydrolase: EC 3.2.1.2], pullulanase (700 U/mL) from *Klebsiella planticola* (amylopectin 6-glucoanhydrolase; EC 3.2.1.41), isoamylase (1000 U/mL) from *Pseudomonas sp*. (glycogen 6-glucoanhydrolase; EC 3.2.1.68), and lichenase (1000 U/mL) from *Bacillus subtilis* (endo-1,3-β-D-glucanase: EC 3.2.1.73) were sourced from Megazyme International (Wicklow, Ireland).

Starch extraction

Starch was extracted from barley flour based on the method by Carciofi et al. (2011), with modifications. Briefly, 5 g of milled barley was mixed with 25 mL of 5 mM dithiothreitol containing 1% sodium dodecyl sulphate for 30 min at room temperature, and subsequently centrifuged at 3300 x g for 15 min. The pellet was then washed twice with water and filtered through a 70 µm mesh cloth. The filtrate was then centrifuged and 50 mL of 20 mM NaH_2PO_4 buffer (pH 6.5) was added. The mixture was incubated in a 50°C water bath for 5 min before the addition of 100 µL lichenase enzyme, after which the sample was incubated for 1 hour, with stirring every 15 minutes. After centrifugation

(3300 x g for 15 min) the pellet was washed twice with distilled water, once with ethanol, followed by air drying overnight.

Starch morphology analysis

Morphology of barley starch granules was observed by light, polarized light, and confocal microscopy. For light microscopy analysis, starch granules were lightly treated with dilute HCl (2.2 M) to gently remove amorphous material and viewed under an Olympus BX40 light microscope (Melville, NY, USA) connected to a digital camera (Olympus DP11-N) and a monitor (Sony PVM-14N5U; Tokyo, Japan) was used obtain digital images. Polarized light images were acquired with the same imaging system using a polarized light filter.

Confocal laser scanning microscopy (CLSM) was conducted according to methods described by Glaring et al. (2006), using a TCS SP2 confocal laser scanning microscope (Leica Microsystems, Germany). Granules were stained prior to scanning with APTS solution (20 mM 8-amino-1,3,6-pyrenetrisulfonic acid) as described by Glaring et al. (2006).

Wide angle x-ray diffraction

X-ray measurements of hydrated samples were acquired using a Rigaku X-ray diffractometer (Rigaku-Denki, Co., Tokyo, Japan) equipped with a 100XL+ micro-focus sealed X-ray tube producing a photon beam with a wavelength of 1.54 Å. The scattering patterns were recorded with a 2D 300 K Pilatus detector from Dectris (Baden, Switzerland). The samples were measured in the Wide-angle X-ray scattering (WAXS)

setting covering a q-range from about 0.06 to 2.8 $Å^{-1}$ with an exposure time of 600 seconds. The latter corresponds to an upper 2θ value of 40.15 degrees or 2.24 Å. The water content of samples was adjusted by water phase sorption for 10 days in desiccators at a relative humidity of 90% using a saturated salt solution of barium chloride. Hydrated samples were then sealed between thin mica films to prevent any significant change in water content during the measurement, which was performed in vacuum. Relative crystallinity was calculated according to the methods described in Brückner (2000) and Frost et al. (2009). Amorphous background scattering was estimating using an iterative smoothing algorithm in MATLAB (Natick, Massachusetts, USA). The relative crystallinity was then estimated from the peak and total areas as:

$$Relative\ Crystallinity = \frac{Area\ of\ Peaks}{Total\ Area}$$

where the areas are numerically integrated using built in MATLAB functions. The relative amounts of different crystal polymorph types were determined following subtracting the estimated amorphous background and fitting with a series of Gaussian peak profiles. From these fits, the amounts of V-type polymorph can be estimated as the ratio of the area under the characteristic V-type peaks at roughly 2θ = 13° and 20° compared to the total peak area of all fitted Gaussian peaks, whereas the A-type polymorph was estimated utilizing the fitted characteristic main peaks at 2θ = 15° and 23° and the unresolved doublet at 17° and 18° 2θ.

Differential scanning calorimetry

The thermal properties of native starch samples were analyzed by differential scanning calorimetry (DSC) using a Discovery DSC from TA instruments (New Castle, DE, USA).

Scans were performed from 25°C to 85°C at a rate of 5°C/min. All starch samples were analyzed in slurries of 2 mg starch and 10 µL 10 mM NaCl buffer in duplicates. Onset temperature (T_o), peak temperature (T_p), completion temperature (T_c) and enthalpy change (ΔH) were derived from the thermal profiles.

Starch molecular structure

To determine the size distribution of barley starch with gel permeation chromatography (GPC), duplicate starch samples (8 mg) were dissolved in 90% DMSO (200 µl) and gently stirred overnight at room temperature. Following dilution with warm water (800 µl, 80°C), the dissolved starch sample (400 µL) was then applied to a Sepharose CL 2B (Pharmacia, Uppsala, Sweden) column (1.6 x 32 cm) and eluted with 0.01 M NaOH at 0.5 mL/min. Even numbered fractions (1 mL) were collected and analysed for carbohydrate content with the phenol-sulfuric acid method (Dubois et al.,1956). The maximum wavelength of absorption (λ_{max}) of the iodine-glucan complex was determined in the collected odd numbered fractions. 1 mL of 0.01 M HCl was added to the fractions and following neutralization, 0.1 mL of 0.01 M I_2/0.1 M KI solution was added. Wavelength spectra were recorded from 300-800 nm with a WPA Spectrawave S800 diode array spectrophotometer (Harvard Bioscience, Holliston, MA, USA).

β-Limit dextrins of barley starches were prepared by dissolving starch in 90% DMSO and stirring overnight as described above. The following day, 2 µL of β-amylase along with 100 µL of 0.01 M sodium acetate buffer (pH 6.0) were added and the mixture was stirred overnight. The following day, the sample was diluted to 1 mL with water, heated to deactivate the enzyme, and 400 µL was applied to the Sepharose CL 2B

column. Fractions (1 mL) were analysed for carbohydrate content and maximum wavelength of iodine absorption as described above.

Chain length analysis of barley starch with GPC was completed according to methods described by Kalinga et al. (2013). Briefly, duplicate samples of barley starch were debranched with isoamylase and pullulanase whereafter the sample was applied on a column (1 x 90 cm) of Sepharose CL 6B (GE Healthcare, Uppsala, Sweden) and eluted with 0.5 M NaOH at 1 mL/min. Fractions (1 mL) were analysed for carbohydrate content as above. By dividing the chromatograms at the lowest points between the two peaks, the relative content of amylose and amylopectin were determined according to Sargeant (1982). In order to further characterize the long chain and short chain components of amylose, the amylose fraction was divided into the fraction eluted at the void of the gel, and the fraction which eluted between the void volume and amylopectin chain fraction, respectively.

Statistical analysis

All analyses were conducted in duplicate and analyzed using SPSS (IBM Corporation, Armonk, NY, USA). Significant differences were determined by comparing means by Tukey's test at a significance level of $p < 0.05$.

Results

Morphology of starch granules

Following the treatment of isolated starch granules with dilute HCl, growth rings were observed in starch granules from WBS and NBS grown under both diurnal and constant light conditions (Figure *2*.1). This observation was unexpected and did not align with earlier findings reported by Buttrose (1960), and Tester et al. (1991) wherein growth rings were not observed in barley starch when grown under constant illumination conditions. The presence of the maltese cross in all starch samples regardless of growing conditions observed under polarized light indicates that the radial arrangement of starch molecules (Jane et al., 2003) was preserved under both growing conditions (Figure 2.2). The appearance of growth rings in WBS and NBS barley grown under constant light conditions was also confirmed by CLSM analysis (Figure 2.3). In this analysis, the reducing ends of starch components were labelled with the fluorescent probe APTS, with smaller molecular components exhibiting greater fluorescence intensity due to their greater molar ratio of reducing ends per anhydrous glucose residues, and consequent greater amount of fluorescent labelling by weight (Blennow et al., 2003). NBS granules exhibited strong fluorescence in the hilum regardless of lighting regime, whereas this was not observed in WBS granules.

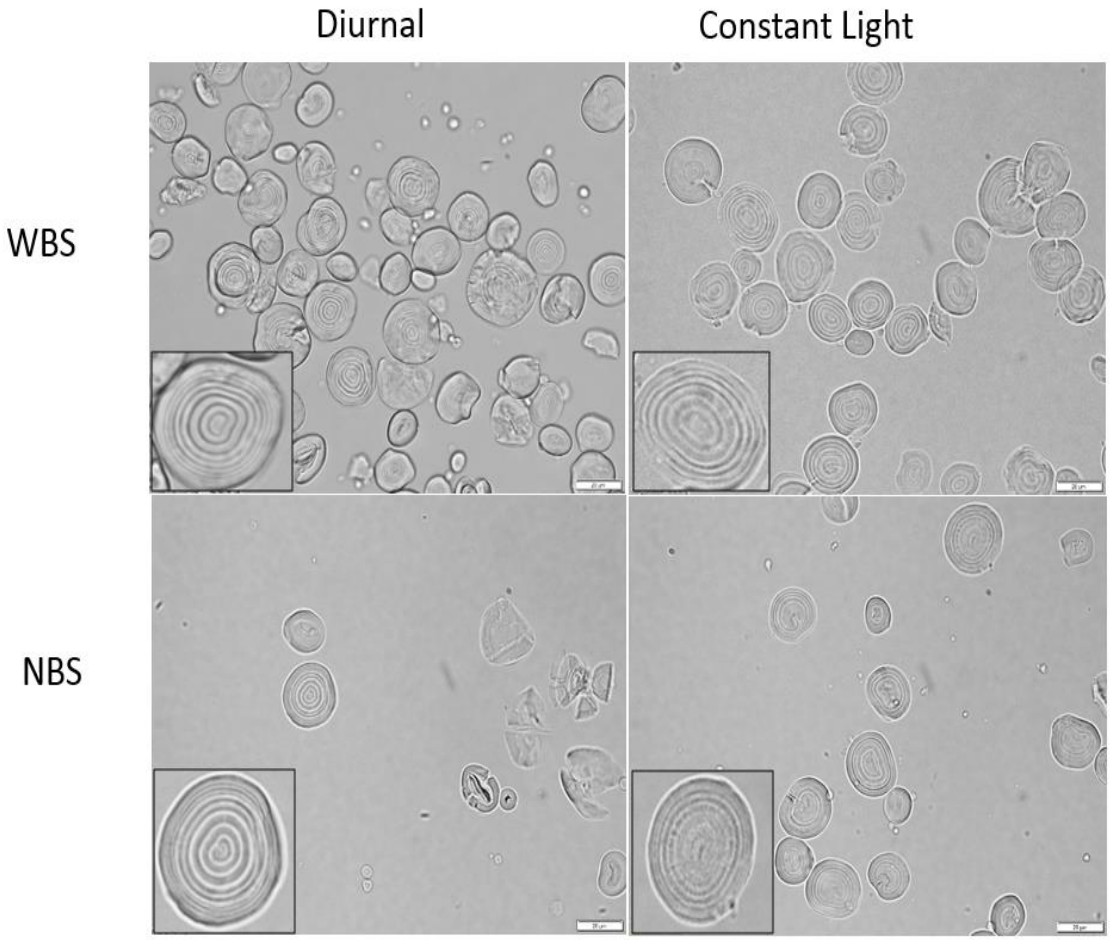

Figure 2.1: Acid treated NBS and WBS granules displaying presence of growth rings viewed by light microscopy. Scale bar represents 20 µm. Inset displays granules at higher magnification.

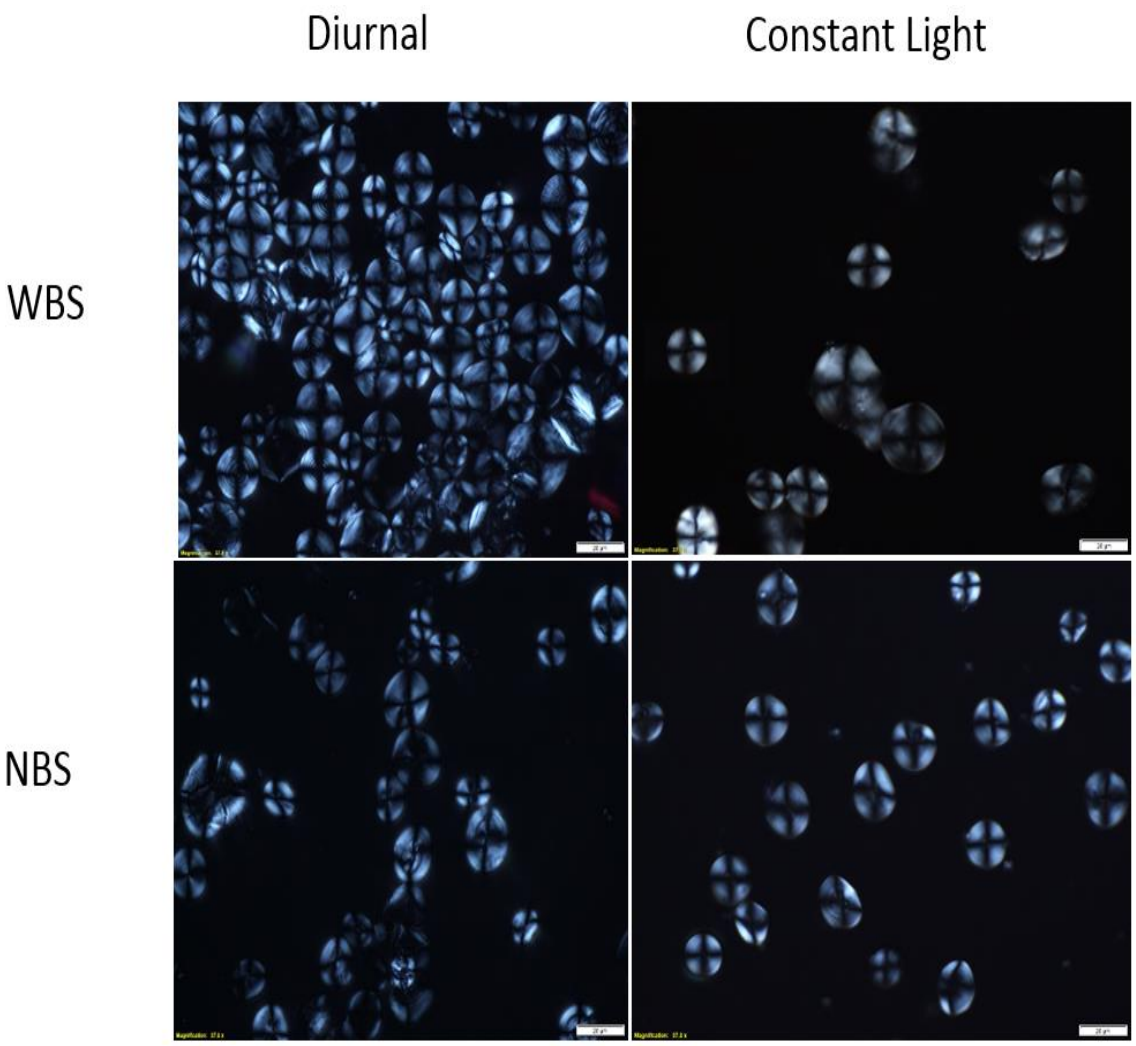

Figure 2.2: Diurnal and constant light NBS and WBS granules viewed by polarized light microscopy. Scale bar represents 20 µm.

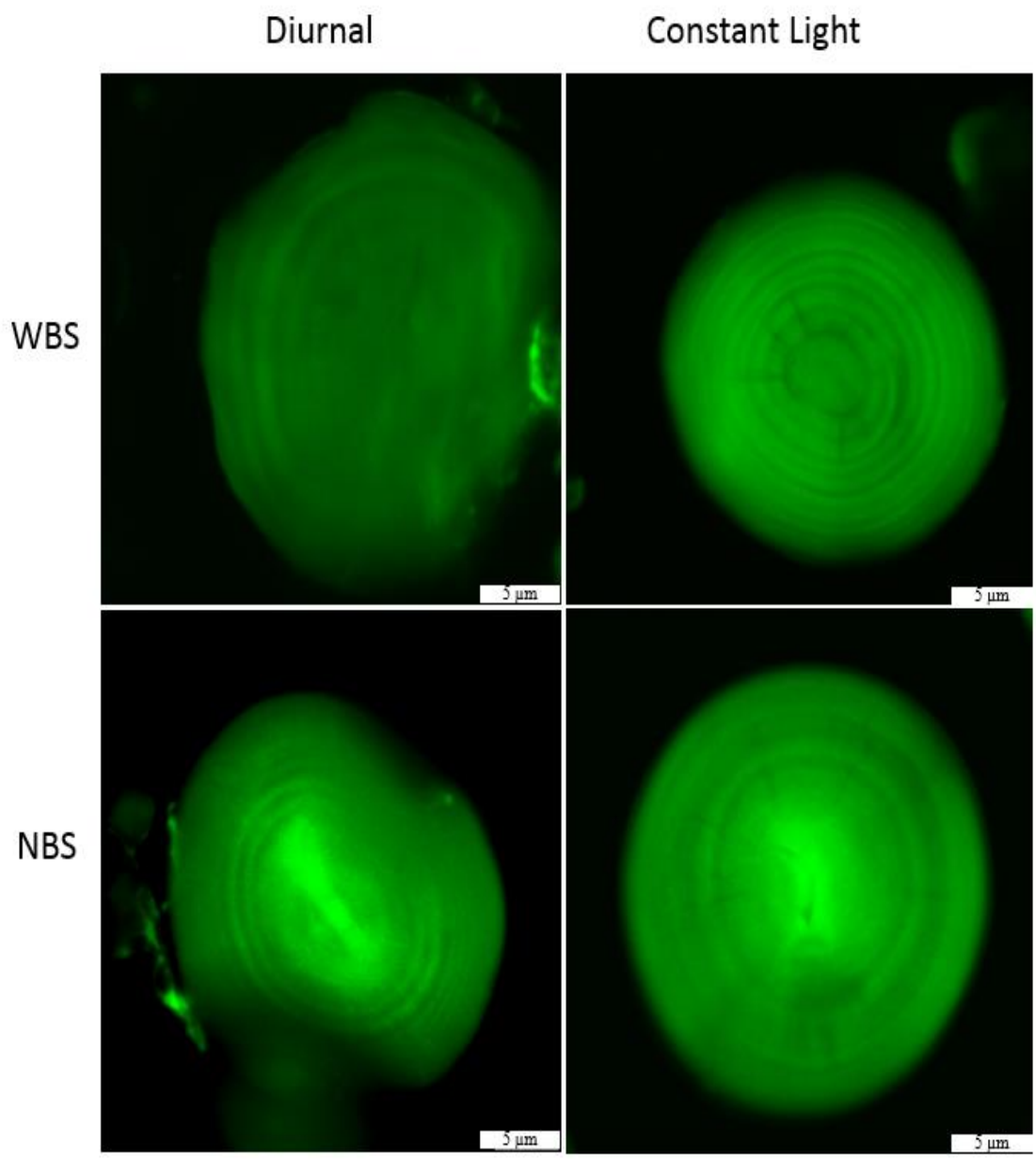

Figure 2.3: Diurnal and constant light NBS and WBS granules viewed by CLSM. Scale bar represents 5 µm.

Architecture of diurnal and constant light barley starch granules

The polymorphism of barley starch granules cultivated under diurnal or constant light photosynthetic conditions was determined by WAXS. X-ray diffraction patterns can be seen in

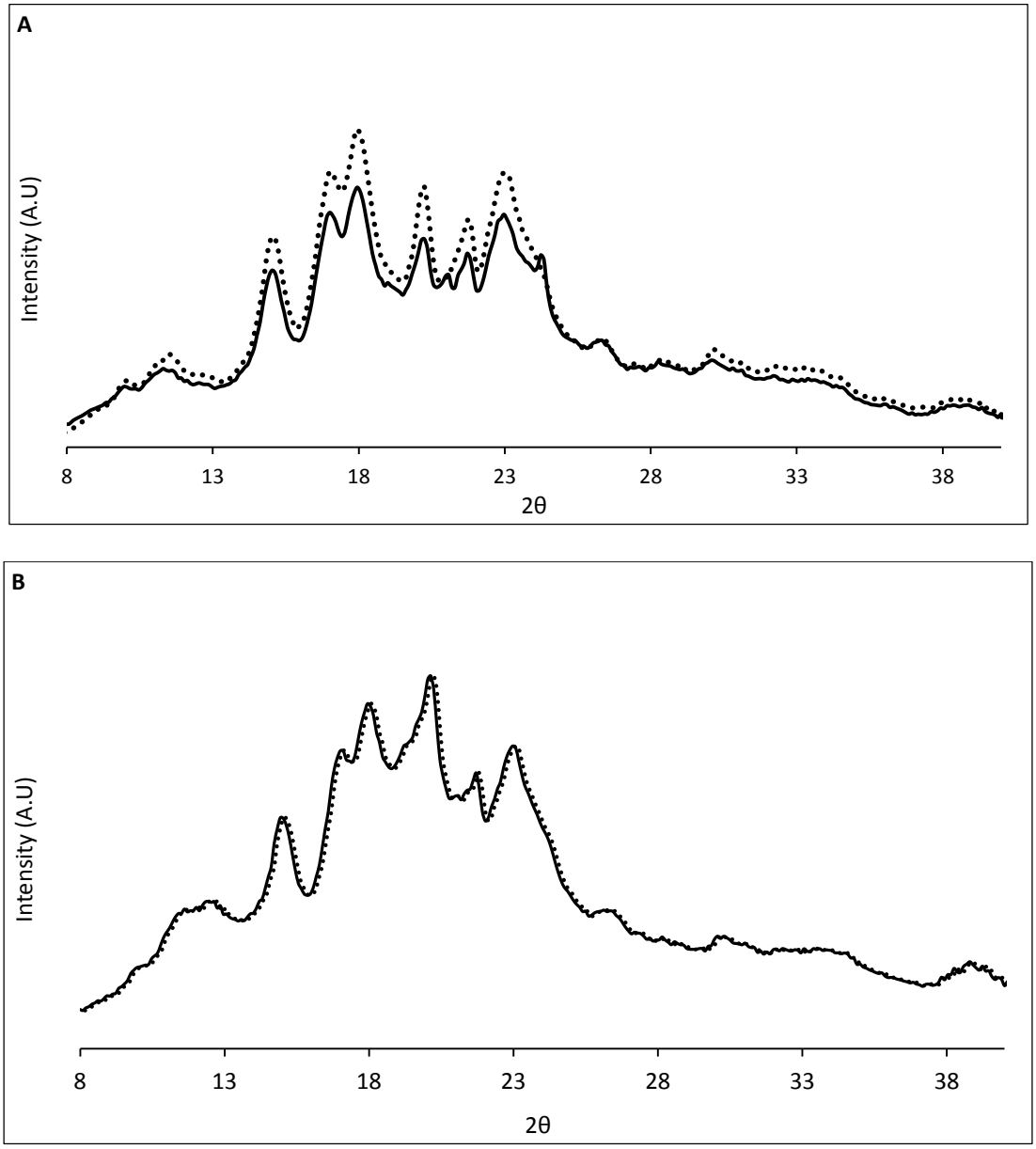

Figure 2.4: Wide angle X-ray scattering pattern of WBS (A) and NBS (B) grown under diurnal (⋯⋯) and constant light conditions (—).

Figure 2.4. All barley samples exhibited primarily A-type and V-type crystallinity**.** The relative crystallinity of NBS was not influenced by diurnal or constant light growing conditions (Table 2.1), whereas the relative crystallinity of WBS starch was suppressed when grown under the constant lighting regime (15.7%) compared to diurnal conditions

(20.4%). Diurnally grown WBS starch also exhibited a greater contribution of V-type crystals to the relative crystallinity (18.1%) compared to WBS barley grown under constant light conditions (11.1%).

Table 2.1: Relative crystallinity (RC) of diurnal and constant light WBS and NBS granules.

	RC (%)	A-type (% of total)	V-type (% of total)	V-type (% of crystals)
Diurnal NBS	19.5	16.9	2.5	12.9
Constant Light NBS	19.2	16.7	2.4	12.6
Diurnal WBS	20.4	16.7	3.6	18.1
Constant Light WBS	15.7	13.9	1.7	11.1

When starch is heated in the presence of moisture, it undergoes a series of irreversible physical changes commonly referred to as gelatinization (Svensson and Eliasson, 1995). During gelatinization, the organization of the crystalline amylopectin lamellae is disrupted and lost in an irreversible phase transition (Slade and Levine, 1988). The thermal properties of gelatinization of WBS and NBS cultivated under diurnal or constant light conditions were determined by DSC analysis, and the gelatinization transition temperatures (T_o, T_p, T_c) and enthalpy of gelatinization (ΔH) were recorded. It is well accepted that T_p is an indicator of crystalline perfection, whereas ΔH represents the energy required to rupture hydrogen bonds within double helices (Cooke and Gidley, 1992). Illumination conditions appeared to influence the gelatinization profiles of both WBS and NBS (Figure 2.5). NBS grown under diurnal conditions exhibited lower T_o, T_p, and T_c and ΔH values compared to its counterpart cultivated under continuous

illumination (Figure 2.5). Interestingly, the opposite trend was observed in WBS, as diurnal WBS exhibited higher T_o and T_p values indicating higher crystalline perfection in diurnally grown WBS. The T_c and ΔH were very similar between the two light regimens, indicating that WBS grown under constant light conditions displayed a broader, more heterogeneous distribution of crystalline quality, as shown by the broader temperature range (T_c– T_o).

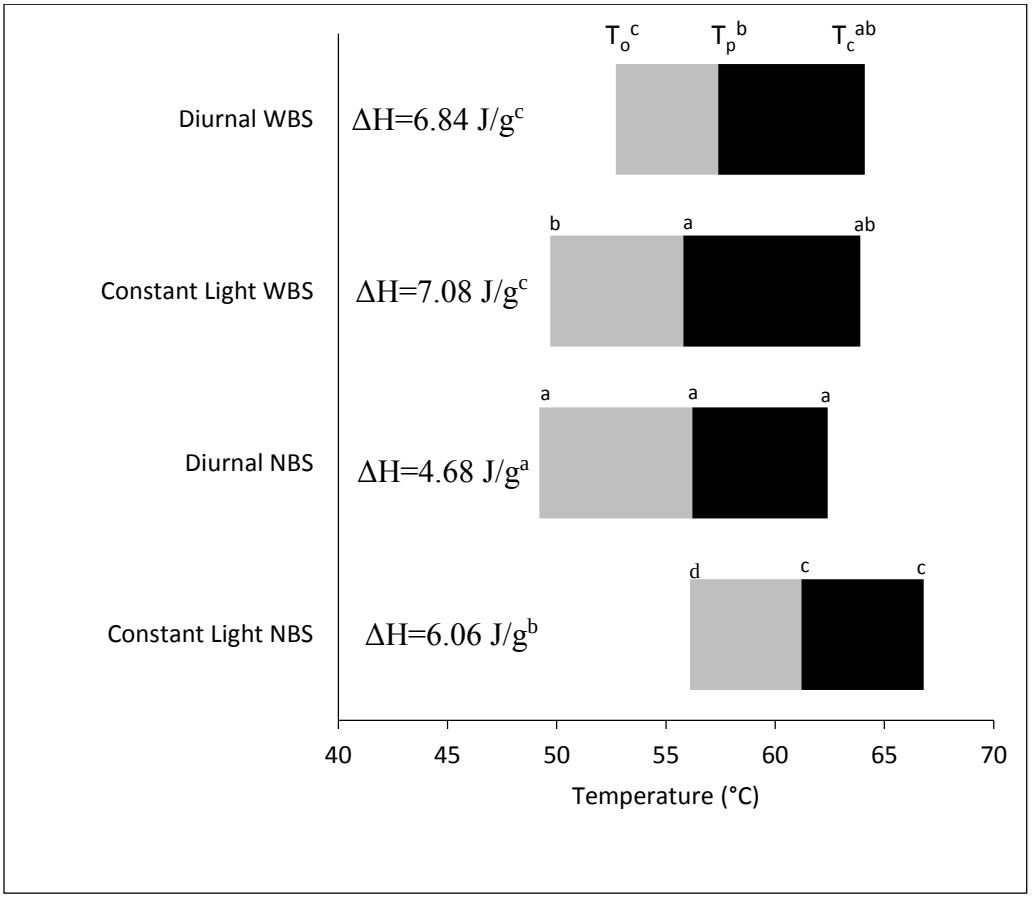

Figure 2.5: Gelatinization parameters of NBS and WBS cultivated under diurnal or constant light conditions (To= Onset temperature; Tp = Peak melting temperature; Tc= Conclusion temperature; ΔH= Enthalpy of gelatinization. Values with same letters are not significantly ($p < 0.05$) different.

Molecular structure of starch

The molecular size distribution of native and β-amylase treated WBS and NBS grown under diurnal or constant light conditions determined by GPC on Sepharose CL 2B are shown in in Figure 2.6 and Figure 2.7, respectively. WBS grown under both diurnal and constant light conditions displayed a single peak eluting at the void volume, with the diurnal sample displaying a slightly broader size distribution. λ_{max} was similar under diurnal and constant light growing conditions (approximately 540 nm). When WBS was treated with β-amylase, which cleaves successive maltose units from the non-reducing ends of glucan polymers until a branch point is reached, the size of the residual β-limit dextrin (β -LD), as well as the quantity of maltose produced, can be determined. The β-LD profile of diurnal and constant light WBS was comparable as the size of the β-LD remained very large and was eluted at the void volume. In addition, similar quantities of maltose were produced (approximately 63 wt%), which was seen as a peak at the total volume of the gel. The λ_{max} of the β-LD of WBS was similar to that of the original WBS (i.e. 540 nm regardless light conditions). NBS displayed a bimodal molecular size distribution profile, which also was similar regardless the light conditions (Figure 2.7). Amylopectin components of NBS, which were eluted at or near the void volume, exhibited similar λ_{max} (approximately 560 nm) regardless of lighting regime. Interestingly, the λ_{max} of the NBS amylopectin was greater than the WBS amylopectin component, indicating an altered relationship between amylopectin glucan chains and iodine between the two barley varieties. The larger amylose components of NBS, which eluted following the amylopectin peak, displayed similar λ_{max} values independent of lighting conditions during growth. However, constant light NBS maintained greater λ_{max} values than diurnal NBS for the smaller amylose components eluting between fractions

47-59. Similar quantities of maltose were produced following the addition of β-amylase to NBS (approximately 41 wt%) regardless the lighting regime. As for WBS, the λ_{max} values of the β-LD of the NBS amylopectin were similar under the two lighting regimes. However, the λ_{max} of the β-LD of branched amylose components, which eluted after fraction 35, were slightly higher in constant light NBS than in diurnal NBS.

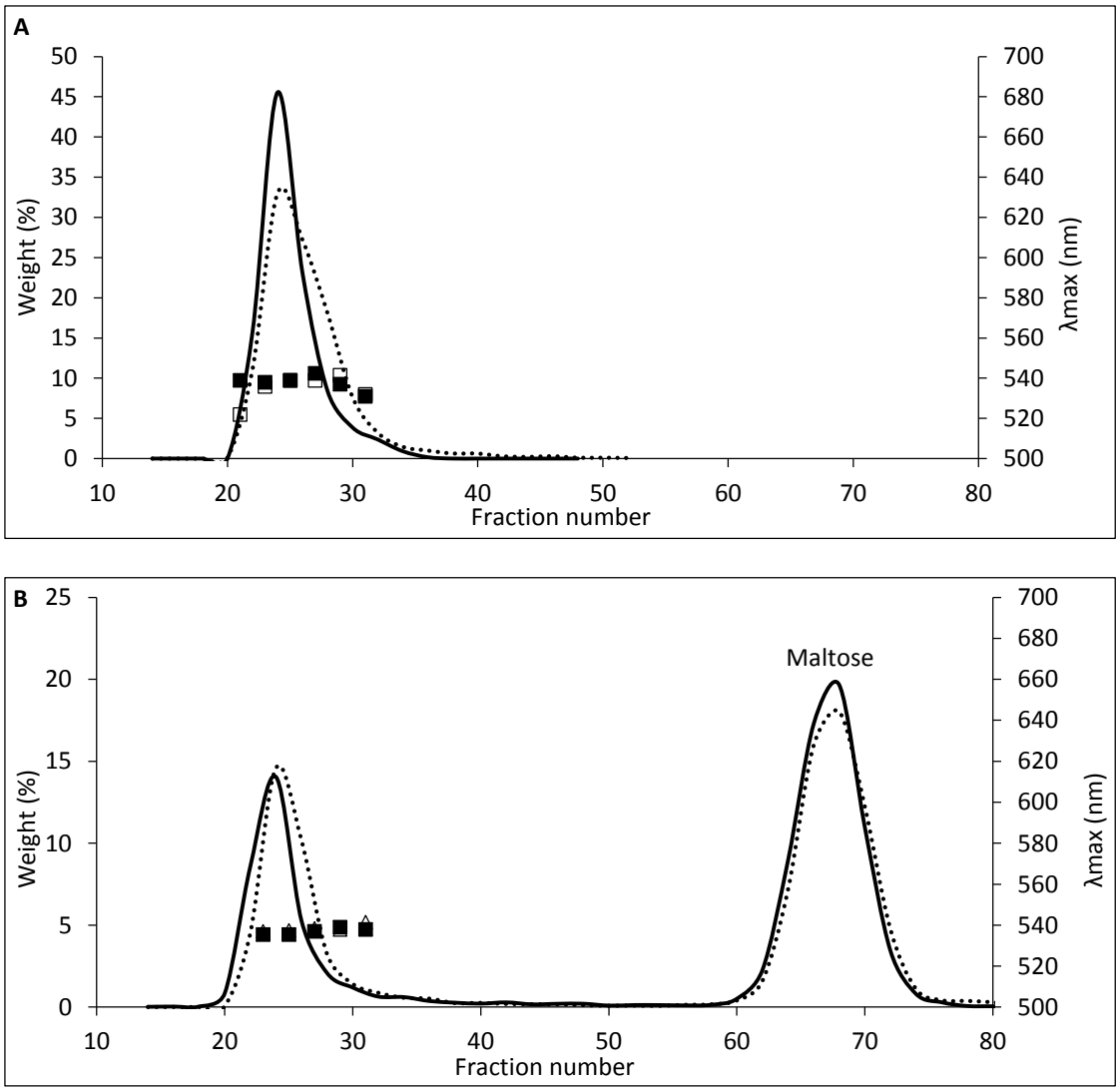

Figure 2.6: Molecular size distribution of native (A) and β-amylase treated WBS (B) grown under diurnal (……) and constant light conditions (—) determined by GPC on Sepharose CL 2B, with corresponding λ_{max} for diurnal (□) and constant light (■) conditions.

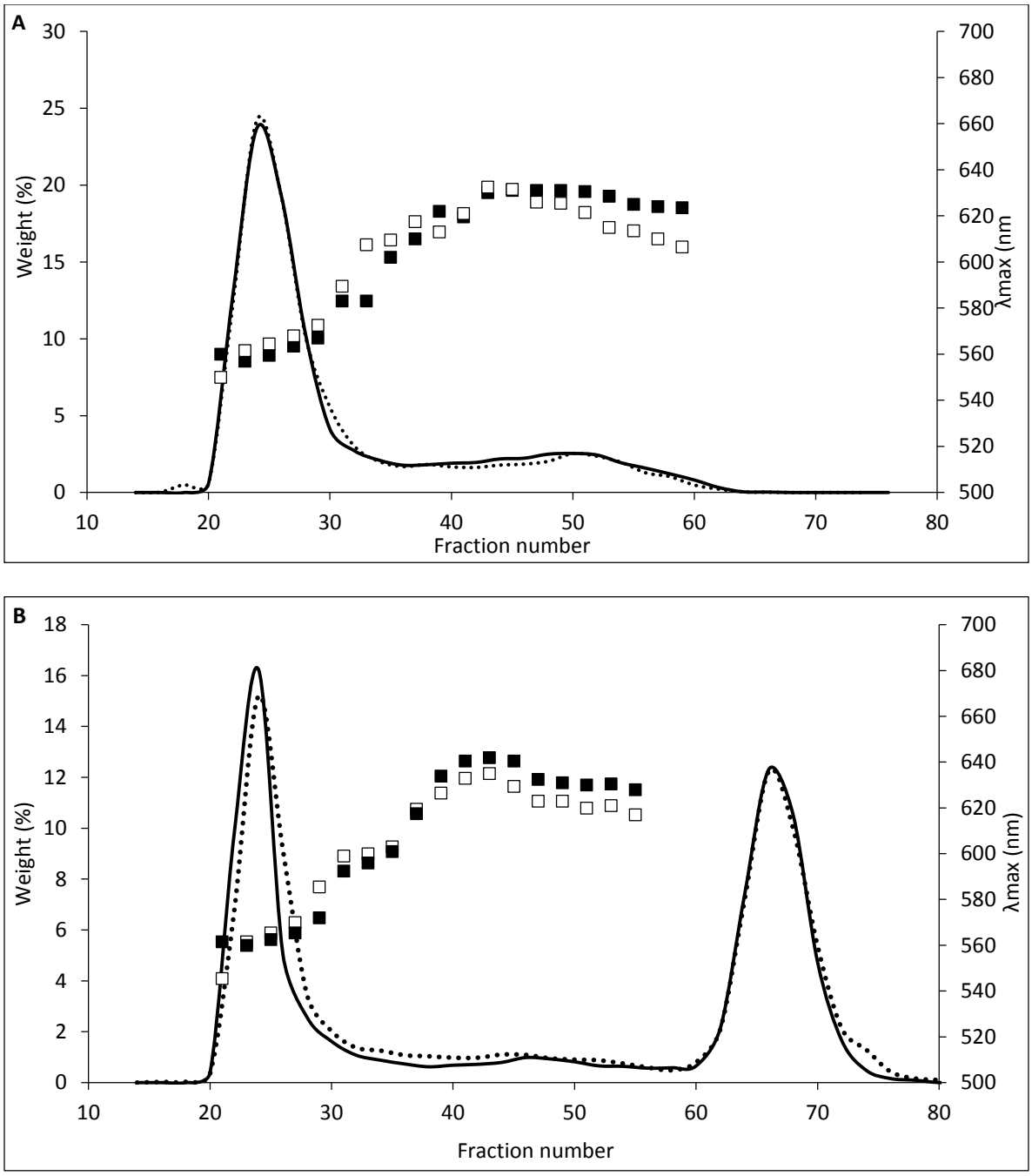

Figure 2.7: Molecular size distribution of native (A) and β-amylase treated NBS (B) grown under diurnal (……) and constant light conditions (—) determined by GPC on Sepharose CL 2B, with corresponding λ_{max} for diurnal (□) and constant light (■) conditions.

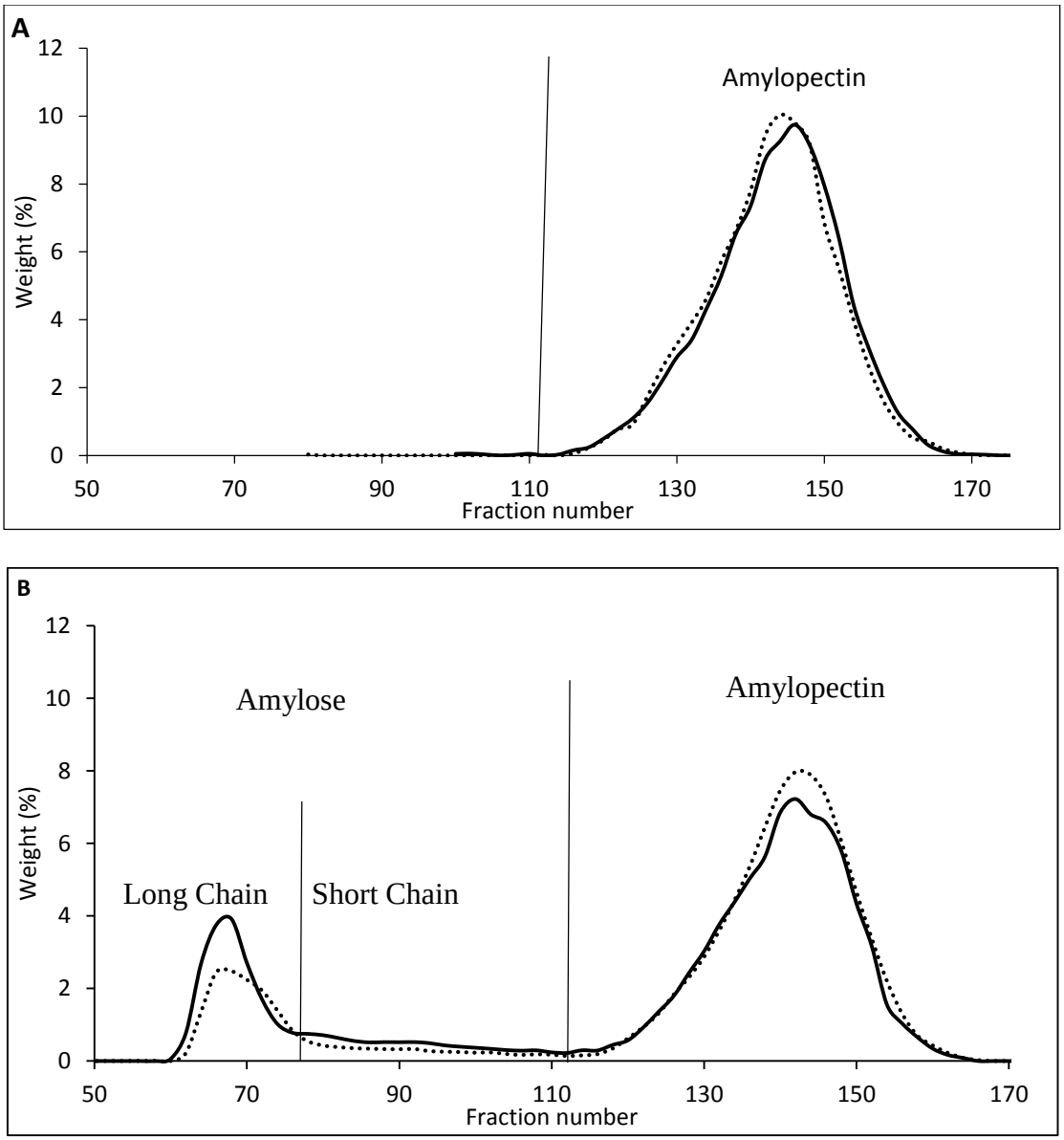

Figure 2.8: Debranched profiles of diurnal (……) and constant light conditions (—) cultivated WBS (A) and NBS (B) determined by GPC on Sepharose CL 6B.

Following the addition of isoamylase and pullulanase, which hydrolyze α-(1,6)-glucosidic linkages present in starch, the size distribution of the debranched components were determined by GPC on a column of Sepharose CL 6B (Figure 2.8). In this analysis, the long chains of amylose eluted in the early fractions, followed by the elution of the shorter amylopectin chains in later fractions. The chain length distribution of WBS

appeared similar when grown under the two lighting regimes, and the same was true for the amylopectin component in NBS. However, the apparent amylose content of NBS markedly increased from 18.7% when grown under diurnal conditions to 23.1% when grown under constant light conditions (Table 2.2). The molecular structure of the amylose component was also altered by the lighting conditions as the ratio of long chains:short chains decreased from 4.2 in NBS cultivated under constant light to 2.7 when grown diurnally, indicating that the diurnal cycle influences the structure and composition of NBS granules.

Table 2.2: Amylose and amylopectin content of WBS and NBS cultivated under diurnal or constant light conditions[1].

	Apparent Amylose (%)	Long chain amylose: short chain amylose ratio	Amylopectin (%)
Diurnal WBS	0	-	100[c]
Constant Light WBS	0	-	100[c]
Diurnal NBS	18.7[a]	2.7[a]	81.3[b]
Constant Light NBS	23.1[b]	4.2[b]	76.9[a]

[1]Values with same letters are not significantly ($p < 0.05$) different.

Discussion

The occurrence of growth rings irrespective of diurnal or constant light growing conditions (Figure 2.1 and 2.3) may indicate the growth ring formation is not controlled by diurnal photosynthetic activity. It is not clear why growth rings were observed in barley starch cultivated under constant light in this study, but not observed in barleys

cultivated under constant light conditions by Tester et al. (1991) and Buttrose (1960). One complicating factors is that previous studies on diurnal photosynthetic activity and constant light conditions utilized different light sources for plant illumination as Bakhuyzen (1925), and Buttrose et al. (1960) used mercury lamps, Tester et al. (1991) used either mercury or sodium lamps, and Pilling and Smith (2003) used an unspecified light source. In this investigation mercury lamps were used and it remains thus unclear how the light source, or the intensity of illumination, influences the appearance of growth rings. Structural analysis of NBS indicated that under constant light growing conditions the concentration of amylose increased (Table 2.2 and Figure 2.8). Jenkins and Donald (1995) postulated that increasing amylose content corresponds to an increased size of the crystalline lamellae and a corresponding decreased size of the amorphous lamellae, as amylose acts to disrupt the packing of amylopectin double helices. Therefore, as amylose apparently influences the organization of the amorphous and crystalline lamellae, and one semi-crystalline growth ring may contain a zone of ~10 lamellar repeats (Pilling and Smith, 2003) followed by an amorphous growth ring, it is a possibility that the altered organization of lamellae due to increased amylose may interfere with the contrast of semi-crystalline and amorphous rings, making them difficult to decipher without treatment with enzymes or dilute acid. In this study, growth rings present in NBS were not readily visible in their native state, and were only revealed following treatment with dilute (2.2M) HCl. Similarly, Pilling and Smith (2003) treated cracked starch granules with α-amylase from porcine pancreas to reveal the presence of growth rings in potato starch cultivated under constant light. It is important to note that certain previous studies, which reported the absence of growth rings under continuous illumination conditions

(Van De Sande-Bakhuyzen, 1926, Tester et al., 1991), did not treat the granules with acids or enzymes prior to visualization.

The structural properties of amylose were postulated to influence the appearance of growth rings in NBS when viewed by CLSM, as amylose is a smaller molecule in relation to amylopectin and therefore contains a greater molar ratio of reducing ends per anhydrous glucose residue, resulting in a greater amount of fluorescent labelling by weight compared to amylopectin (Blennow et al., 2003). The presence of alternating light and dark growth rings observed in NBS by CLSM analysis (Figure 2.3) can therefore be rationalized as the greater quantitative binding of the fluorescent probe by the amylose component compared to amylopectin, and the supposedly predominant deposition of amylose in the amorphous growth rings (Montgomery and Senti, 1958) compared to the semi-crystalline growth rings composed mainly of amylopectin. However, there are conflicting views on the location of amylose within the starch granule as Blennow et al. (2003) found a high concentration of amylose in the center of the granule, which was supported in this analysis as normal barley starch displayed strong fluorescence in the hilum (Figure 2.3), whereas Jane and Shen (1993) postulated that amylose components were more concentrated at the periphery of the granule than in the core following chemical gelatinization of normal potato starch with calcium chloride (which chemically gelatinized starch starting at the periphery). As WBS is devoid of amylose (Table 2.2), the appearance of growth rings in WBS cannot be explained by the greater fluorescent label binding by weight of the amylose component, and rather, must be explained by differences in fluorescent label binding by the amylopectin component. It is therefore postulated that the alteration of higher and lower fluorescent rings in WBS may be due to

the fluorescent labelling of low and high molecular weight amylopectin components, respectively, located in the amorphous and semi-crystalline growth rings.

Alternative explanations for the occurrence of growth rings in all samples regardless of lighting conditions include circadian rhythms and physical mechanisms (Pilling and Smith, 2003). Circadian rhythms may influence the appearance of growth rings through the periodic regulation of starch synthesizing enzymes such as granule bound starch synthase and starch synthase III, which have been shown to directly influence the presence of growth rings (Pilling and Smith, 2003). Growth ring formation may also be influenced by physical restraints as it is hypothesized that during the packing of double helices from adjacent external amylopectin chains, it may become energetically unfavorable to continue synthesizing crystalline components, resulting in a generation of amorphous components (Pilling and Smith, 2003). The generation of amorphous component may then relieve any stresses induced on the matrix and allowing for the granule to synthesize new semi-crystalline areas (Pilling and Smith, 2003).

The physical and thermal characteristics of NBS and WBS were determined by X-ray diffraction (Figure 2.4) and DSC analysis (Figure 2.5), respectively. Diurnal or constant lighting regimes did not influence the diffraction patterns of NBS. The elevated amylose content (+4.4%), and consequently lower amylopectin content in NBS exposed to constant light did not appear to have an impact on the relative crystallinity. This observation supported findings reported elsewhere wherein similar differences in apparent amylose content of normal barley starch did not have a noticeable influence on the relative crystallinity (Waduge et al., 2006). While the relative crystallinity determined by WAXS provides an indication of the percentage of crystallinity with respect to the

total material (Lopez-Rubio et al., 2008), the DSC endotherm obtained during the gelatinization of starch provides information on the quality and organization of the crystalline lamella (Vamadevan et al., 2013). The lower onset and peak melting temperatures of diurnally grown NBS can be interpreted that the starch was of lower crystalline quality than NBS cultivated under constant light conditions, as it has been suggested that the peak melting temperature represents a measure of starch crystalline perfection (Tester and Morrison, 1990). The lower enthalpy values of the diurnally grown NBS indicated that a lower quantity of double helices was synthesized compared to constant lighting conditions.

When considering WBS, it was interesting to observe the substantial drop in relative crystallinity of the constant light samples compared to the diurnally grown sample. The presence of the V-type crystal polymorph in WBS, which is typically associated with amylose-lipid complexes, was surprising, although its presence has been reported in other waxy barley starches, with the complex postulated to be formed between the outer branches of amylopectin and native lipids (Waduge et al., 2006).Within the literature there are numerous reports citing the relationship between lower relative crystallinity and lower onset gelatinization temperatures (Vamadevan et al., 2013, Gomand et al., 2010b, Vandeputte et al., 2003), and indeed, that relationship was also observed for WBS in this analysis. It has been suggested by Tester et al. (2001) that the crystalline lamellae restricts the hydration of amorphous regions. Therefore, a higher relative crystallinity might imply that the amorphous region hydrates less readily resulting in a delayed initiation of swelling and gelatinization (Vandeputte et al., 2003). The fact that the enthalpy remained similar between diurnal and constant light exposed

WBS implied that a similar quantity of double helices were synthesized, although in constant light growing conditions a population of those helices may have been disoriented (unpacked) or the ordering at the ends of existing double helices were unpacked in the crystallites (Kozlov et al., 2007).

The molecular size distribution of WBS (Figure 2.6) did not appear to be largely impacted when grown under constant lighting conditions compared to diurnal conditions. When the native starch was analyzed by GPC on Sepharose CL 2B, similar elution patterns were observed with the entire sample eluting at the void volume of the gel. In addition, when the granules were treated with β-amylase to produce β-LDs, a similar quantity of remaining internal components was observed. The similar quantities of maltose produce independent of lighting regime may be indicative of a similar proportion of external chains independent of growing conditions. Moreover, similar λ_{max} values were observed for WBS and its β-LDs regardless the light conditions. It has been reported that the nature of the iodine inclusion complex with glucan polymers is dependent on the availability of glucan polymers to bind with iodine (Banks et al., 1971). Greater λ_{max} values correlate with the length of the glucan chain, which formed the complex. Amylopectin may interact with iodine to form inclusion complexes with either the external amylopectin chains, or the internal amylopectin chains involved in the connection of clusters (Kalinga et al., 2013). The observed WBS λ_{max} values implied that the nature of the complex-forming segments in the external and/or internal parts of the macromolecule were similar and independent of the light conditions.

The β-limit value of WBS (~61 wt%) was greater than that of NBS (42 wt%), implying that the structure of the branched amylose component influenced the quantity of

maltose produced by β-amylase. Like WBS, NBS displayed a similar molecular size distribution profile and λ_{max} values independent of growing conditions (Figure 2.7), although under constant light the λ_{max} values for smaller amylose molecules, (fractions 49-59) were higher. These differences in λ_{max} values suggested that the amylose component, but not the amylopectin, was affected by the lighting conditions. The differences in λ_{max} values of the amylose component complement and support the different size distribution profiles of debranched NBS when studied by GPC on Sepharose CL 6B (Figure 2.8). NBS cultivated under constant light conditions exhibited an increased amylose content, as well as an increased ratio of long:short amylose chains (Table 2.2) compared to diurnal NBS. Considering these differences, one may infer that diurnal photosynthetic activity influences the structure of the amylose component.

NBS grown under constant light conditions may contain a greater concentration of ADP-glucose in the plastid compared to the diurnal sample due to continually ongoing photosynthesis. Clarke et al. (1999) reported that the rate of starch synthesis and the amylose:amylopectin ratio is correlated with the concentration of ADP-glucose in developing pea embryos. It is broadly agreed that the affinity of granule bound starch synthase I (GBSSI), a key enzyme involved in the synthesis of amylose, for ADP-glucose is lower than that of the key amylopectin synthesizing enzyme soluble starch synthase (Clarke et al., 1999). Therefore, an increase in ADP-glucose will potentially increase the amylose:amylopectin ratio. As the concentration of ADP-glucose in NBS grown under constant light conditions may be greater than that of diurnally grown NBS, the increased amylose content may align with expectations of Clarke and colleagues.

Conclusion

The observation of growth rings in all samples could not confirm earlier reports of the absence of growth rings in barley starch cultivated under constant light, and disproves the notion that growth rings in barley starch are due to diurnal photosynthetic rhythms. The decreased amylose content, decreased long:short chain ratio of amylose components, and altered gelatinization profiles obtained from NBS cultivated under diurnal conditions compared to constant light conditions provide direct evidence that diurnal photosynthetic activity influences the structure and organization of NBS yielding altered thermal profiles. The greater relative crystallinity and higher melting temperatures of diurnally grown WBS implies that the diurnal photosynthetic activity facilitates a greater amount of crystalline registration and perfection in the waxy variety, while for NBS the relative crystallinity is not largely influenced by light conditions, but the crystalline order was influenced by diurnal photosynthetic activity. As WBS, but not NBS, lacks GBSS activity, it appears that diurnal photosynthetic activity influences barley differently based on its enzyme composition.

Chapter 3: Effect of diurnal photosynthetic activity on the fine structure of amylopectin from normal and waxy barley starch.

Summary

In this study, the impact of diurnal photosynthetic activity on the fine structure of amylopectin from normal barley (NBS) and waxy barley (WBS) starches was determined following the cultivation of barley in a greenhouse under normal diurnal or constant light growing conditions. Amylopectin fine structure was investigated by characterizing whole amylopectin and its φ,β-limit dextrins, as well as its clusters and building blocks after their partial and complete hydrolysis with α-amylase from *Bacillus amyloliquefaciens,* respectively. Similar average chain lengths for the unit and internal chains of amylopectin of NBS and WBS were observed when determined by anion-exchange chromatography regardless of lighting conditions. Clusters of amylopectin from diurnally grown NBS and WBS contained larger average chain lengths, and were larger compared to clusters of amylopectin grown under constant light conditions. Diurnally grown clusters from NBS and WBS also contained a greater number of building blocks, and shorter inter-block chain lengths compared to clusters grown under constant light. These results indicate that diurnal photosynthetic activity influenced the fine structure of the amylopectin component of NBS and WBS.

Introduction

Starch is the major storage polysaccharide in a vast range of photosynthetic organisms. It is found in insoluble, semi-crystalline granular form of varying sizes (~0.1-200 μm),

depending on botanical origin (Pérez and Bertoft, 2010). The major constituents of starch are amylose and amylopectin. Amylose is an essentially linear polysaccharide composed of α-(1,4)-linked D-glucosyl units, comprising 20-35% of the granules in most plants, whereas amylopectin is a branched macromolecule containing α-(1,4)-linked D-glucosyl chains and ~5% α-(1,6)-linkages.

The synthesis of starch in the endosperm of higher plants is controlled by various enzymes in four key steps (Morell et al., 2003). The four steps involve the synthesis of ADP-glucose, the monomer precursor of starch, from glucose 1-phosphate and ATP by the enzyme ADPglucose pyrophosphorylase. ADP-glucose is then transferred to the non-reducing end of an already present glucose residue by one of several isoforms of starch synthase enzymes. Starch branching enzymes then act to introduce branch points by cleaving α-(1,4)-linked glucans and transferring them to an acceptor chain, forming α-(1,6)-linkages (Morell et al., 2003). Finally, starch debranching enzymes play a role in the synthesis of starch, as they facilitate the formation of water-insoluble, semi-crystalline polymers (Smith, 2012). Smith et al. (2004) investigated the diurnal changes in the expression patterns of genes encoding enzymes involved in starch synthesis, and reported that the transcription encoding of two starch synthases, granule bound starch synthase and starch synthase II, increased appreciably during the transition from dark to light.

Photosynthetic plants produce the necessary substrates required to synthesize starch by the conversion of light energy, carbon dioxide, and water into carbohydrates and oxygen through a complex interplay of light dependent and light independent reactions (Whatley et al., 1963). In 1895, Meyer postulated that the presence of alternating layers of increasing/decreasing levels of crystallinity, commonly referred to as

growth rings, which is a universal feature present in starch granules from differing botanical origins, is the result of diurnal activity. This hypothesis was supported by Van De Sande-Bakhuyzen (1926) and Buttrose (1960) wherein no growth rings were observed in wheat and barley starch, which was cultivated under constant light growing conditions. Recently, in an unexpected observation, growth rings were observed in starch from normal and waxy varieties of barley when grown under constant light conditions as viewed by light and confocal microscopy (Chapter 2). However, it was also observed that the molecular structure and gelatinization properties of normal barley starch was influenced by diurnal photosynthetic activity, as normal barley starch grown under constant light contained increased amylose content, as well as an increased ratio of long amylose chains:short amylose chains, and higher onset and peak gelatinization temperatures compared to normal barley starch cultivated under diurnal conditions (Chapter 2). The crystallinity and thermal properties of waxy barley starch was also influenced by diurnal photosynthetic activity (Chapter 2). Whereas this previous report suggested diurnal photosynthetic activity influences the molecular composition and physical properties of barley starch, its impact on the fine structure of the amylopectin component has not been determined.

Amylopectin contains a variety of structural elements, which can be elucidated by treatments with various debranching, exo-acting, and endo-acting enzymes (Bertoft, 2013). The most studied structural element of amylopectin, the unit chain profile, can be analyzed by the addition of debranching enzymes, such as isoamylase and pullulanase, which hydrolyze α-(1,6)-linkages allowing for analysis of the chain length distribution of glucan chains. The two main categories of chains identified in most samples are long (DP

> 36) and short (DP < 36) chains. The external chains of amylopectin are found in crystalline regions of the molecule, whereas the internal chains, containing numerous branch points, are considered to be in the amorphous regions. If amylopectin is successively treated with phosphorylase *a* and β-amylase, a φ,β-limit dextrin is obtained wherein all the external segments of B-chains (chains substituted with other chains) and the external A-chains (unsubstituted chains) are converted to glucosyl and maltosyl stubs, respectively (Bertoft, 1989). The chains of the φ,β-limit dextrin can be analyzed quantitatively to determine the chain length distribution of internal amylopectin components.

Clusters of amylopectin, which are defined as groups of short chains with an internal chain length < 9 (Bertoft, 2007), are important structural elements in the amylopectin molecule. They can be isolated via the partial hydrolysis of amylopectin with α-amylase from *Bacillus amyloliquefaciens* (Bertoft, 2013). Clusters can be isolated following a time course α-amylolysis, stopping the enzymatic reaction when the reaction rate slows down. The φ,β-limit dextrin of isolated clusters can then be obtained following treatment with phosphorylase *a* and β-amylase, allowing for analysis of important cluster structural parameters. During the preparation of clusters new chains are formed and released from amylopectin by the α-amylase and, therefore, chains in isolated clusters are designated with lowercase letters (a-chains and b-chains) to differentiate from the chain categories in the whole amylopectin (Bertoft et al., 2012b). The unit chain profiles of isolated clusters determined following debranching provides valuable insight on the composition of clusters. In the φ,β-limit dextrin of clusters, the majority of a-chains are maltosyl stubs, with a lower amount of a-chains being maltotriosyl stubs, as a small

number of very short a-chains produced by the α-amylase are not attacked by either phosphorylase or β-amylase (Bertoft, 2007). The different categories of b-chains in clusters are directly related to the number of inter-block segments (IB-S) they are involved in, wherein b0-chains (DP 4-6) lack IB-S, b1-chains (subdivided into b1a and b1b with DP 7-10 and 11-18, respectively) are involved in one IB-S, b2-chains (DP 19-27) are involved in two IB-S, and b3-chains (DP ≥ 28) are involved in three IB-S (Bertoft et al., 2012b). Building blocks inside clusters can be isolated following extensive α-amylolysis using the same α-amylase of *B. amyloliquefaciens* at higher concentration, yielding linear or branched α-limit dextrins which are the basic structural units of amylopectin according to the 'building block backbone model', which has been described extensively elsewhere (Bertoft, 2013). Building blocks can be classified into different groups dependent on their size. The smallest building blocks (DP 5-9) generally are singly branched (i.e. consist of two chains) and are named group 2 building blocks. Building blocks containing three chains (DP 10-14) are referred to as group 3 building blocks, whereas group 4 building blocks (DP 15-19) possess 4 chains. Group 5 building blocks have been reported to contain a more complicated mixture of α-limit dextrins containing between 5-7 chains (DP 20-35), while group 6 building blocks (DP > 35) contain an average of 10-12 chains (Bertoft, 2015).

As barley was utilized in previous studies to investigate the role of diurnal photosynthetic activity on the presence of growth rings, it was selected for this study to compliment previous systems studied in the literature. The objective of this study was to investigate the influence of diurnal photosynthetic activity on the structure of amylopectin components such as unit chains, clusters, and building blocks. Knowledge

generated from this study will allow for a greater understanding of the influence of diurnal photosynthetic activity on the fine structure of amylopectin in waxy and normal barley starch.

Materials and methods

Materials

Waxy barley starch (WBS, Cinnamon variety) and normal barley starch (NBS, Golden Promise variety) were cultivated as previously described in Chapter 2. Briefly, barley was grown under diurnal or constant light conditions in a greenhouse located at the University of Copenhagen (Copenhagen, Denmark). Constant light conditions were maintained by illuminating barley plants under constant artificial light using mercury lamps for 3 months from planting to maturation. Constant light samples were shielded from natural sunlight. Diurnal samples were grown under ambient conditions, with supporting illumination from 4 am-8 pm. No significant differences in the rate of maturity were observed between the two lighting regimes.

Starch extraction and amylopectin fractionation

Barley starch was extracted according to the method of Carciofi et al. (2011) with modifications to the procedure reported in Chapter 2. Amylopectin was fractionated from NBS according to the method of Klucinec and Thompson (1998) with modifications reported by Annor et al. (2014). Purity of fractionated amylopectin was verified by gel

permeation chromatography (GPC) on a column of Sepharose CL 6B after debranching with isoamylase and pullulanase as described by Laohaphatanaleart et al. (2010).

Production of φ,β-limit dextrins from amylopectin

φ,β-Limit dextrins from amylopectin were produced according to the method of Laohaphatanaleart et al. (2010). Briefly, amylopectin was dissolved in of dimethyl sulfoxide (DMSO) by gentle stirring overnight. The amylopectin sample was treated twice with phosphorylase *a*, followed by two β-amylase treatments. Following each enzyme treatment, the products glucose 1-phosphate (from phosphorylase *a*) and maltose (from β-amylase), respectively, were removed via tangential flow filtration using a membrane with a molecular weight cut off of 10 000 Da (Minimate^{TM} TFF system, Canton, MA, USA). Following the final filtration, the φ,β-limit dextrins were recovered and freeze-dried.

Cluster isolation and production of their φ,β-limit dextrins

Clusters from barley amylopectin were isolated following α-amylolysis (120 min) with α-amylase from *Bacillus amyloliquefaciens* (0.09 U/mL) at 25 °C according to method reported by Kong et al. (2009). φ,β-Limit dextrins of the isolated clusters were produced as described for amylopectin above, however, the products glucose 1-phosphate or maltose were removed from the clusters via GPC through two coupled PD-10 columns (GE Healthcare Life Sciences, NJ, USA) (Kong et al., 2009). The resulting φ,β-limit dextrins of clusters were freeze dried and their size distribution was determined by GPC on a column of Sepharose CL 6B (GE Healthcare, Uppsala, Sweden) as described by

Bertoft (2007). The column was calibrated with branched dextrins of known DP as described by Bertoft and Spoof (1989).

Analysis of the unit chain distribution

The composition of chains of amylopectin, and of φ,β-limit dextrins of amylopectin and clusters, were studied according to the methods of Bertoft et al. (2008). In short, amylopectin or φ,β-limit dextrins were debranched overnight by a combination of isoamylase and pullulanase. Following boiling in hot water to deactivate enzymes and filtration with a 0.45 µm nylon filter, the sample was analysed by high-performance anion-exchange chromatography (HPAEC) with a Dionex ICS 5000^{+} system (Dionex Corporation, Sunnyvale, CA, USA) containing a CarboPac PA-100 ion-exchange column (4 x 250 mm) and accompanying guard column (4 x 50 mm) coupled with a pulsed amperometric detector (PAD). An eluent gradient was utilized using a combination of 150 mM sodium hydroxide (Eluent A) and 150 mM sodium hydroxide containing 0.5 M sodium acetate (Eluent B) as described elsewhere (Bertoft et al., 2008). Areas under peaks were corrected to carbohydrate concentration according to Koch et al. (1998).

Building block preparation and structural analysis

Building blocks were isolated from clusters according to methods reported by Bertoft et al. (2012b). The size distribution of building blocks was analyzed with a column (1.6 x 90 cm) of Superdex 30 (GE Healthcare Life Sciences, NJ, USA) as reported by Kalinga et al. (2014). The column was calibrated using commercial dextrins (Sigma-Aldrich, St. Louis, MO, USA) of known degree of polymerization (DP 1-7) and with larger, branched α-dextrins of known DP (Bertoft and Spoof, 1989). The size and chain length distribution

of building blocks were determined as reported by Bertoft et al. (2012b) with the same HPAEC equipment described above, but with a different eluent gradient for building block analysis.

Statistical analysis

All analyses were conducted in duplicate and analyzed using SPSS (IBM Corporation, Armonk, NY, USA). Significant differences were determined by comparing means by Tukey's test at a significance level of $p < 0.05$.

Results

Unit chain profile of amylopectin

The unit chain profile of amylopectin may be distinguished into different chain categories, which provide robust insight into the structure of the amylopectin component. Two major groups of chains are short (DP 6-36) and long (DP > 37) chains, which are distinguished from each other by a groove position at ~DP 36 depending on the sample. A comparison of the amylopectin unit chain profiles of normal barley starch (NBS) and waxy barley starch (WBS) grown under diurnal or constant light conditions are seen in Figure 3.1. The chain distribution profiles of amylopectin from NBS and WBS appeared to be similar regardless the lighting conditions, exhibiting similar peak (DP 12) and groove positions for all samples analyzed. Small differences in the quantities of short chains at DP 13-14 and at DP 18-19 were observed in NBS under the different growing conditions.

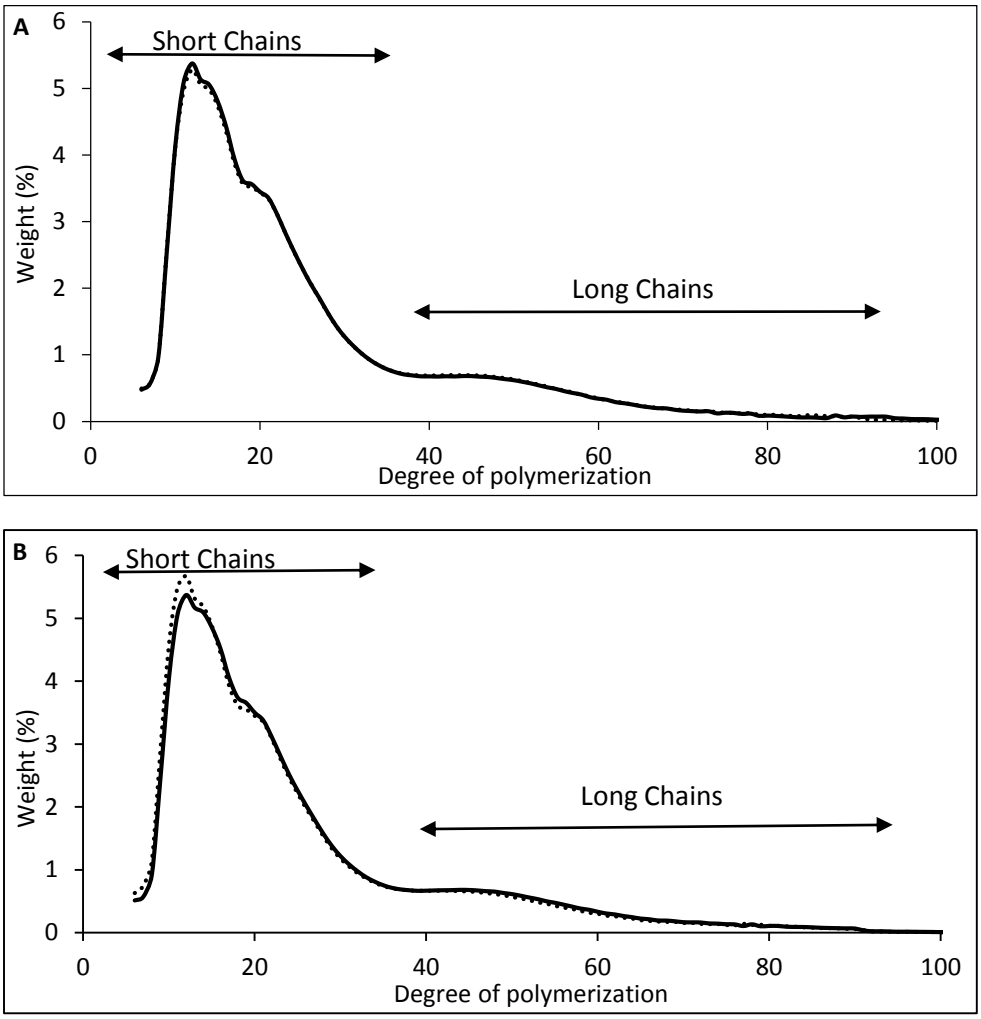

Figure 3.1: Unit chain profile of amylopectin from WBS (A) and NBS (B) cultivated under diurnal (-----) or constant light (——) conditions.

The internal chain profile of φ,β-limit dextrins from NBS and WBS cultivated under constant light or diurnal conditions is shown in Figure 3.2. The lighting regime did not appear to influence the internal unit chain distribution of NBS, as the two chain distributions overlapped each other. However, the internal chain profile of WBS amylopectin, particularly in the short chain region, did appear to be influenced as the

location of the groove position distinguishing the separation between short B-chains and long B-chains was slightly different under constant or diurnal light conditions.

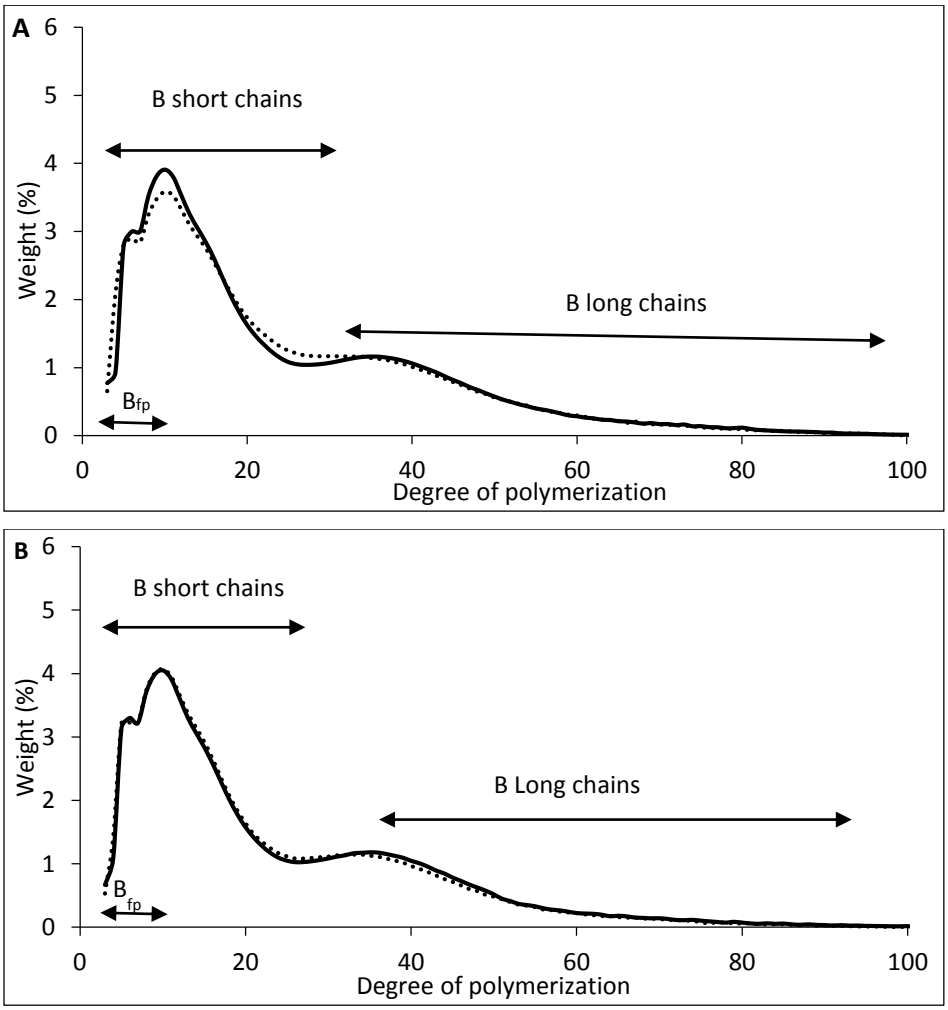

Figure 3.2: Unit chain profile of φ,β-limit dextrins of amylopectin from WBS (A) and NBS (B) cultivated under normal diurnal (-----) or constant light (——) conditions. Arrows indicate regions of fingerprint B-chains (B_{fp}), short B-chains, and long B-chains.

In addition, differences in the elution profile of 'fingerprint' B_{fp}-chains (DP 3-7), which are the shortest chains and appear to be specific for each plant (hence 'fingerprint' chains) (Bertoft et al., 2008), and BS_{major} chains (DP 8-27) (Bertoft et al., 2008) were observed in the φ,β-limit dextrins from WBS barley grown under different illumination conditions.

Table 3.1: Average chain length of various chain segments and φ,β-limit value of barley amylopectin[1]

Sample	CL	SCL	LCL	ECL	ICL	TICL	CL_{LD}	BS-CL_{LD}	BL-CL_{LD}	φ,β-limit value
Diurnal WBS	18.3^{b}	15.8^{b}	51.5^{bc}	11.8^{a}	5.5^{b}	13.9^{b}	8.0^{b}	9.9^{a}	40.3^{a}	56.2^{b}
Constant Light WBS	17.9^{ab}	15.7^{ab}	50.9^{ab}	11.3^{a}	5.5^{b}	13.1^{b}	8.0^{b}	10.0^{a}	40.7^{a}	54.9^{a}
Diurnal NBS	17.6^{a}	15.4^{a}	50.9^{a}	11.5^{a}	5.1^{a}	12.3^{a}	7.5^{a}	9.9^{a}	39.8^{a}	56.9^{a}
Constant Light NBS	18.2^{ab}	15.8^{b}	51.6^{c}	11.8^{a}	5.3^{ab}	12.7^{ab}	7.8^{ab}	9.9^{a}	40.0^{a}	56.9^{a}

[1] CL = chain length, SCL= CL of short chains, LCL = CL of long chains, ECL (external chain length) = CL × (φ,β-limit value/100) + 1.5 , ICL (internal chain length) = CL – ECL – 1, TICL (total internal chain length) = B-CL_{LD} -1 , φ,β-limit value is determined by the difference between in CL between amylopectin and its φ,β-limit dextrin, CL_{LD} = average CL of φ,β-limit dextrin, BS-CL_{LD} = CL of short B chains of φ,β-limit dextrin, BL-CL_{LD} = CL of long B chains of φ,β-limit dextrin.

Values with different letters in columns are significantly different ($p < 0.05$) from each other.

A comparison of the average chain length values of selected chain segments is shown in Table 3.1. The average chain length (CL) of amylopectin from diurnal photosynthetic NBS (17.6) was slightly lower than that of NBS grown under constant light (18.2), whereas the diurnal WBS exhibited a slightly greater CL of 18.3 compared to constant light WBS (17.9), although none of the differences were significant. The length of short (SCL) and long (LCL) chains of WBS amylopectin was similar regardless of the lighting regime. For NBS, the SCL and LCL were slightly, and significantly,

smaller in diurnal NBS compared to constant light NBS. The average φ,β-limit value, which reflects the length of external amylopectin chains, was slightly lower in WBS grown under constant light conditions (54.9) compared to diurnal conditions (56.2), whereas the φ,β-limit value was nearly identical in diurnal and constant light cultivated NBS. Non-significant differences were observed between growing conditions for the average length of the internal chains (chains between branches), total internal chains (the whole internal B-chains), and short and long B-chains of the φ,β-limit dextrins.

Table 3.2: Relative molar amounts (%) of amylopectin chain categories in NBS and WBS [1]

Sample	A chains	A_{fp}	$A_{crystal}$	B chains	B_{fp}	BS_{major}	BL
Diurnal WBS	49.8^{a}	7.1^{a}	42.3^{a}	50.2^{a}	17.5^{b}	26.7^{a}	6.0^{b}
Constant Light WBS	49.7^{a}	7.1^{a}	42.6^{a}	50.2^{a}	16.0^{a}	28.2^{b}	6.0^{b}
Diurnal NBS	50.7^{a}	7.1^{a}	43.6^{a}	49.2^{a}	16.6^{ab}	27.4^{ab}	5.1^{a}
Constant Light NBS	50.1^{a}	7.1^{a}	43.0^{a}	49.8^{a}	16.4^{a}	27.7^{b}	5.6^{b}

[1] A-chains were determined following debranching, A_{fp} = 'fingerprint' A-chains of DP 6-8 in original amylopectin, $A_{crystal}$ = A-chains – A_{fp} chains, B chains= chains with DP > 3 in φ,β-limit dextrin which are further subdivided into B_{fp} (DP 3-7), BS_{major} (DP 8-27), and BL (long B chains, DP $\geq$28) in the φ,β-limit dextrin.

Values with different letters in columns are significantly different ($p < 0.05$) from each other.

The relative molar amounts of various chain categories are shown in Table 3.2. Non-significant differences between lighting conditions were observed in NBS and WBS amylopectin for quantities of fingerprint A-chains and crystalline A-chains, which are A-

chains believed to be not long enough to participate in crystal structure formation (Gidley and Bulpin, 1987), and A-chains likely involved in crystalline formation (Annor et al., 2014), respectively. Lighting conditions did not appear to largely influence the total molar quantity of B-chains. However, when considering the sub-fractions within B-chains, the relative molar quantity of BS_{major}-chains (DP 8-27) (Table 3.2) significantly decreased from 28.2% to 26.7% when grown in diurnal conditions compared to constant light conditions. Further, the relative molar quantity of B_{fp}-chains (DP 3-7) (Table 3.2) significantly increased in diurnal WBS amylopectin (17.5%) compared to constant light WBS amylopectin (16.0%), although no change in the quantity of long B-chains (BL-chains) was observed under the different lighting regimes. Less significant differences were observed in the sub-fractions of B-chains in NBS amylopectin, as similar quantities of BS_{major}- and B_{fp}-chains were observed regardless of lighting regime. However, diurnal NBS amylopectin contained a significantly lower quantity of BL-chains (5.1%) than constant light NBS (5.6%).

Cluster structure

Clusters of amylopectin from NBS and WBS were isolated following a time course α-amylolysis with α-amylase from *B. amyloliquefaciens*. Throughout the time course analysis aliquots of sample were removed and neutralized every 20 minutes, followed by GPC analysis on Sepharose CL 6B. Changes in the molecular size distribution of barley amylopectin is shown in Figure 3.3A. The α-amylolysis pattern exhibited by amylopectin from NBS and WBS grown under diurnal or constant light conditions was similar to patterns previously reported for other starches

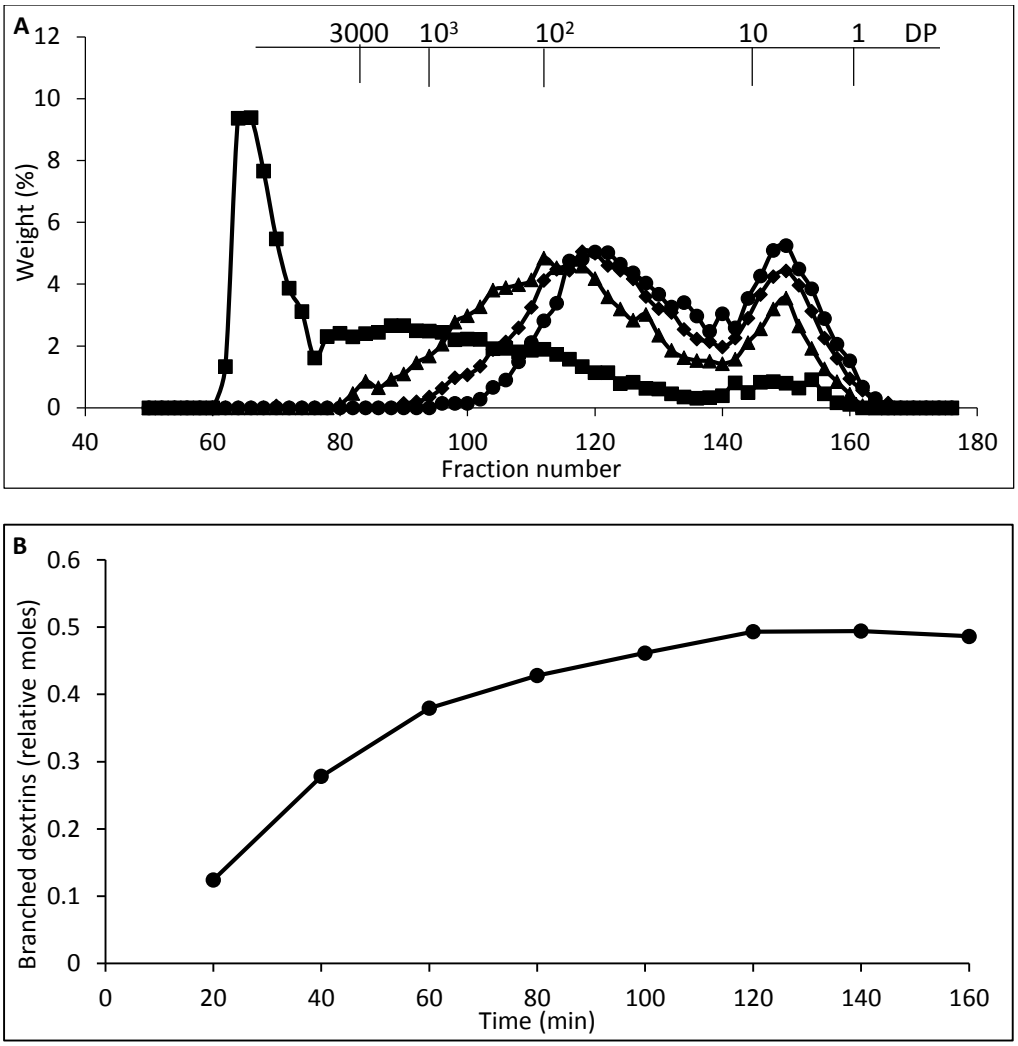

Figure 3.3: Representative time course α-amylolysis of amylopectin from NBS analyzed by GPC on Sepharose CL 6B depicting shift in size distribution of amylopectin following incubation with α-amylase from B. amyloliquefaciens at different time intervals of 20 min (■), 60 min (▲), 100 min (♦), and 140 min (●)(A) and development of branched dextrins (DP > 30) during time course α-amylolysis (B). Numbers in (A) indicate degree of polymerization.

(Kalinga et al., 2014, Zhu et al., 2015), producing groups of clusters (DP > 30) and small fragments (DP < 30) from the hydrolysis of external chains (Bertoft, 1989). The evolution of the relative number of branched dextrins with DP > 30 is shown in figure 3.3B. An initial rapid increase in branched dextrins was achieved until a plateau was

reached at 120 min. This phenomenon can be rationalized as during the early stages of the α-amylolysis reaction, the nine

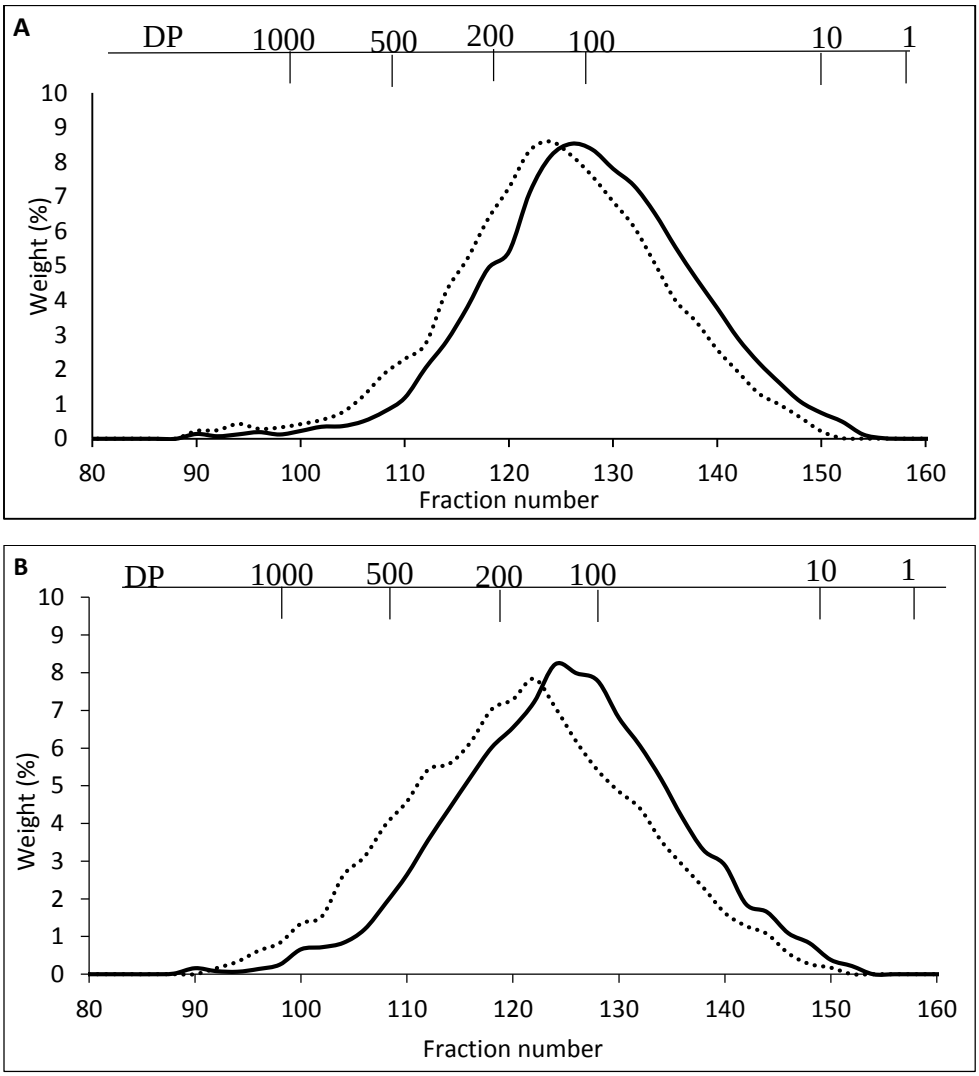

Figure 3.4: Size distribution of clusters of amylopectin from waxy (A) and normal (B) barley starch cultivated under normal diurnal (-----) or constant light (——) conditions determined by GPC on Sepharose CL 6B. Numbers indicate degree of polymerization.

subsites of the α-amylase can readily be filled with D-glucosyl units. When the enzyme can no longer fill all subsites, the reaction slows considerably. As nearly no increase of branched dextrins was observed past 120 minutes of enzyme treatment, 120 minutes was utilized for cluster preparation.

The molecular size distribution of the φ,β-limit dextrins of clusters were determined by GPC with Sepharose CL 6B (Figure 3.4). Diurnal growing conditions resulted in larger clusters for both varieties. The average DP of diurnal WBS clusters was 105.2 compared to 74.9 for constant light WBS, whereas the average DP of diurnal NBS clusters was 123.1 compared to an average DP of 93.9 for constant light NBS clusters (fractions containing < 1% carbohydrate were excluded) (Table 3.3). When the φ,β-limit dextrins of clusters were debranched, a number of other structural parameters could also be estimated (Table 3.3).

Table 3.3: Characterization of φ,β-limit dextrin of barley starch clusters[1]

Sample	DP	NC	DB(%)	CL	ICL
Diurnal WBS	105.2^{b}	16.4^{b}	14.7^{a}	6.4^{b}	4.2^{b}
Constant Light WBS	74.9^{a}	13.2^{a}	16.2^{b}	5.6^{a}	3.5^{a}
Diurnal NBS	123.1^{c}	19.5^{c}	15.0^{a}	6.3^{b}	4.0^{b}
Constant Light NBS	93.9^{b}	16.2^{b}	16.2^{b}	5.7^{a}	3.5^{a}

[1] DP= average degree of polymerization determined by GPC, NC = number of chains determined by DP/ CL, DB (degree of branching) = (NC-1)/DP×100, CL= average chains length of clusters determined by high performance anion exchange chromatography, ICL (internal chain length) = (CL – ECL)×NC/(NC-1) wherein NC-1 relates to internal chain segments and ECL is 1.5 due to action of phosphorylase and β-amylase.

Values with different letters in columns are significantly different ($p < 0.05$) from each other.

The number of chains significantly increased in both WBS and NBS when cultivated under diurnal conditions compared to constant light conditions, whereas, the degree of branching was lower in clusters grown under diurnal conditions decreasing from 19.5 to 16.2% and from 16.4 to 13.2% for NBS and WBS clusters, respectively, compared to clusters

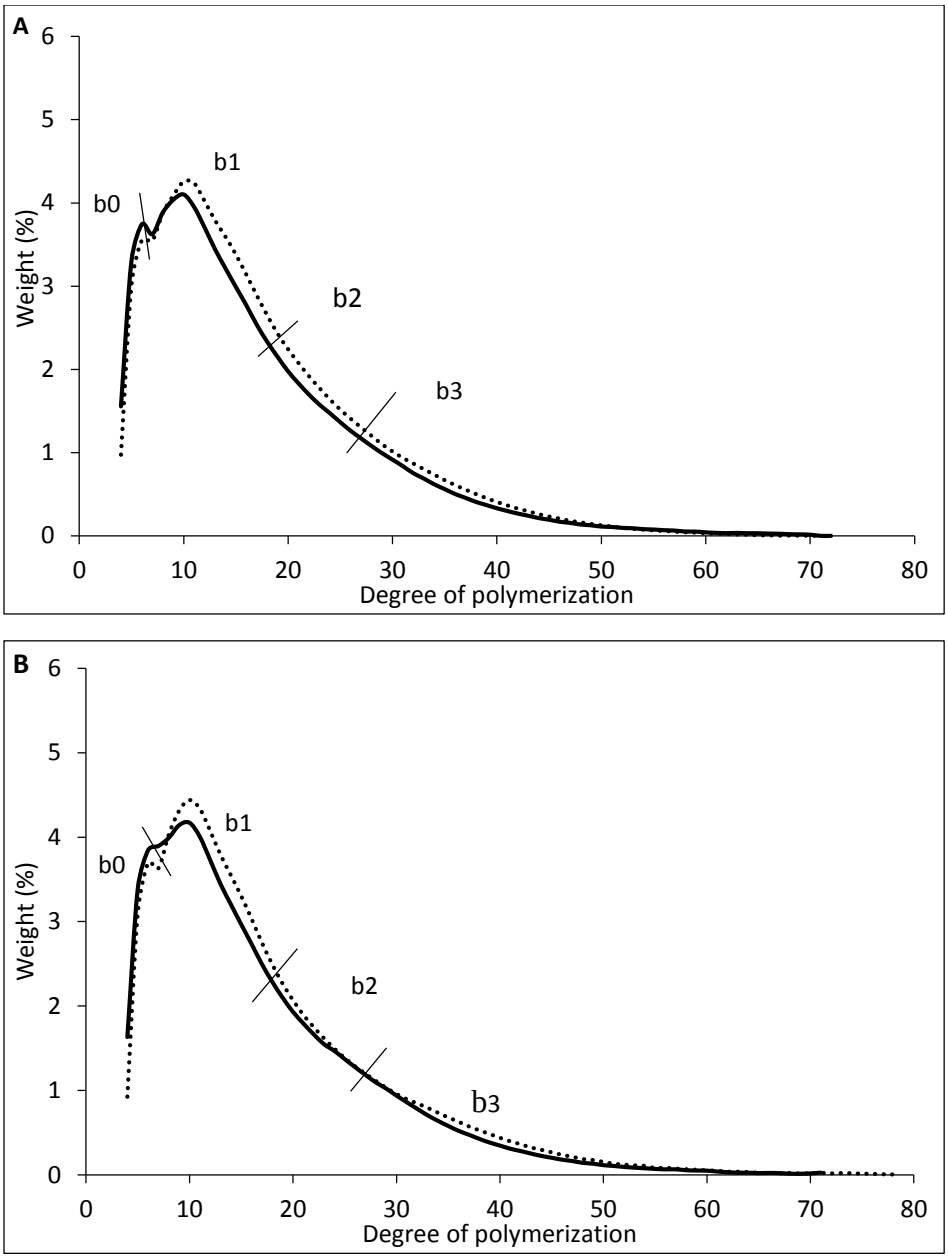

Figure 3.5: Chain length distribution of debranched φ,β-limit dextrins of clusters from WBS (A) and NBS (B) cultivated under normal diurnal (-----) or constant light (——) conditions. Chain categories of clusters are indicated.

grown under constant light conditions. The average CL of NBS and WBS clusters were higher in diurnal samples than in those cultivated under constant light, increasing from 5.6 to 6.4 and from 5.7 to 6.3, respectively. Diurnally grown clusters maintained longer

ICL increasing from 3.5 to 4.0 and from 3.5 to 4.0 for NBS and WBS amylopectin, respectively, compared to their counterparts cultivated in constant light growing conditions.

When grown under diurnal conditions, the internal chain profile of WBS clusters exhibited an increased quantity of glucan chains from DP 7 to approximately DP 29 compared to constant light WBS clusters (Figure 3.5). The internal chain profile of NBS clusters grown under diurnal conditions exhibited a similar trend. The relative molar distribution of selected chain categories of NBS and WBS amylopectin is shown in Table 3.4. In the φ,β-limit dextrins of clusters, DP 2 chains are solely produced from the hydrolysis of a-chains ("true" a-chains), whereas DP 3 represents an unknown combination of a- and b-chains, and DP $\geq$ 4 solely represent b-chains ("true b-chains") (Bertoft et al., 2012b). Lighting conditions did not influence the quantity of "true" a-chains, although clusters of diurnal WBS amylopectin contained significantly ($p < 0.05$) decreased molar amounts of the mixture of chains at DP 3, and significantly greater quantities of "true" b-chains. All sub-categories of b-chains (b1a-, b1b-, b2-, and b3-chains) displayed significantly ($p < 0.05$) greater quantities when grown under diurnal conditions compared to constant light conditions, except the b0- chain category for which no significant differences were observed. The same trend was observed with diurnal NBS clusters compared to constant light NBS clusters.

Table 3.4: Molar distribution of chain categories of clusters of amylopectin from waxy and normal barley [1]

Sample	DP2	DP3	DP≥4	b0	b1a	b1b	b2	b3
Diurnal WBS	49.2[a]	9.5[a]	41.2[b]	9.2[a]	12.0[b]	12.9[b]	4.7[c]	2.3[b]
Constant Light WBS	51.0[a]	12.9[b]	35.9[a]	9.5[a]	10.5[a]	10.3[a]	3.7[a]	1.8[a]
Diurnal NBS	49.6[a]	9.4[a]	40.9[b]	9.5[a]	12.5[b]	12.3[b]	4.2[b]	2.3[b]
Constant Light NBS	50.1[a]	12.5[b]	37.2[a]	9.9[a]	11.1[a]	10.4[a]	3.7[a]	1.9[a]

[1] DP 2 = "true" a-chains, DP 3= mixture of a- and b-chains, DP ≥ 4= "true" b-chains, b0 = DP 4-6, b1a = DP 7-10, b1b = DP 11-18, b2 = DP 19-27, b3= DP ≥ 28

Values with different letters in columns are significantly different ($p < 0.05$) from each other.

Building block composition

The isolated φ,β-limit dextrins from WBS and NBS clusters were further extensively hydrolyzed with α-amylase from *B. amyloliquefaciens* to produce α-limit dextrins termed 'building blocks' (Bertoft et al., 2010). The structure and composition of the isolated building blocks reflect the branching structure found in the amylopectin component (Bertoft et al., 2012b). Slightly different size distribution profiles determined by GPC on Superdex 30 were observed for building blocks from WBS and NBS cultivated under diurnal and constant light growing conditions (Figure 3.6). The building blocks were also analyzed by HPAEC prior to and following debranching, to obtain their size distribution and unit chain distribution profiles, respectively (Figure 3.7). A number of structural parameters for building blocks can be calculated utilizing a combination of the GPC and HPAEC data, which are presented in Table 3.5. Diurnal light growing conditions

significantly increased the relative abundance of the branched building blocks in the clusters compared to constant light growing conditions.

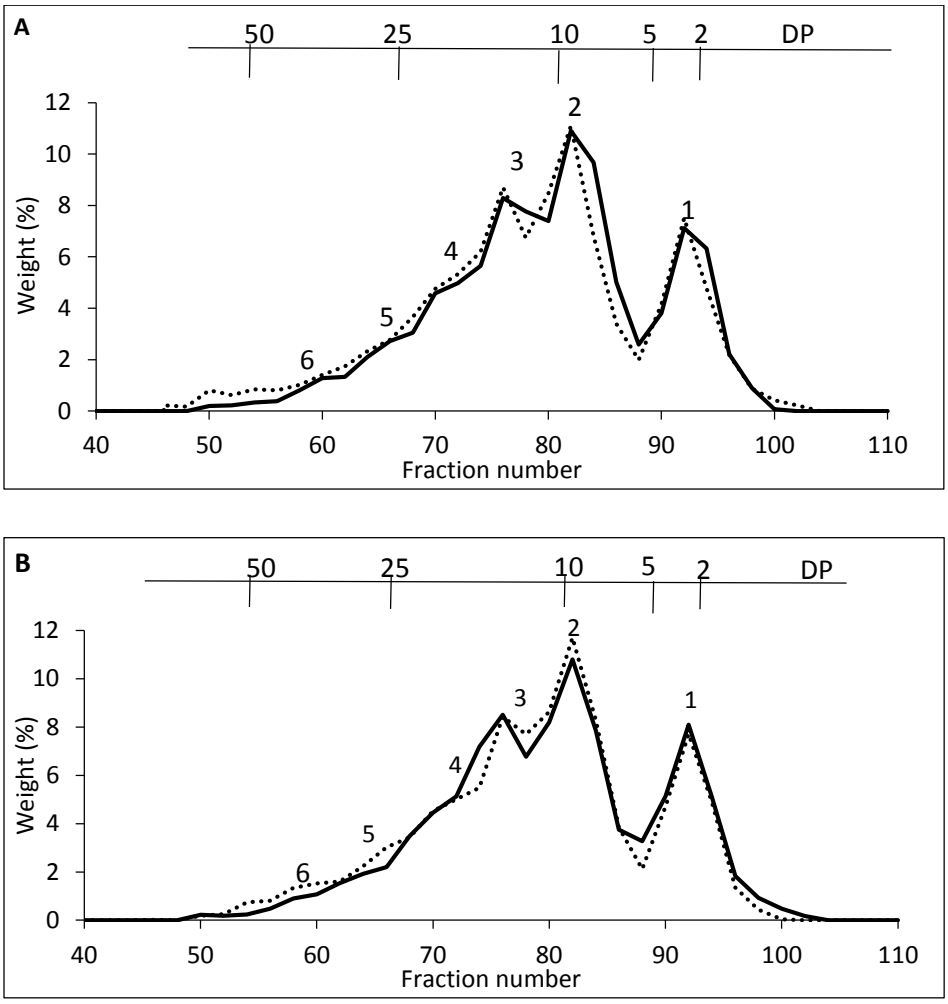

Figure 3.6: Size distribution of building blocks in clusters of amylopectin from waxy (A) and normal (B) barley starch cultivated under normal diurnal (---) or constant light (——) conditions obtained by GPC on Superdex 30. Groups of building blocks are indicated by numbers.

The average DP values for the branched building blocks, and the average number of building blocks in the clusters (NBbl) were greater when grown under diurnal conditions compared to constant lighting conditions for both starches. Diurnal or constant light growing conditions did not influence the density of building blocks (DBbl) in NBS and

WBS clusters. WBS and NBS clusters formed under constant light conditions exhibited greater inter-block chain lengths (IB-CL) than their clusters grown under diurnal conditions.

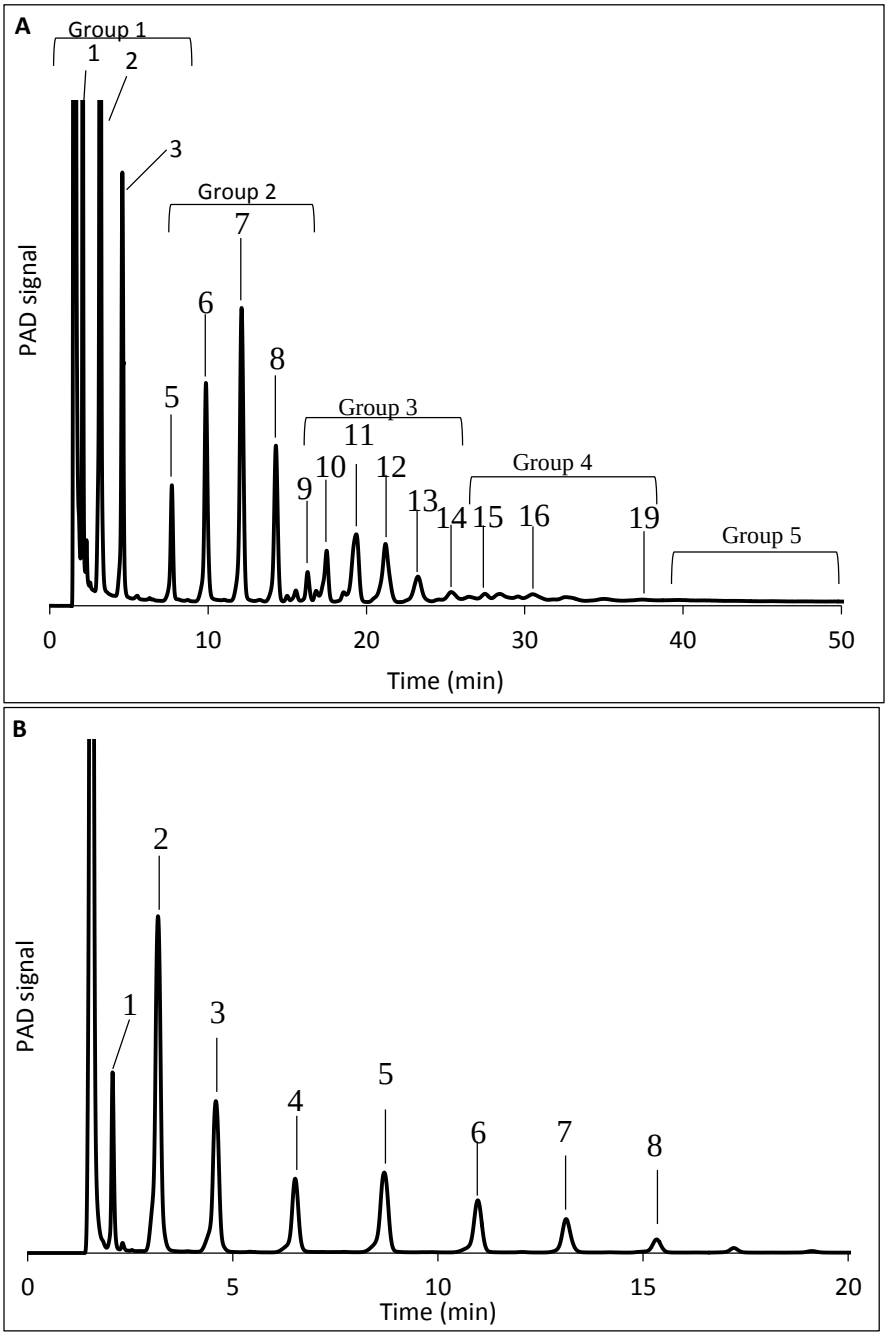

Figure 3.7: Typical HPAEC chromatograms of building blocks from clusters of barley starch (ex. constant light NBS) prior to (A) and following (B) debranching. Groups of building blocks are highlighted in (A), and numbers represent DP.

Table 3.5: Structural parameters of building blocks in cluster from waxy and normal barley starch[1]

	Linear Dextrins		**Branched Blocks**					
	Mole (%)	DP	Weight (%)	Mole (%)	DP	NBbl	DBbl (%)	IB-CL
Diurnal WBS	49.6[a]	1.9[a]	83.8[d]	50.3[c]	10.0[c]	8.8[c]	8.4[a]	5.9[a]
Constant Light WBS	60.0[c]	1.9[a]	75.9[b]	39.9[a]	9.1[a]	6.2[a]	8.2[a]	6.9[c]
Diurnal NBS	51.1[b]	1.9[a]	82.0[c]	48.8[b]	9.5[b]	10.4[d]	8.4a	6.0[b]
Constant Light NBS	60.9[c]	1.9[a]	74.5[a]	39.0[a]	9.0[a]	7.7[b]	8.3[a]	7.0[d]

[1] Linear dextrins = fragments with DP 1-3, Branched blocks = DP $\geq$ 5, NBbl (average number of building blocks) = (Weight% branched building blocks/ 100) x (DP clusters/DP branched building blocks), DBbl (Density of building blocks) = (NBbl / DP cluster)* 100, IB-CL (Inter block chain length) = (mole% linear dextrins x DP linear dextrins) / mole% branched building blocks + 4.

Values with different letters in columns are significantly different ($p < 0.05$) from each other.

The molar distribution of branched building block groups are shown in Table 3.6. Diurnal growing conditions appeared to suppress the relative molar distribution of group 2 building blocks in NBS and WBS compared to constant light conditions. The quantity of group 3 building blocks was greater in barley samples grown diurnally, although the difference was only significant in diurnal NBS. No differences were observed for the relative molar distribution of group 4 building blocks in WBS for the different lighting regimes. However, diurnal NBS contained significantly more of group 4 building blocks than constant light NBS. The relative quantity of group 5 and 6 building blocks was significantly higher in clusters from NBS and WBS cultivated in diurnal conditions.

Table 3.6: Relative molar distribution of branched building blocks in clusters of amylopectin from waxy and normal barley starch[1]

	Group 2	Group 3	Group 4	Group 5	Group 6
Diurnal WBS	63.7^{a}	24.2^{b}	5.0^{b}	5.6^{c}	1.2^{c}
Constant Light WBS	67.1^{bc}	23.7^{b}	5.0^{b}	3.9^{b}	0.3^{a}
Diurnal NBS	65.6^{ab}	24.6^{b}	5.0^{b}	4.0^{b}	0.5^{b}
Constant Light NBS	68.3^{c}	22.8^{a}	4.6^{a}	3.6^{a}	0.3^{a}

[1] Groups of building blocks are classified dependent on their size. Group 2 = DP 5-9, Group 3= DP 10-14, Group 3= DP 15-19, Group 4= DP 20-35, Group 5= DP > 35.

Values with different letters in columns are significantly different ($p < 0.05$) from each other.

Discussion

The impact of diurnal photosynthetic activity on the structure, crystallinity and gelatinization parameters of starch isolated from waxy and normal barley grown under diurnal and constant light conditions has been described elsewhere (Chapter 2). This study focused on the impact of diurnal photosynthetic activity on the fine structure of the amylopectin component. The analysis of amylopectin from WBS grown diurnally confirmed previously reported values for the same variety (Bertoft et al., 2011).

Starch biosynthesis and diurnal photosynthetic activity

The supply of substrates required for starch synthesis is influenced by diurnal rhythms, wherein the rate of sucrose supply is higher during the day than at night (Geigenberger and Stitt, 2000). In addition, a number of studies on crops have reported diurnal oscillation of starch synthetic gene expression such as the diurnal oscillation of starch

branching enzyme (SBE) expression in sorghum endosperm (Mutisya et al., 2009), the diurnal oscillation of genes encoding the catalytic subunit of AGPase in potato tubers (Geigenberger and Stitt, 2000), and the diurnal oscillation of genes encoding for SBEI and SBEII in cassava (Baguma et al., 2003).

ADP-glucose is the sole precursor for starch synthesis, with ADP-glucose pyrophosphorylase acting as the rate-limiting enzyme in the pathway. Van den Koornhuyse et al. (1996) investigated the fine structure of amylopectin synthesized in a mutant of *Chlamydomonas reinhardtii*, an algae and model organism for molecular biology in higher plants. Mutants studied by Van den Koornhuyse et al. (1996) had disruptions at the *STA1* structural gene, which rendered ADP-glucose pyrophosphorylase less responsive, and thus, altering the supply of ADP-glucose necessary for starch synthesis. The fine structure of amylopectin from the mutant and wild type samples were characterized, revealing clear differences in the size distribution of small glucans (Van den Koornhuyse et al., 1996). The mutant amylopectin contained greater quantities of glucan chains of DP 3-7, and lower quantities of DP 12-15 compared to the wild type. Therefore, a precedence exists wherein the altered supply of ADP-glucose influences the structure of amylopectin. As the supply of ADP-glucose may be different in normal and waxy barley grown under normal diurnal or constant light photosynthetic conditions, it is possible that these differences in ADP-glucose concentration promoted the differences in amylopectin fine structure observed in this study. Potential mechanisms for the differences in amylopectin structure observed are (i) changes in the concentration of ADP-glucose may influence the relative activities of starch synthesizing enzymes and therefore influence starch structure (Clarke et al., 1999), and (ii) the concentration of

sucrose produced via photosynthesis could impact a wide range of metabolite concentrations and potentially the concentration of other cellular components, which may influence the organization of the amylopectin component (Pilling and Smith, 2003). In addition, diurnal activity may influence the reported enzyme regulation functionality of protein complexes comprised of key enzymes of amylopectin synthesis (Tetlow, 2011).

Influence of diurnal photosynthetic activity on amylopectin structure

The unit chain composition of amylopectin from normal WBS (Figure 3.1, Table 3.1) were comparable when cultivated under diurnal or constant light conditions, exhibiting similar average chain length values and elution profiles as determined by HPAEC. However, NBS exhibited slightly, though significantly, greater average short and long chain lengths when grown under constant light conditions compared to diurnal conditions. It has been reported elsewhere that environmental conditions such as a maximum daylight temperature influences the chain length distribution of amylopectin from wheat (Shi et al., 1994). On the other hand, the biosynthesis of starch has previously been reported to contain compensatory mechanisms, which regulate starch structure and metabolism (Stitt and Zeeman, 2012). The similar average chain length distribution and chain length profiles of WBS may be indicative of a conserved unit chain profile of amylopectin under diurnal and constant light growing conditions.

Nevertheless, subtle differences in the molar amount of certain internal chain length categories were observed in amylopectin from NBS and WBS (Table 3.2), which suggested differences in the organization and architecture of the amylopectin component. Decreases in the molar quantity of long B-chains (DP $\geq$ 27) observed in NBS cultivated

under diurnal conditions indicated that the molar quantity of long B-chains was suppressed under the normal diurnal lighting regime. The increased relative molar quantity of B_{fp}-chains in WBS cultivated under diurnal conditions (17.5) compared to constant light conditions (16.0), and decreased relative molar quantity of BS_{major} chains in diurnal WBS (26.7) compared to constant light WBS (28.2) suggested an altered organization of amylopectin under the different lighting regimes, as B_{fp}-chains have been reported to participate in tightly branched building blocks in clusters (Bertoft and Koch, 2000). This may be due to differences in the expression of starch synthase II, which has been reported to participate in the synthesis of unit chains between DP 12-38 (Zhang et al., 2008). Unit chains of this length correspond to the internal B_{fp}- and BS_{major}-chains in the φ,β-limit dextrins, as the ECL of amylopectin from WBS and NBS was DP ~11. Further, starch synthase II has been shown to exhibit diurnal rhythms as lower levels of the expression patterns for the enzyme have been observed during darkness, which increase substantially in the transition from dark to light (Smith et al., 2004). On the other hand, the higher quantity of B_{fp}-chains may be a result of altered activity of debranching isoamylase enzymes, rendering greater amounts of B_{fp}-chains under the diurnal lighting regime.

When amylopectin is hydrolyzed with α-amylase from *B. amyloliquefaciens*, external and long internal chains are hydrolyzed producing relatively resistant clusters comprised of short chains (Bertoft et al., 2012b). The average size of clusters (Figure 3.4, Table 3.3) was consistently larger when barley was cultivated diurnally compared to constant light conditions, with the significantly greater NBbl in diurnally grown barleys providing a structural basis for the larger clusters. It was thus apparent that diurnal

photosynthetic activity influences the biosynthesis and structure of amylopectin at the cluster structural level.

The unit chain composition of isolated clusters from NBS and WBS appeared to systematically change when cultivated under the different lighting regimes (Table 3.4). The significantly lower quantity of chains with DP 3 (mixture of a- and b-chains) and greater quantity of "true" b-chains observed in diurnal samples compared to constant light conditions suggested that the mode of branching catalyzed by SBE, or glucan trimming catalyzed by starch debranching enzymes (Kalinga et al., 2014), is influenced by environmental lighting conditions. With the exception of b0-chains, all sub-categories of b-chains increased in the diurnally grown barleys indicating a greater proportion of internal chains compared to constant light conditions. According to the backbone model of amylopectin, the backbone consists of long amylopectin chains, with the building blocks distributed along the backbone (Bertoft, 2013). It has been suggested that the longer b2- and b3-chains are more preferentially distributed along the backbone of amylopectin (Zhu et al., 2013), indicating that diurnal growing conditions may have influenced the backbone structure of amylopectin. The significantly greater quantities of b2- and b3-chains may be a result of altered activity of the starch synthase III enzyme under the diurnal lighting regime as starch synthase III has been reported to function in the provision of long amylopectin chains, which extend between clusters (James et al., 2003).

Clear differences in the size distribution and composition of building blocks isolated from NBS and WBS were evident when comparing their structures when cultivated under the two different lighting regimes (Figure 3.6, Table 3.6). Significantly

lower quantities of group 2, and greater quantities of the large blocks of group 5 and 6 were present in diurnally grown samples. The abundance of group 5 and 6 building blocks provided a structural basis for the greater average cluster size in diurnally grown samples. The greater quantity of group 5 and 6 building blocks also supported the greater molar quantity of B_{fp}-chains observed in diurnal WBS, which likely are found especially in the larger building blocks. Moreover, barleys cultivated under the diurnal light conditions possessed clusters with significantly shorter IB-CL. All together, the results suggested that diurnally grown barley maintains a more compact molecular structure.

It has previously been reported that a relationship exists between the internal structure of amylopectin and the thermal properties of starch wherein the alignment of chains in the crystalline lamellae is dependent on the flexibility of spacers within or between building blocks located in the amorphous lamellae. Therefore, the internal structure of amylopectin can be utilized to predict trends in thermal properties (Vamadevan et al., 2013). Vamadevan et al. (2013) systematically investigated correlations between gelatinization parameters and amylopectin structural data obtained from starches which were classified into groups based on their internal unit chain profiles obtained from their φ,β-limit dextrins. It was determined that the onset temperature of gelatinization was negatively correlated with the NBbl and positively correlated with IB-CL (Vamadevan et al., 2013). Interestingly, this relationship may explain the differences observed in the thermal profiles of diurnal and constant light NBS reported in Chapter 2, wherein the diurnally grown NBS, which contained significantly greater NBbl and shorter IB-CL than constant light NBS, displayed a significantly lower onset gelatinization temperature. Shorter IB-CL may act to increase the number of non-parallel

double helices due to unfavorable combination of spacer arms, with their short length decreasing the flexibility of internal chains (Vamadevan et al., 2013).

Conclusion

It has been established that diurnal photosynthetic activity results in a more branched structure of amylopectin in NBS and WBS compared to barley cultivated under constant light conditions. This is manifested as larger clusters containing a greater number of building blocks, and lower inter-block chain lengths. Although numerous differences in amylopectin fine structure were observed, the average chain lengths of the unit chains of amylopectin remained similar regardless of lighting regime, perhaps indicating this structural feature is conserved during starch biosynthesis.

Chapter 4: Molecular structure of lintners of barley starches containing 0 to 100% amylose

Summary

In this study, the structure and morphology of a novel amylose-only barley starch (AOS) produced using a chimeric RNAi hairpin, which suppressed all known genes coding for starch branching enzymes (SBE I, SBE IIa, SBE IIb) in the grain, was probed utilizing acid hydrolysis along with light, transmission electron, and confocal laser scanning microscopy. Normal barley starch (NBS) and waxy barley starch (WBS) were also studied to allow for the characterization of starches ranging from zero to 100% amylose content. AOS granules exhibited an irregular morphology containing multi-lobed granules with a rough surface texture compared to the morphology of A- and B-type granules present in NBS and WBS. When viewed by transmission electron microscopy, nanocrystals from AOS lintners displayed strongly textured aggregates with an organization unlike any specimen viewed previously, whereas nanocrystals from NBS and WBS displayed an expected lamellar structure comprised of stacks of elongated elements with a width of 5-7 nm. Amylose containing starches displayed lower rates of acid hydrolysis than WBS, and AOS reached a plateau at ~45% acid hydrolysis. High performance anion-exchange chromatography of lintners at equivalent levels of acid hydrolysis (45 wt%) revealed the average degree of polymerization (DP_n) of AOS lintners was 21, substantially smaller than that of NBS and WBS (DP_n 42). AOS lintners contained the lowest number of chains per molecule (NC 1.1) compared to NBS (2.8) and WBS (3.3), with NC correlating with amylose content. The average chain length of AOS

lintners was 19 compared to 15 for NBS and 13 for WBS. The size distribution profile of AOS revealed a repeat-size of the molecules corresponding to 5-6 glucose residues, i.e. the approximate number of residues per turn of the helical structure of amylose.

Introduction

Starch is the main storage polysaccharide in higher plants and is a globally important food and industrial material (Tetlow, 2011). Starch is a cheap, renewable, and biodegradable material comprised of two principle components, amylose and amylopectin. Amylopectin is a branched macromolecule composed of α-(1,4)-linked D-glucosyl chains containing α-(1,6)- branches, whereas amylose is a mostly linear macromolecule containing α-(1,4)-linked D-glucosyl units. Although the chemical composition of starch is not complex, the structure of native starch granules varies significantly between plant species (Wang and Copeland, 2015). Variability in the structure of starch produced from different plant species is due to differences in the genes that encode starch biosynthetic enzymes, along with environmental factors (Wang and Copeland, 2015). Variability in starch structure drives numerous food and industrial uses of native starch, however, native starches do have natural limitations and modification can greatly enhance their desired functionality (Hermansson and Svegmark, 1996, BeMiller and Huber, 2015).

The physicochemical properties of starch contribute to its rate and extent of digestion (Regina et al., 2015). The proportion of amylose in starch has a relationship with the rate of digestion, with high-amylose starches generally being more resistant to enzymatic digestion and containing greater quantities of health promoting resistant

starch. It was previously believed that the amylopectin component of starch was required for the generation starch granules in wild-type and waxy starches devoid of amylose (Ball et al., 1996). Further, it was postulated that amylopectin biosynthesis is sufficient to explain the major features of starch granule biosynthesis, and that double helices from the amylopectin component were responsible for the crystallinity present in starch (Ball et al., 1996). However, it has recently been shown that semi-crystalline starch granules can be synthesized with only the amylose component through the silencing of all known genes coding for starch branching enzymes (SBE I, SBE IIa, SBE IIb) in barley using a single RNAi hairpin (Carciofi et al., 2012). When this so called amylose-only starch (AOS) was gelatinized, it contained very high contents of resistant starch (65%) compared to the control starch (29%) (Carciofi et al., 2012). The high content of resistant starch may be explained by decreased accessibility of amylose chains to digestive enzymes due to retrogradation, i.e. the formation of stable double-helical structures during cooling following gelatinization (Li et al., 2008). AOS has great potential to be incorporated into food products designed to have a low glycemic impact, coinciding with a slow and sustained glucose release. To date, it has been determined that AOS exhibits unique thermal and crystallinity properties (Carciofi et al., 2012), although an understanding of its crystalline structure at the molecular level has not yet been studied.

A common approach utilized to investigate the crystalline architecture of starch granules exploits the principle that crystalline starch components are more resistant towards dilute acid catalyzed hydrolysis than amorphous starch components (Kainuma and French, 1971). The insoluble residues, which remain following acid hydrolysis, are referred to as lintners or Nägeli amylodextrins, when starch is incubated in the presence

of HCl (2.2 M) or H_2S0_4 (15%), respectively. The remaining dextrins following acid hydrolysis are typically either linear (average degree of polymerization (DP) 13-17) or single branched (average DP 24-30) dextrins (Yamaguchi et al., 1979). The single branched dextrins consist of chains of almost equal length (Srichuwong et al., 2005). In addition, a small amount of multiple branched dextrins may also be present (Jacobs et. al., 1998). Investigating the kinetics of acid hydrolysis, as well the structure of the residual insoluble residues provides insightful information pertaining to the molecular structure, architecture, and dynamics of the crystalline components of starch in granules (Wikman et al., 2013).

In this study, lintners of AOS from barley were investigated by acid hydrolysis and compared to lintners from normal (NBS) and waxy barley starch (WBS). This study will not only provide novel insight into the crystalline structure of health promoting AOS, but will allow for an enhanced understanding of the molecular structure of crystalline components present in starch granules containing zero to 100% amylose.

Materials and methods

Barleys

Barley (*Hordeum vulgare)* with suppressed genes coding for starch branching enzymes, achieved by using a chimeric RNAi hairpin and containing amylose-only starch, was produced according to methods described by Carciofi et al. (2012). Normal barley starch (NBS; Golden Promise variety; 18% amylose, 82% amylopectin) and waxy barley starch (WBS; Cinnamon variety; 100% amylopectin) were cultivated in a greenhouse at the

University of Copenhagen, Denmark. Amylose content was determined by gel permeation chromatography of starch debranched with isoamylase and pullulanase on a column (1 x 90 cm) of Sepharose CL 6B (GE Healthcare, Uppsala, Sweden) according to the method of Sargeant (1982), as reported in Chapter 2.

Starch extraction

Starch was extracted from ground barley flour according to method of Carciofi et al., (2011) with modifications described by Goldstein et al., (Chapter 2).

Lintnerization

Starch granules were suspended in 2.2 M HCl (200 mg/8 mL HCl) and incubated at 35°C or 40°C according to the method by Robin (1974). Starch suspensions were gently mixed daily. The rate of acid hydrolysis was determined by taking small aliquots (15 µL) at regular intervals, diluting to 1.5 mL with distilled water, centrifuging at 2000 x g, and analyzing the supernatant for carbohydrate content using the phenol-sulphuric acid reagent (Dubois et al., 1956). For structural analysis, large aliquots of sample prepared at 40°C were taken at ~45% hydrolysis, neutralized with 0.1 M NaOAc, washed twice with distilled water, and the insoluble residue was recovered by lyophilization.

Enzyme treatment

Freeze dried lintners were enzymatically treated in three different manners. Firstly, lintners were treated with β-amylase to obtain their β-limit dextrins according to methods

by Bertoft (2004a). Secondly, lintners were debranched with the addition of isoamylase and pullulanase according to methods reported by Wikman et al. (2013). Lastly, following debranching, lintners were treated with β-amylase to obtain the β-limit dextrin of debranched components according to Wikman et al. (2013).

Size distribution analysis

The size distribution of lintners at 45% acid hydrolysis was determined by gel-permeation chromatography (GPC) on a column (1 x 90 cm) of Sepharose CL 6B (GE Healthcare, Uppsala, Sweden) as described by Bertoft (2007). The GPC column was calibrated at low DP values using commercial dextrins of glucose, maltose, and maltoheptaose (Sigma-Aldrich, St. Louis, MO), and at larger DP values with debranched WBS, which had been analyzed by high-performance anion-exchange chromatography (HPAEC). A standard curve for the GPC column was obtained by comparing the elution of dextrins from debranched WBS with HPAEC analysis on a weight basis, and the standard curve was extended linearly past the last clearly resolved DP-peak of 60 by HPAEC analysis to cover the remaining volume of the GPC column.

Anion-exchange chromatography

Lintners and enzymatically treated lintners at 45% hydrolysis were analyzed by HPAEC with a pulsed amperometric detector (PAD) (Dionex-ICS 5000^{+}, Sunnyvale, CA) equipped with a Carbo-Pac PA-100 column and similar guard column according to methods reported by Wikman et al. (2013). Areas under peaks were corrected to

carbohydrate content according to Koch et al. (1998), and dextrins of DP > 35, which were not resolved as peaks, were quantitatively approximated by a continuous area division of the chromatograms (Bertoft, 2004b).

Microscopy

Transmission electron microscopy (TEM) analysis of barley starch lintners at 45% hydrolysis was acquired according to methods reported by Putaux et al. (2003). Scanning electron microscopy analysis (SEM) of starch granules were acquired with a Hitachi 4700 FE-SEM (Hitachi High Technologies, Tokyo, Japan) following sputter coating with ~20 nm of Au. Polarized light microscopy images were acquired according to methods described in Chapter 2.

Statistical analysis

All analyses were conducted in duplicate and analyzed using SPSS (IBM Corporation, Armonk, NY, USA). Significant differences were determined by comparing means by Tukey's test at a significance level of $p < 0.05$.

Results

The molecular structure of NBS and WBS utilized in this study were previously reported by Goldstein et al. (Chapter 2), whereas the structure and architecture of their amylopectin components were reported by Goldstein et al. (Chapter 3).

Morphological characterization

When visualized with SEM, NBS and WBS contained the well-known combination of large disc-shaped A-type granules and small spherical B-type granules (Figure 4.1), previously described by many authors (Vasanthan and Hoover, 2009, Stark and Yin, 1986, Tang et al., 2001). AOS from barley exhibited an elongated and multi-lobed morphology, with some granules exhibiting a rough surface morphology in agreement with that reported by Carciofi et al. (2012). The morphology observed in AOS has not been not been typically observed in NBS and WBS granules.

Starch granules were observed under polarized light microscopy prior to and following acid hydrolysis. Native AOS starch did not display any birefringence (not shown), which indicated that there was no main molecular direction of the glucan chains, aligning with observations reported by Carciofi et al. (2012). Native NBS and WBS displayed maltese crosses as shown in Chapter 2. At 45% acid hydrolysis, the AOS lintner exhibited fragmented birefringence with no clear organization. Maltese crosses were still present in NBS and WBS lintners following acid hydrolysis (Figure 4.1).

As part of the sample preparation for TEM analysis, lintners were placed in a suspension of water and were briefly homogenized with a benchtop homogenizer to generate fragments (Putaux et al., 2003), which were separated from the whole lintner. It is these fragments that were sampled to view by TEM and thus it is important to consider that the structures observed by TEM may not be representative of the structure of the whole lintner. TEM analysis of AOS, NBS, and WBS lintners (Figure 4.1) at 45% acid hydrolysis revealed the presence of micrometer-size aggregates, which were comprised of fragments of lintnerised granules. The fragments from WBS revealed a lamellar structure comprised of stacks of elongated elements with a width of 5-7 nm, believed to

represent crystalline amylopectin side chains viewed longitudinally. NBS lintners contained the same lamellar structure observed in WBS, although its degradation was not as complete. Long fibrillar fragments in NBS lintners were observed and certain regions appeared undisrupted. AOS lintners were composed of strongly textured aggregates of nanocrystals with an organization unlike any specimen viewed previously (Putaux et al., 2003, Angellier-Coussy et al., 2009). It should be noted, however, that the extent of acid hydrolysis of lintners viewed by TEM in this study differed greatly from analyses completed in other studies, such as Putaux et al. (2003), where the authors investigated waxy maize lintners at 70% and 95% hydrolysis, while Angéllier-Coussy et al., (2009) reported on waxy maize Nägeli amylodextrins at 84% acid hydrolysis.

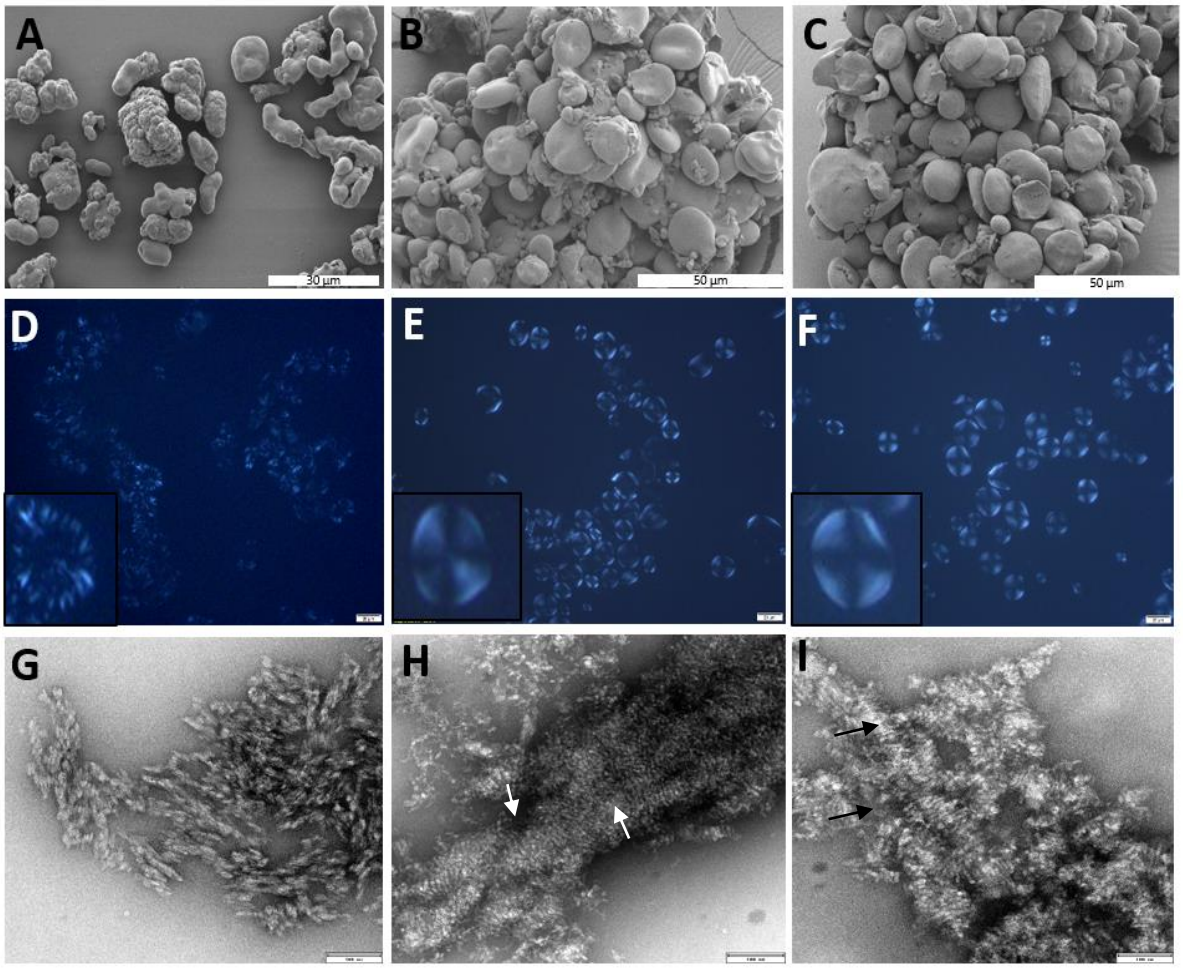

Figure 4.1: Morphological characterization of native and acid hydrolyzed barley starches. SEM of native AOS, NBS, and WBS granules displayed in A, B, and C, respectively. Polarized microscopy of AOS, NBS, and WBS lintners displayed in D, E, and F, respectively. TEM of AOS, NBS, and WBS lintners displayed in G, H, and I, respectively. Scale bar in A represents 30 µm while scale bar in B and C represents 50 µM. Scale bar in D, E, F, represents 20 µm. Scale bar in G, H, I represents 100 nm. Inset in D, E, and F represents lintners at higher magnification. Arrows in H, and I indicate lamellar stacks of platelets formed by the crystallization of amylopectin side chains.

Rate of lintnerization

The kinetics of lintnerization of the three starch samples were determined under two different incubation temperatures (Figure 4.2). Typically, acid hydrolysis patterns of starch exhibit two stages, an initial fast hydrolysis of the amorphous regions, followed by slower hydrolysis of the amorphous and crystalline regions (Wang et al., 2012). The more

rapid hydrolysis of the amorphous regions can be explained by the looser packing of amorphous components compared to their crystalline counterparts (Kainuma and French, 1971). The two-stage pattern was more evident at the lower incubation temperature (35°C). The presence of amylose appeared to retard the solubilization of starch in dilute HCl as WBS exhibited the fastest rate of hydrolysis followed by NBS, with AOS exhibiting the slowest rate of solubilization. The incubation temperature strongly influenced the rate of solubilization of WBS and NBS, with WBS reaching ~80% solubilization in 3 days at 40°C and 6 days at 35°C, whereas NBS reached ~80% solubilization in 5 days at 40°C compared to 14 days at 35°C incubation. Interestingly, the incubation temperature did not influence the kinetics of lintnerization of AOS, as similar hydrolysis profiles were observed during incubation at 35°C and 40°C. In addition, AOS was highly resistant to acid hydrolysis plateauing at ~45% hydrolysis.

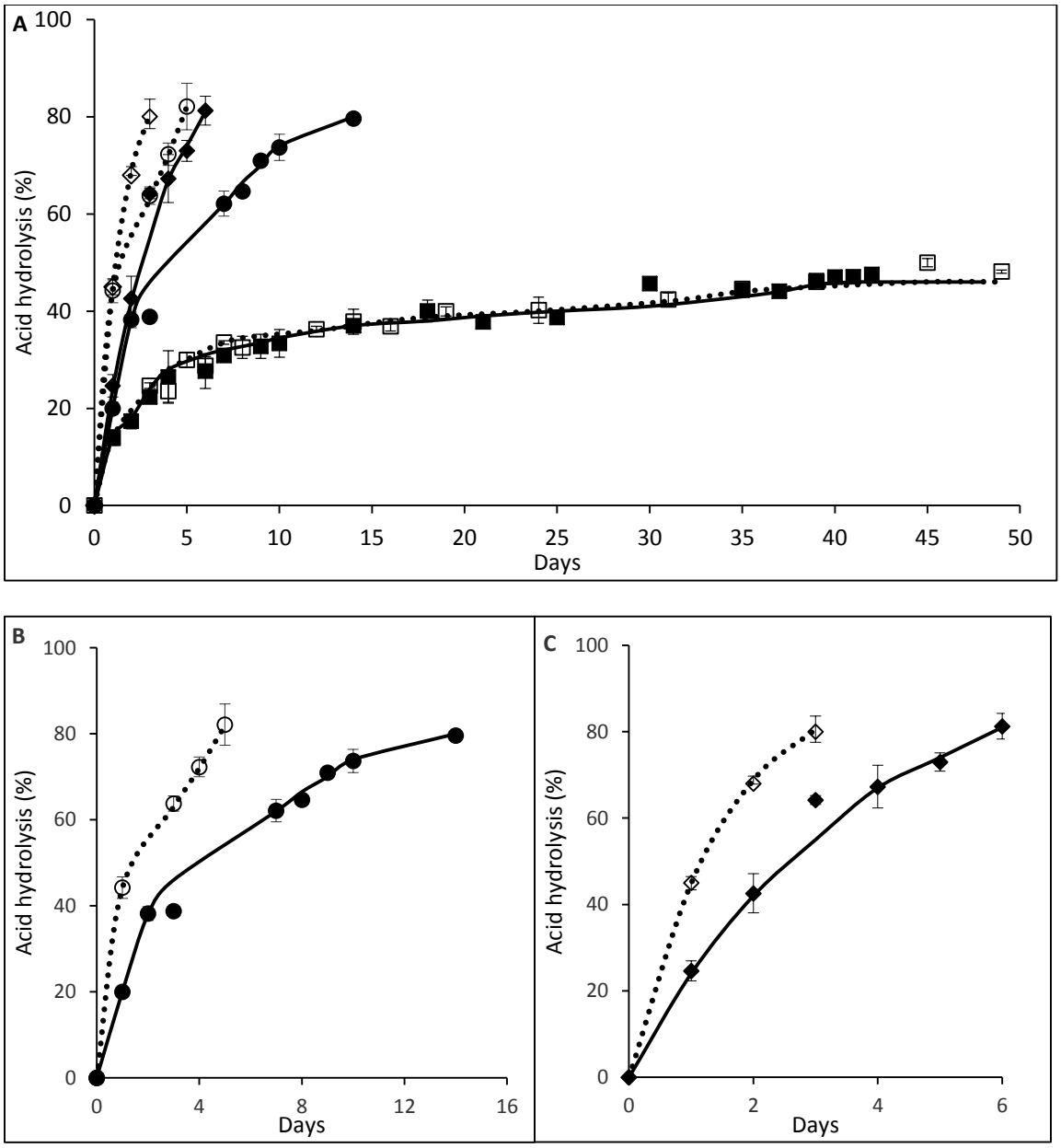

Figure 4.2: (A) Acid hydrolysis of AOS (■). NBS (●) and WBS (◆) incubated at 35°C (filled symbols) and 40°C (open symbols), including enlarged profiles for (B) NBS and (C) WBS. Scatter plot markers represent experimental data, whereas hydrolysis curves are fitted.

Molecular composition of lintners

The size distribution of acid hydrolyzed barley starches obtained at 40°C was determined by GPC using Sepharose CL 6B. In this analysis, solubilized dextrins were separated on

the basis of their size, or more specifically, their hydrodynamic volume (Trathnigg, 2000). The size distributions of lintners from AOS, NBS, and WBS at ~45% hydrolysis are shown in Figure 4.3. NBS and WBS displayed similar size distribution profiles with WBS containing a slightly greater concentration of smaller components with DP < 40. The average DP_n of NBS and WBS lintners determined by GPC were 46 and 48, respectively. AOS exhibited a narrower size distribution than WBS and NBS, with an average DP_n of 31.

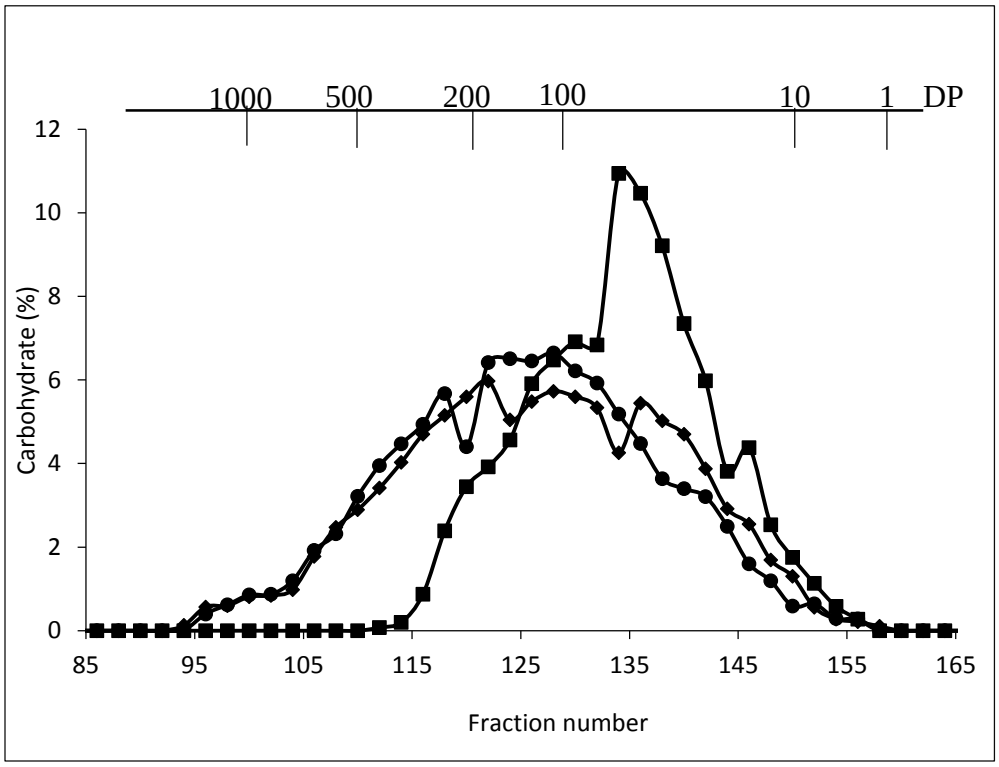

Figure 4.3: Size distribution of AOS (■). NBS (●) and WBS (◆) lintners at 45% acid hydrolysis prepared at 40°C determined by gel permeation chromatography on Sepharose CL 6B. Numbers indicate the degree of polymerization.

The molecular size distributions of the lintners were acquired in greater detail by HPAEC analysis with representative chromatograms shown in Figure 4.4. NBS and WBS

exhibited similar profiles (NBS not shown). A small quantity of small dextrins (DP ≤ 6) in NBS and WBS was detected. However, this population of dextrins was not considered to be part of the granular structure as it was observed previously that it was easily removed following extensive washing (Angéllier-Coussy et al., 2009). The first population of dextrins in WBS lintner with a peak at DP_n 12 represent linear dextrins, the second population with a peak at DP_n of 24 is single branched dextrins, and the third population starting at DP_n 37 is comprised of multiple branched dextrins (Yamaguchi et al., 1979, Jacobs et al., 1998). Therefore, the dextrins contained in the lintners from WBS and NBS were divided into three populations consisting of small dextrins of DP_n 6-18 (Fraction I), intermediate-sized dextrins of DP_n 19-36 (Fraction II), and larger dextrins with $DP_n \geq 37$ (Fraction III).

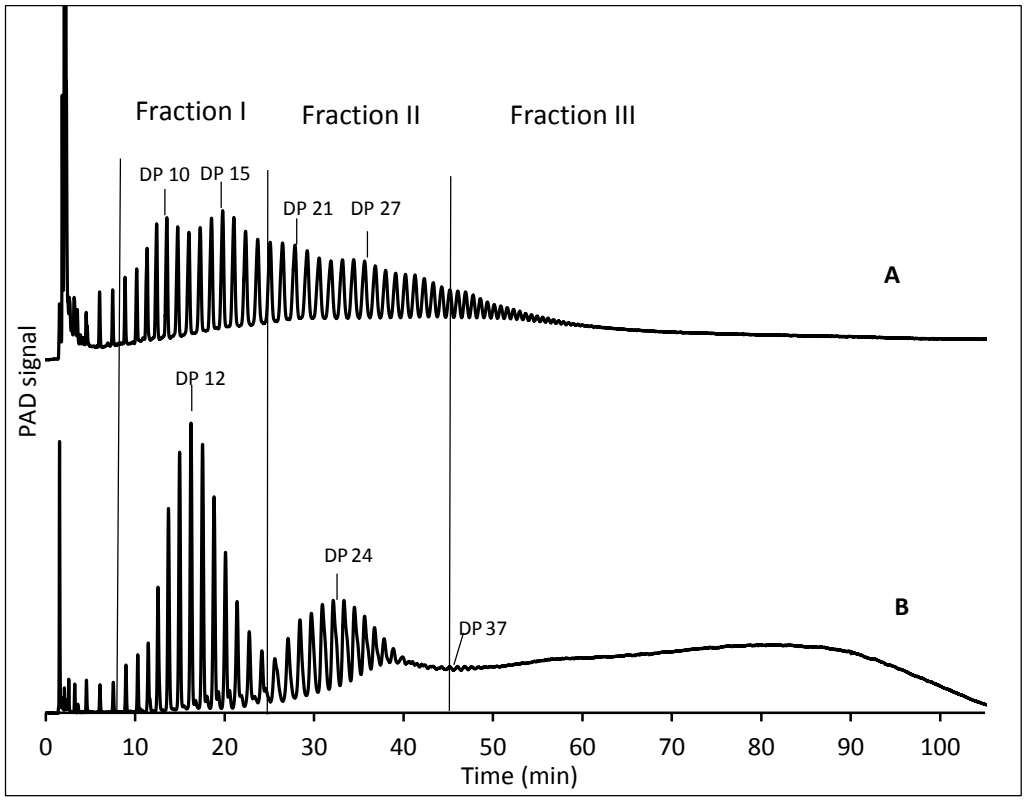

Figure 4.4: Size distribution of AOS (A) and WBS (B) lintners at 45% solubilization prepared at 40°C determined by HPAEC.

The AOS lintner did not display a comparable elution profile to NBS and WBS. Rather, it displayed a profile with peaks and shoulders with an apparent periodicity of 5-6 glucose residues. Although the three dextrin populations found in NBS and WBS lintners were not apparent in the AOS lintner, the chromatogram was divided into the similar fractions to allow for a quantitative comparison between all three samples. AOS contained significantly greater relative molar quantities of Fraction I and II (together 89%), and therefore significantly lower quantities of Fraction III (11%) than NBS and WBS (Table 4.1). NBS and WBS displayed very similar relative molar compositions, although WBS statistically maintained a significantly greater quantity of Fraction I compared to NBS. The relative molar composition of NBS and WBS were much more evenly distributed across the three fractions than in the AOS lintner.

Table 4.1: Relative molar composition (%) of lintnerized starches prepared at 40°C.

	AOS	NBS	WBS
Fraction I[1]	48[c]	32[a]	34[b]
Fraction II	41[b]	29[a]	29[a]
Fraction III	11[a]	37[b]	36[b]

[1] Fraction I includes dextrins of DP 6-18, fraction II DP 19-36, and fraction III DP≥ 37.
Values in rows with different letter are significantly different at $p < 0.05$.

The molecular size distribution of lintners analyzed by HPAEC analysis provides resolution of peaks considerably higher than GPC analysis (Bertoft, 2004b). Utilizing HPAEC analysis, Bertoft (2004b) determined the average chain length of a debranched waxy maize starch by continuously dividing the HPAEC chromatograms into successive areas past the last clearly resolved peak for each chain, and reported that the average chain lengths were comparable between GPC and HPAEC analysis. In the HPAEC

analysis of lintners, chains longer than DP 35 are not clearly resolved, however, using an approach in line with that utilized by Bertoft (2004b), the amount of chains past the last clearly resolved HPAEC peak were estimated by a continuous division of the chromatogram into successive areas. The average DP_n values of NBS (42) and WBS (42) lintners (Table 4.2) determined by HPAEC were nearly identical and they were more than double the average DP_n of the AOS lintner (21), which supported the substantially smaller size distribution of the AOS lintner determined by GPC. The average DP_n values were comparable between GPC and HPAEC analysis for NBS and WBS lintners. However, the average DP_n of the AOS lintner was considerably smaller when estimated by HPAEC analysis. Apparently, this was due to considerable differences in the average DP_n

Table 4.2: Structure of lintnerized starches prepared at 40°C.

	AOS	NBS	WBS
DP_n (GPC)[1]	31[a]	46[b]	48[b]
DP_n (HPAEC)[2]	21[a]	42[b]	42[b]
Chain Length[3]	18[c]	15[a]	13[b]
Number of chains[4]	1.1[c]	2.8[a]	3.3[b]
Fraction I (DP_n) [5]	12[a]	13[b]	12[a]
Fraction II (DP_n)	25[a]	27[b]	25[a]
Fraction III (DP_n)	44[a]	79[b]	83[c]

[1]Average DP_n of lintner determined by GPC on a column of Sepharose CL 6B.
[2]Average DP_n of lintner determined by HPAEC.
[3] Average chain length of lintners determined by HPAEC following debranching with isoamylase and pullulanase.
[4] Number of chains = DP_n whole lintner (HPAEC)/chain length.
[5] Fraction I includes dextrins DP 6-18. Fraction II includes DP 19-36, Fraction III includes DP $\geq$ 37.
Values in rows with different letter are significantly different ($p < 0.05$).

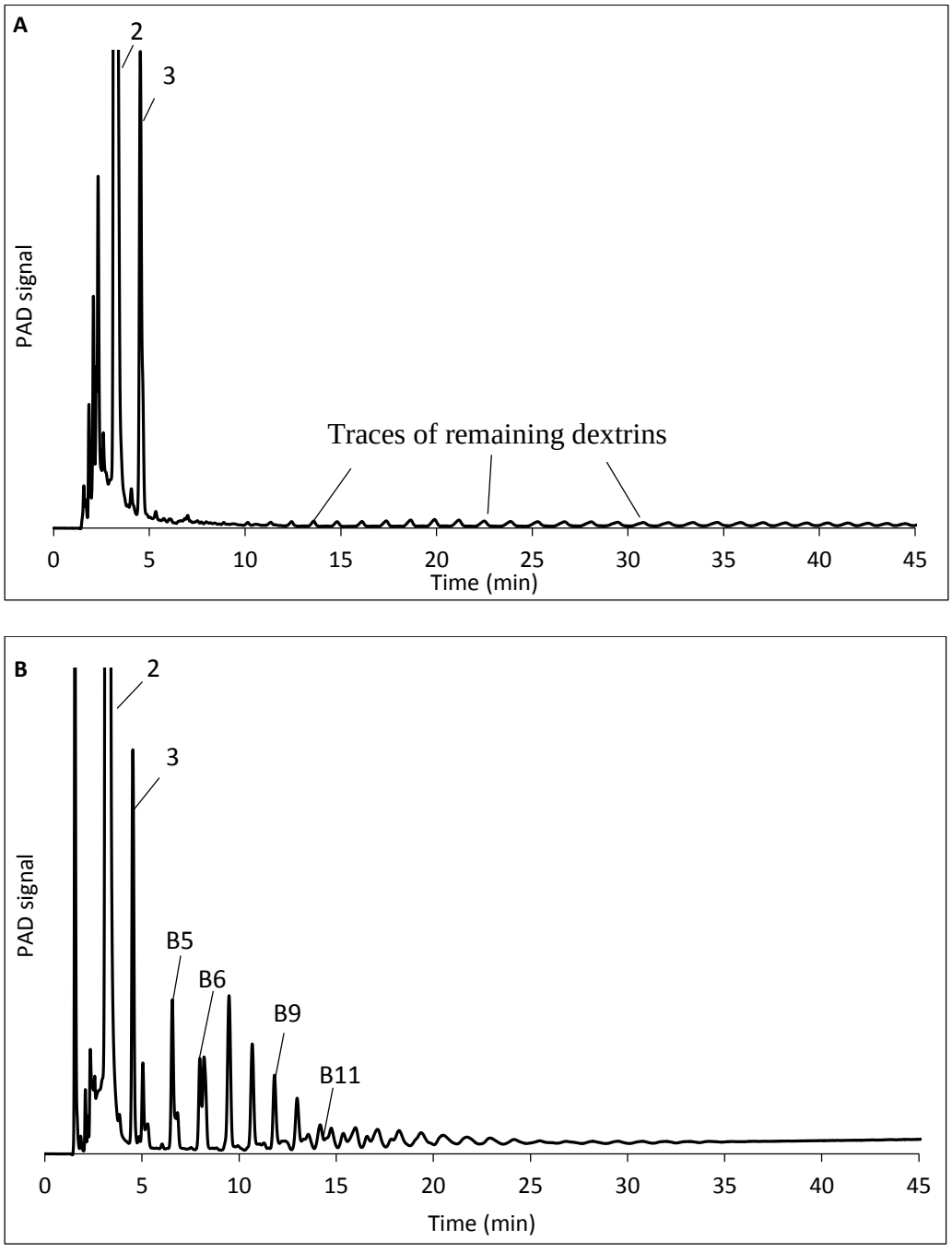

Figure 4.5: Size distribution of β-limit dextrins of AOS (A) and WBS (B) determined by HPAEC. Number indicates the degree of polymerization, and "B" indicates branched dextrins.

of Fraction III containing larger dextrins, with AOS possessing an average DP_n of 44, compared to average DP_n values of 79 and 83 for NBS and WBS lintners, respectively, whereas similar average DP_n values for Fraction I and II were observed across the three lintner samples (Table 4.2).

The β-limit dextrins of lintners were obtained following the addition of β-amylase, which cleaves successive maltose units from the non-reducing end of glucosidic chains until a branch point is reached which cannot be bypassed. The remaining dextrins were present in very low quantity and did not allow for proper quantification (Figure 4.5), however, it was readily apparent that the majority of the remaining dextrins from NBS (not shown) and WBS had branches located near the reducing end of the dextrins, as the majority of the dextrins were of low DP, eluting shortly after maltose and maltotriose (Figure 4.5). Remaining dextrins from AOS lintners following treatment with β-amylase were present in trace amounts. These resistant dextrins maintained a larger size distribution with greater DP values compared to the resistant dextrins from NBS and WBS. This suggested that branch points apparently were not located close to the reducing end as in practice no peaks were observed near the peaks of maltose and maltotriose.

Chain profiles of lintners

The structure of the lintners were further characterized following debranching with the enzymes isoamylase and pullulanase, which hydrolyze the α-(1,6)-branches present in the remaining residues. It is of importance to note that the debranching enzymes utilized in this study are unable to hydrolyze single α-(1,6)-linked glucosyl residues attached to an α-(1,4)-backbone chain (Abdullah and French, 1966). The profile of the chromatograms of the debranched lintners analyzed by HPAEC is shown in Figure

4.6. The debranched profile of different varieties of barley at varying levels of acid hydrolysis have been reported elsewhere (Song and Jane, 2000) and were confirmed for NBS and WBS study. NBS and WBS therefore served as valuable control profiles to compare to that of the unique AOS lintner. Following debranching WBS displayed a population of short dextrins with DP_n 2-7, and a second population of larger dextrins with a maximum at DP_n 12 with gradually smaller peaks eluting as the DP increased. As was the case with the profiles of the chromatograms prior to debranching, WBS and NBS displayed very comparable debranched size distribution profiles (NBS not shown). The chromatogram of the debranched AOS lintner was unique, exhibiting a broad distribution of peaks with no major populations. However, within the broad distribution of peaks a periodicity of 5-6 glucose residues was observed. In Figure 4.7 the molar distributions of the debranched lintners are compared with the distribution of the lintner prior to debranching. The debranched AOS lintner displayed a profile very similar to the lintner prior to debranching, which was indicative of low levels of branching in the lintner, as debranching did not have a large impact on the molar distribution of the lintner. When comparing the molar distribution of NBS and WBS lintners prior to and following debranching, it was apparent that the position of the glucan population with a peak at DP 12 remained essentially the same in both samples, however, the population with a peak at DP 24, believed to represent single branched glucose chains (Wang and Copeland, 2015) largely disappeared in the debranched sample.

The average chain lengths (CL) of the debranched lintners appeared to relate with the amylose content of the samples, as WBS had the lowest CL (13), followed by NBS (15) and AOS (19) (Table 4.2). With knowledge of the CL of debranched lintners and the

average DP_n of lintners, the number of chains (NC) can be approximated. The apparent NC of the AOS lintner was 1.1, compared to 2.8 in NBS, and 3.2 in WBS, again implying a relationship with the amylose content.

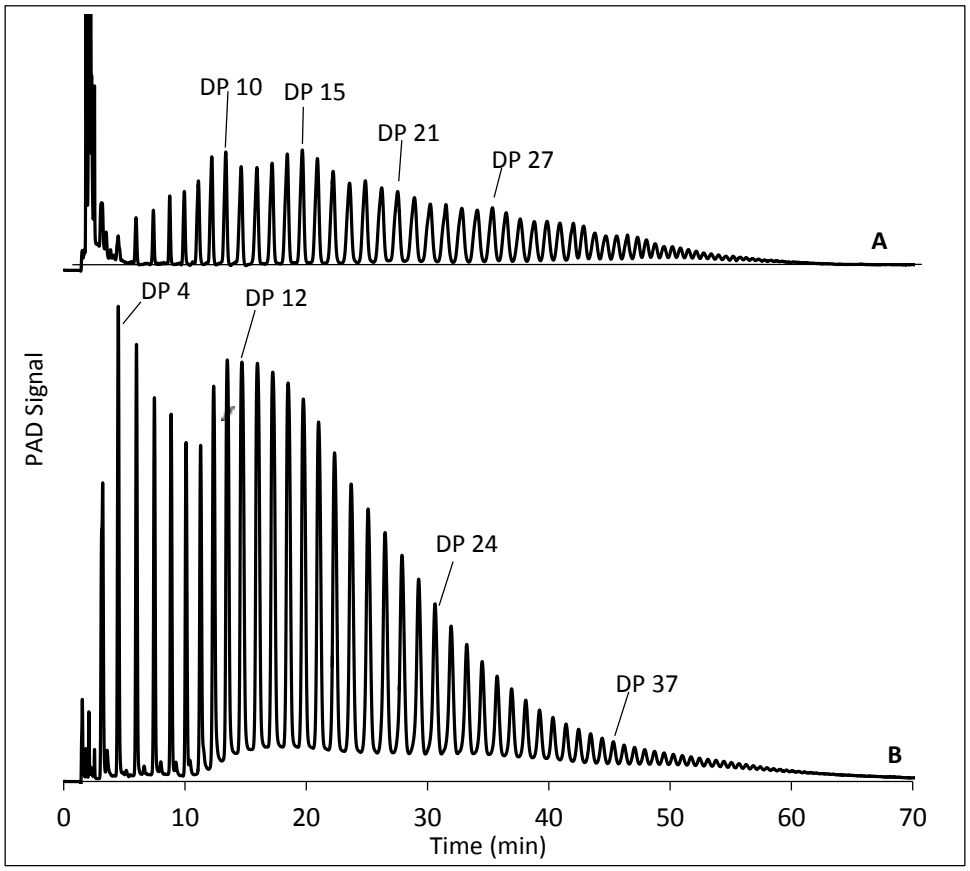

Figure 4.6: Size distribution of debranched AOS (A) and WBS (B) lintners prepared at 40°C determined by HPAEC. Numbers indicate degree of polymerization.

In order to investigate the presence of α-(1,6)-branches resistant to the action of the debranching enzymes, the lintners were subjected to β-amylase treatment following debranching. If debranching was complete, β-amylase could digest the debranched lintners into a combination of maltose and maltotriose. The presence of other dextrins is therefore indicative of the presence of resistant branch points, which block the action of

β-amylase. As was the case with the addition of β-amylase directly to lintners prior to debranching described above, the remaining dextrins

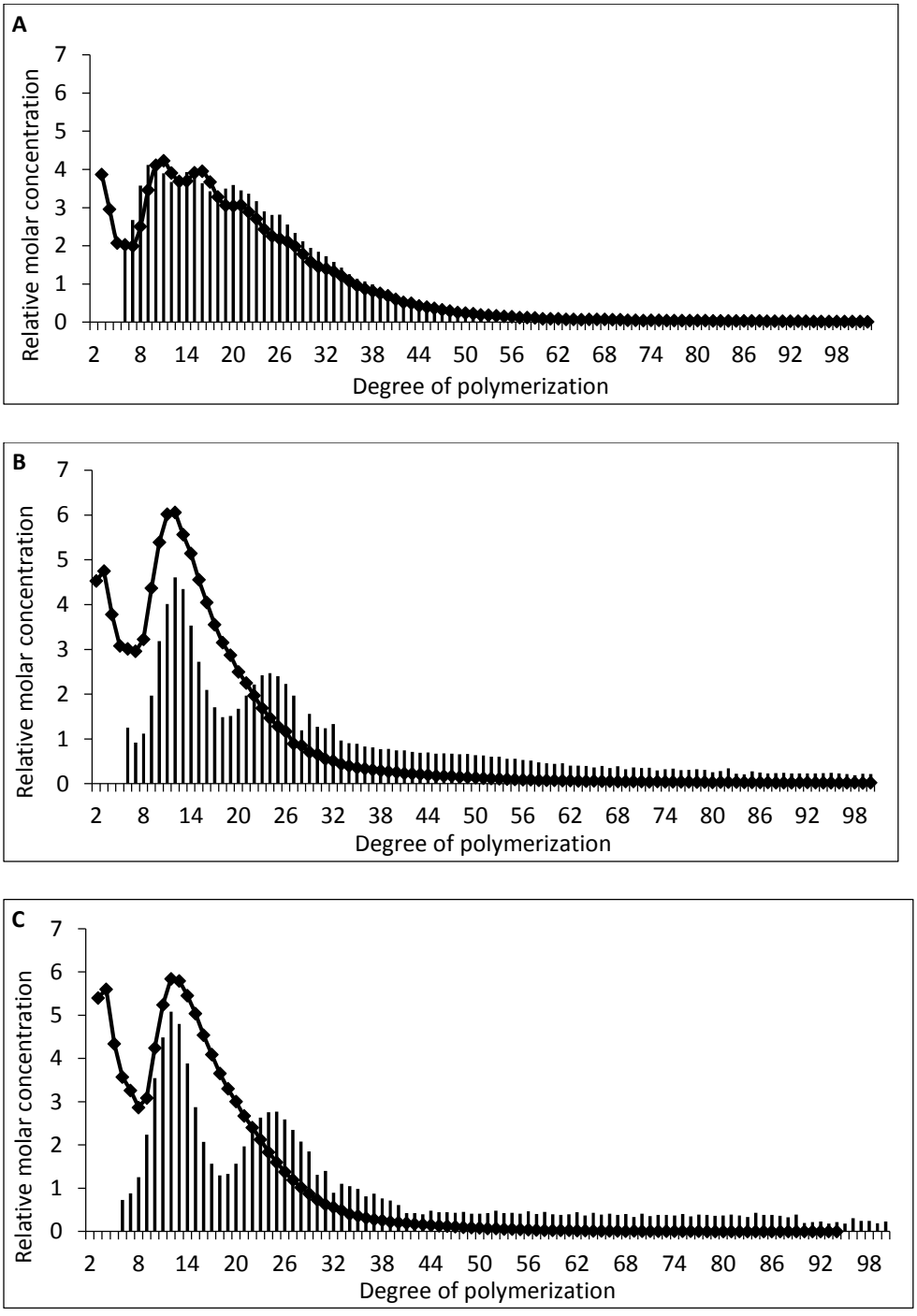

Figure 4.7: Molar distribution of lintners (bar graphs) and their components after debranching (scatter plot) for AOS (A), NBS (B), and WBS (C) determined by HPAEC.

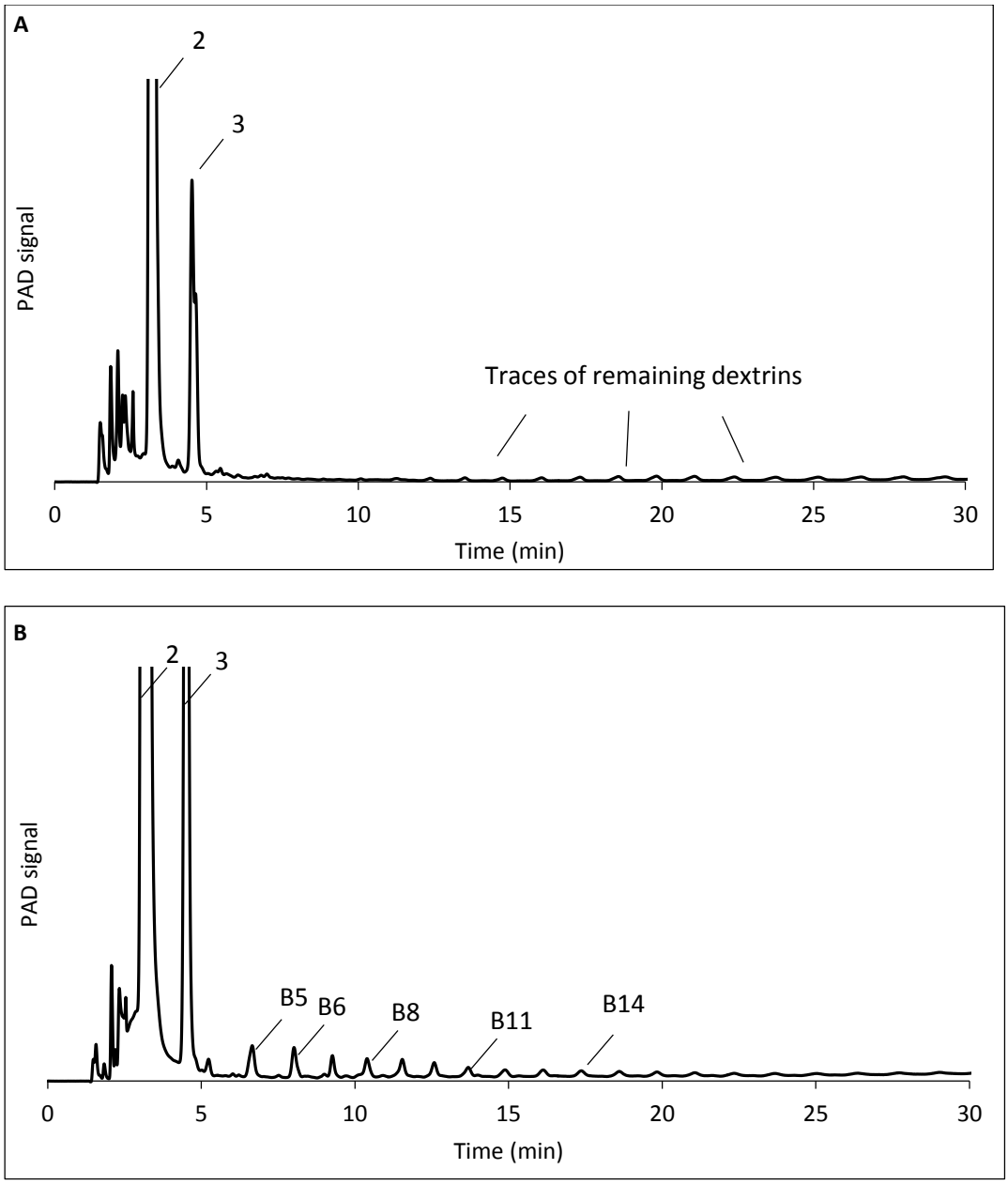

Figure 4.8: Distribution of dextrins of debranched lintners of AOS (A) and WBS (B) treated with β-amylase. Number indicates the degree of polymerization, and "B" indicates branched dextrins.

were present in such minute amounts that it did not allow for quantification (Figure 4.8). The profile of remaining dextrins in NBS and WBS were very similar displaying a distribution with a group of dextrins between DP_n 4-14, and a group of larger dextrins

with DP_n values ≥ 15, with the larger group likely representing the presence of resistant branch points located near the non-reducing end of at least two chains within the same molecule (Wikman et al., 2013). The AOS lintner did not display a similar distribution of remaining dextrins to that seen in NBS and WBS. No small limit dextrins existed, showing that branches were not located near the reducing end in AOS lintners. Rather, a single broad distribution of trace amounts of dextrins indicative of resistant branches near the non-reducing end of the molecules was observed.

Discussion

In this study the structure and composition of lintners from a novel AOS was probed using the technique of acid hydrolysis. In addition, NBS and WBS were characterized under the same conditions to compare the structure of starch granules containing amylose between zero and 100%.

The relationship reported elsewhere (Bertoft, 2004a, Wikman et al., 2013) that amylose retards the kinetics of acid hydrolysis was confirmed in this study, as amylose containing starch was hydrolyzed slower than WBS. The observation of AOS reaching a plateau at ~45% hydrolysis was not unexpected, as a similar plateau was observed in acid hydrolyzed high-amylose containing maize starch, reaching ~60% hydrolysis after 102 days of incubation in sulfuric acid (15.3% v/v) (Jiang et al., 2010). AOS is composed of a combination of B-type (55% contribution) and V-type (45% contribution) crystallinity, with a relative crystallinity of 25% (Carciofi et al., 2012), i.e. a different polymorphic structure than the A-type and V-type WBS and NBS (Waduge et al., 2006). A similar combination of B- and V-type polymorphs have previously been observed in high-

amylose maize starches (Gérard et al., 2002), although the high-amylose maize also contained the A-type polymorph. Gérard et al. (2002) reported that the V-type polymorphs were preferentially degraded in the initial stages of acid hydrolysis, coinciding with an increase in the proportion of B-type. A preferential hydrolysis of the V-type polymorph of AOS starch was also observed by Putaux (personal communication), as it disappeared after the first days of acid hydrolysis as determined by wide-angle X-ray diffraction analysis. Moreover, the loss of the V-type polymorph in AOS lintners coincided with an increase in the relative crystallinity of the B-type polymorph (Putaux, personal communication), aligning with the observation by Gérard et al. (2002). It has been reported that B-type crystals from high-amylose maize starch exhibited greater resistance to hydrolysis than A-type crystals, perhaps due to the ability of longer chains from B-type crystals to form more stable structures (Gérard et al., 2002), or the ability of amylose chains to intertwine and form B-type crystals (Jayakody and Hoover, 2002). Bertoft (2004a) investigated the susceptibility of waxy maize and waxy potato starch containing A-type and B-type polymorphs, respectively, and could not support the observation of differences in susceptibility of differing crystals type, reporting similar kinetics of hydrolysis between A- and B- type crystals from granules made of pure amylopectin. Therefore, the resistance of B-type crystals from high-amylose maize starch could not be considered representative of B-type crystals from starch in general (Bertoft, 2004a), and the plateau observed in AOS cannot be attributed to its B-type crystal structure *per se*. As the acid hydrolysis of AOS plateaued at ~45%, and the relative crystallinity was 25% (Carciofi et al., 2012), the inability of AOS to be hydrolyzed further implied that amorphous material was present in the materials resistant

to further hydrolysis. The plateau may be indicative of an association between the crystalline and amorphous components of amylose preventing further degradation. In comparison, the relative crystallinity of NBS and WBS were 19.5% and 20.4% (Chapter 2), and acid hydrolysis progressed past 80% (Figure 4.2) indicating the majority of amorphous material was hydrolyzed.

The incubation temperature has been shown to have a great impact on the rate of acid hydrolysis (Jane et al., 1997). Branch-structure difference in starches of A- and B-type X-ray patterns were revealed by their Nägeli dextrins (Jane et al., 1997) or lintners (Bertoft, 2004a, Wikman et al., 2013). The fact that the incubation temperature did not influence the kinetics of acid hydrolysis of AOS was therefore unexpected and appeared to reflect the nature of the molecules in the amorphous areas, as it is that part of the granules which the acid preferentially hydrolyzes (Bertoft, 2004a). The impact of amylose content on the semi-crystalline structure of barley starches was investigated by Jenkins and Donald (1995). They reported that increased amylose content corresponded to an increased size of the crystalline lamellae, and subsequently decreased size of the amorphous lamellae, as amylose acts to disrupt the packing of amylopectin double helices by two proposed mechanisms. The first mechanism was the co-crystallization of amylose with amylopectin, which act to pull amylopectin helices into the amorphous lamellae (increasing the size of the crystalline lamellae). The second suggested mechanism was the penetration of amylose oriented transverse to the lamellar stack into the amorphous lamellae introducing disorder (Jenkins and Donald, 1995). Biliaderis et al. (1981) reported a relationship between the kinetics of acid hydrolysis of the amorphous lamellae and the molar ratio of short:long chains of the branched polysaccharide

component of legume starches, wherein a greater resistance to acid hydrolysis was observed in starches containing greater short:long chain ratios. Vamadevan et al. (2013) postulated that the length of internal chain segments along the amorphous backbone of amylopectin influences the organization of double helices in the crystalline lamellae, implying that the organization of the amorphous components impacts the nature of crystallinity. It is thus apparent that a large number of factors influence the structure of the amorphous lamella and its subsequent hydrolysis. It is therefore likely that no single factor is responsible for the insensitivity of incubation temperature of AOS to acid hydrolysis. However, it should be noted here that to-date it is not known if a lamellae organization exists in the granules of AOS. Indeed, the lamellae in normal starch granules are formed by the amylopectin component, which is absent in AOS. It is a possibility that the arrangement/packing of the amylose chains in the amorphous parts of the AOS granules is such that their hydrolysis becomes rate limiting at the concentration of hydrochloric acid and incubation temperatures utilized in this study. A lower susceptibility of high-amylose starches to dilute acid hydrolysis has been attributed a greater extent of inter-chain associations between starch molecules, leading to a more compactly organized amorphous region (Hoover and Manuel, 1996) and limited swelling (Nakazawa and Wang, 2003).

The morphology and structure of starch granules and their lintners were probed by utilizing polarized light, scanning electron and transmission electron microscopy. The three techniques complemented each other in confirming that the AOS starch and its lintner did not possess an organization and structure typical of starch granules. This notion was supported by (i) the lack of birefringence in native granules viewed under

polarized light indicative of no main organization of glucan chains (Carciofi et al., 2012), (ii) multi-lobed and elongated morphology containing rough surface texture when viewed by SEM (Figure 4.1), (iii) the presence of strongly textured aggregates of nanocrystals (Figure 4.1) obtained for lintners with an unusual organization compared to other nanocrystals (Putaux et al., 2003, Angéllier-Coussy et al., 2009), and (iv) fragmented birefringence displayed by AOS lintners when viewed under polarized light at 45% acid hydrolysis. In addition, the presence of alternating regions of semi-crystalline and amorphous materials commonly referred to as growth rings (Pilling and Smith, 2003) could not be observed in the AOS granules. It is thereby clear that the silencing of genes coding for SBE's had a large influence on the biosynthesis of the AOS granule resulting in a unique morphology and structure.

It is important to acknowledge that while the hydrolysis of AOS reached a plateau and could not be degraded further, at 45% acid hydrolysis the NBS and WBS lintners could be degraded substantially further as seen by their time-course of hydrolysis in Figure 4.2. The structure of barley starches subjected to more extensive acid hydrolysis with 15% (v/v) H_2S0_4 was reported by Song and Jane (2000). They found that the size distribution profiles of WBS (87% acid hydrolyzed) and NBS (67% acid hydrolyzed) lintners prior to debranching displayed peaks at DP_n 12, 25, and greater DP_n up to DP 40, corresponding to linear, single branched, and double branched molecules, respectively, which were similar to those observed in this study (Figure 4.4). Although Song and Jane (2000) did not present quantitative data, the largest dextrins were likely present in much greater number and reached larger DP_n in the samples investigated in this study, due to the lower extent of acid hydrolysis of the lintners investigated. Upon debranching with

isoamylase and pullulanase, WBS and NBS displayed a major population with a peak at DP_n 12 (Figure 4.6), which has been described for many other starch lintners as well and shows that the larger, branched dextrins are composed of chains with an average DP around 12 (Jane et al., 1997, Song and Jane, 2000). Debranching of WBS and NBS also gave rise to a second population of very short chains at DP 2-6 (Figure 4.6), which was not found in the barley starch lintners described by Song and Jane (2000). This could be due to the much lower extent of lintnerisation in this work, as it has been shown that as hydrolysis progresses, the quantity of short chains (DP 2-8) produced after debranching diminishes, as the short chains may represent defective structures of crystallites which are selectively hydrolyzed at higher levels of acid hydrolysis (Jane et al., 1997, Bertoft 2004a). However, Song and Jane (2000) debranched the lintners with isoamylase alone, whereas in this work isoamylase was used together with pullulanase and it has been shown that the debranching reaction becomes more complete when both enzymes are used (albeit resistant branches always remains in the dextrin mixture) (Bertoft, 2004a). The lintners also contained small amounts of chains with DP up to about 50 and greater in very minute amounts (Figure 4.6), which was similar to the reported chains in barley lintners by Song and Jane (2000) despite the large differences in the extent of hydrolysis. If these dextrins really are single chains or branched dextrins that escapes the attack by the debranching enzymes is difficult to know.

Watanabe and French (1980) reported that the inability of β-amylase to completely digest acid hydrolyzed starches into maltose and maltotriose indicated that branch points were present in structured regions were resistant to acid hydrolysis. As the lintners in this study were not completely converted to maltose and maltotriose, the

remaining dextrins provided insights towards the presence of branch points resistant to the action of β-amylase and/or the action of the debranching enzymes isoamylase and pullulanase in all three lintner samples. The location of branch points influences the extent of β-amylase digestion, with a greater β-amylase digestion attained when branch points are located near the reducing end of the dextrin (Watanabe and French, 1980). It was particularly interesting to observe the presence of resistant branch points in the AOS lintner as all genes coding for known starch branching enzymes had been silenced (Carciofi et al., 2012). The presence of branch points were detected in very low amounts (0.2%) in AOS by nuclear magnetic resonance (NMR) analysis (Blennow, personal communication), which supports the result of the AOS lintner not being completed digested into maltose and maltotriose following treatment with β-amylase. These results therefore indicate that some still unknown enzyme is involved in the biosynthesis of branches in the amylose component of starch.

The presence of resistant branch points in β-limit dextrins of lintners from waxy starches previously reported elsewhere (Watanabe and French, 1980, Bertoft, 2004a, Wikman et al., 2013) was confirmed in this study. The profile of residual dextrins following β-amylolysis of WBS and NBS was similar to that reported by Bertoft (2004a) wherein peaks of small dextrins where detected in comparison to very large maltose and maltotriose peaks. It should be noted that the profile of residual β-limit dextrins of lintners is influenced by the extent of acid hydrolysis (Bertoft, 2004a) and the profile of the β-limit dextrins from NBS and WBS may be different at higher levels of acid hydrolysis. It is surprising, however, to notice that general common features and dextrins populations of lintners are already present at 45% acid hydrolysis in lintners from NBS

and WBS. The majority of lintner structure analysis is reported at higher levels of acid hydrolysis (Song and Jane, 2000, Bertoft, 2004a, Jiang et al 2010, Wikman et al., 2013). It has been reported that as the extent of hydrolysis increases, the β-amylosis limit increases and proportion of remaining dextrins decreases, indicating that more branches present in lintners are removed as acid hydrolysis progresses (Bertoft, 2004a). This observation also supports the decrease in production of short dextrins produced following debranching in lintners at extensive levels of acid hydrolysis reported by Jane et al. (1997) discussed above.

Some longer chains may be detected in lintnerized starches of cereals in general, which was attributed to double-helical structures of retrogradated amylose, or segments of amylose-lipid complexes (Wang and Copeland, 2015). Long chains of amylose may be partially hydrolyzed into dextrins (DP < 120) that may retrogradate into double-helices resistant to acid hydrolysis in the early stages of lintnerization (Morrison et al., 1993). NBS at 45% acid hydrolysis contained dextrins of this size and after debranching the longest chains were of DP about 60 (Figure 4.7). Nevertheless, WBS gave the same result implying that the structure of the lintner was derived mostly from the amylopectin component. However, when it comes to AOS, the lintner was, of course, completely derived from amylose. At 45% acid hydrolysis, the average DP_n of the AOS lintner determined by HPAEC analysis was two times smaller than that of NBS and WBS (Table 4.2) and the size-distribution profile of the AOS lintner, which provided insight into the architecture of the acid resistant parts of the granules, was very different from the other samples. The molar distribution of dextrins showed peaks and smaller shoulders, with a repeating distance of 5-6 glucose residues, and this pattern largely remained after

debranching (Figure 4.6 and 4.7). The presence of a repeat distance approximately corresponding to the number of glucose residues required for one turn of a helix (Imberty et al., 1991) may suggest the lintners were composed of amylose helical structures of repeating periodicity. The significantly higher chain length of the AOS lintner and lower number of chains (NC nearly 1 chain per dextrin, Table 4.2) suggested the acid resistant part of AOS was comprised of a helical structure, with very little defects, making it highly resistant to acid hydrolysis.

Conclusion

The structure of the AOS lintner determined by GPC, HPAEC, and TEM was vastly different than that of the NBS and WBS lintners and contained a highly modified granular structure, which was not surprising given the different composition of AOS. It was clearly demonstrated that AOS was significantly impacted by the silencing of all known SBE's resulting in unique morphological and structural attributes, including the presence of semi-crystalline structures despite it lacking the amylopectin component. The unique structural characteristics of AOS and its lintner compared to NBS and WBS implies that the amylopectin component is required to maintain the typical structures observed in barley starch granules. Although the structure of the AOS components resistant to hydrolysis, and the dynamics of hydrolysis of its amorphous components were determined in this study, an understanding of the organization of its crystalline and amorphous components needs additional analytical tools. In addition, the presence of branch points in the AOS lintners is indicative that branching was catalyzed by a currently unknown enzyme.

Summary and Conclusions

In this work normal barley starch (NBS), waxy barley starch (WBS) lacking granule bound starch synthase activity, and amylose-only starch (AOS) lacking activity of starch branching enzymes were utilized. The morphological and structural properties of barley starches (NBS and WBS) cultivated under different lighting regimes, or containing different activities of starch branching enzymes (AOS, NBS, and WBS) were determined to gain insights into the biosynthesis of starch. Contrary to the notion that growth rings in barley starch granules are synthesized due to diurnal photosynthetic activity, it was unequivocally shown that growth rings are not caused by diurnal photosynthetic activity as they appeared in all barley starches regardless of lighting regime. It was shown that the molecular composition of barley starch was influenced by diurnal photosynthetic activity, as amylose content and structure was different when cultivated under constant light conditions compared to diurnal conditions. Further, it was shown that the physical properties of barley starch granules were influenced by the diurnal lighting regime as different relative crystallinity and gelatinization profiles were observed under the different lighting regimes. These results indicate that although the presence of growth rings were conserved, the diurnal lighting regime does influence the structure of normal and waxy barley starches resulting in altered composition and physical properties.

Following the evaluation of the fine structure of amylopectin from NBS and WBS, it was has been shown that diurnal photosynthetic activity influences the organization of amylopectin resulting in altered cluster sizes and altered arrangement of glucan chains. NBS and WBS contained larger clusters with a greater number of building

blocks (NBbl) and lower inter-block chain lengths when grown under diurnal conditions compared to constant light conditions.

The novel, health promoting amylose-only barley starch (AOS) displayed a highly modified granular structure indicating its biosynthesis was heavily influenced by the silencing of starch branching enzymes. It was formerly believed that amylopectin was responsible for the typical features observed in starch granules, such as the alternating semi-crystalline lamellae, and presence of growth rings, as there features were observed in waxy starches which lack the amylose component. The unique structural and morphological properties of AOS confirmed the notion that the amylopectin component is necessary to maintain the typical features observed in starch granules, as these features were not observed in AOS granules. Further, the existence of AOS granules disproved the idea that amylopectin is a mandatory component of starch granules. When investigating the structure of AOS lintners, it was abundantly clear that the morphology and structure of the starch components resistant to acid hydrolysis were vastly different from the structure of lintners of NBS and WBS at equivalent levels of acid hydrolysis. While key insights into the structure of AOS lintners were gleaned, such as an apparent periodicity of 5-6 glucose residues, which is the approximate residues of glucose required for one helical turn, an understanding of the granule organization could not be deciphered beyond the observation that it is highly modified compared to that seen in NBS and WBS.

One can clearly see that diurnal lighting regimes, or expression of starch branching enzymes, have a substantial impact on the molecular composition, organization, and physical properties of barley starches. As the demand for novel food

materials (including starches) with altered health promoting or functional properties rises, a better understanding of the starch biosynthetic pathways and resulting starch compositions and structures will be invaluable in the design of novel food materials. This study represents a solid contribution towards understanding the influence of diurnal photosynthetic activity, and altered expression of starch branching enzymes on the structure of barley starch.

Importance of findings and future research

Although diurnal activity has been established as a critical component of the photosynthetic cycle, an understanding of how it influences the composition, structure, and thermal properties of starch has received little attention in the literature. The scant literature published hypothesized that growth rings in starch were due to a diurnal photosynthetic cycle, with a relatively recent publication (Pilling and Smith, 2003) arguing the contrary in potato starch granules. The research conducted herein on diurnal photosynthetic activity offers a substantial contribution to the literature and provides a better understanding of the universal phenomenon, and is a premier study in characterizing its influence on the composition, amylopectin fine structure, and physical attributes of starches cultivated under diurnal or constant light growing conditions. This work will hopefully catalyze other researchers to rethink previous misconceptions relating to diurnal activity, such as the notion that constant lighting would stimulate greater quantities of crystalline material (disproved in Chapter 2), and revisit the research subject with rigor to characterize the influence of lighting regimes in other core crops such as wheat, corn, and potato. As this work mainly focused on the structural and

morphological attributes of barley starch under different lighting regimes, a large opportunity exists to characterize how these structural differences influence critical functional attributes such as swelling, digestibility, and baking performance. As the diurnal lighting regime is a universal characteristic in grain cultivation, an enhanced understanding of this fundamental lighting regime is essential to the better understanding of the intricacies of starch biosynthesis.

The characterization of the morphology of AOS, and the structure and morphology of its acid hydrolyzed components were of fundamental importance towards the understanding of the structure of a novel, health promoting starch. The efforts to characterize the structure of the AOS granule by studying its components following acid hydrolysis is the first study of its kind, and with recent efforts to increase the concentration of the health-promoting amylose in granules by various methods (Carciofi et al., 2012, Regina et al., 2015), has the opportunity to serve as a preeminent resource for the understanding of the structure of starches containing 100% amylose.

In light of the findings in this dissertation a number of future research areas have been identified:

i) An investigation of the impact of diurnal activity on other core crops such as wheat, potato, and corn is necessary to confirm if similar influences of lighting regime are observed in other plants.

ii) Further investigation is required to better understand how the diurnal lighting regime influences the enzymatic pathways involved in the biosynthesis of starch, as the current investigation could only comment on the resulting morphological, physical, and structural characteristics following cultivation.

iii) The influence of diurnal photosynthetic activity on the functional attributes of starch requires further characterization.

iv) Diurnal photosynthetic activity was seen to influence the molecular structure and composition of starch granules differently depending on their enzyme composition. Therefore, further research may be warranted to better understand how the molecular composition/variety of cereals influences their susceptibility to environmental lighting regimes.

v) Although the study of acid hydrolyzed components of AOS provided insight into the structure and composition of AOS semi-crystalline components, an understanding of the organization of AOS components was not obtained. Further research may investigate the organization of components to better understand the structure of starch granules synthesized under highly modified conditions.

vi) The presence of small amounts of branch points were detected in AOS following acid hydrolysis even though the expression of genes coding for all known starch branching enzymes were silenced, indicating the branching was catalyzed by an unknown branching enzyme. Further investigation may be warranted to identify the unknown branching enzymes, and characterize its role in starch biosynthesis.

References

Abdullah, M., & French, D. (1966). Reversible action of pullulanase. *Nature*, 210, 200

Alvani, K., Qi, X., & Tester, R. F. (2012). Gelatinisation properties of native and annealed potato starches. *Starch/Stärke, 64*, 297-303.

Angéllier-Coussy, H., Putaux, J., Molina-Boisseau, S., Dufresne, A., Bertoft, E., & Perez, S. (2009). The molecular structure of waxy maize starch nanocrystals. *Carbohydrate Research, 344*, 1558-1566.

Annor, G. A., Marcone, M., Bertoft, E., & Seetharaman, K. (2014). Unit and internal chain profile of millet amylopectin. *Cereal Chemistry, 91*, 29-34.

Baguma, Y., Sun, C., Ahlandsberg, S., Mutisya, J., Palmqvist, S., Rubaihayo, P. R., & Jansson, C. (2003). Expression patterns of the gene encoding starch branching enzyme II in the storage roots of cassava (Manihot esculenta Crantz). *Plant Science, 164*, 833-839.

Ball, S., Guan, H. P., James, M., Myers, A., Keeling, P., Mouille, G., Búleon A., Colonna, P. & Preiss, J. (1996). From glycogen to amylopectin: a model for the biogenesis of the plant starch granule. *Cell, 86*, 349-352.

Banks, W., Greenwood, C., & Khan, K. (1971). The interaction of linear, amylose oligomers with iodine. *Carbohydrate Research, 17*, 25-33.

BeMiller, J. N., & Huber, K. C. (2015). Physical modification of food starch functionalities. *Annual Review of Food Science and Technology, 6*, 19-69.

Bertoft, E. (1986). Hydrolysis of amylopectin by the alpha-amylase of B. subtilis. *Carbohydrate Research, 149,* 379-387.

Bertoft, E. (1989). Partial characterisation of amylopectin alpha-dextrins. *Carbohydrate Research, 189,* 181-193.

Bertoft, E. (2004a). Lintnerization of two Amylose-free starches of A-and B-Crystalline types, respectively. *Starch/Stärke , 56,* 167-180.

Bertoft, E. (2004b). On the nature of categories of chains in amylopectin and their connection to the super helix model. *Carbohydrate Polymers, 57*, 211-224.

Bertoft, E. (2007). Composition of building blocks in clusters from potato amylopectin. *Carbohydrate Polymers, 70,* 123-136.

Bertoft, E. (2013). On the building block and backbone concepts of amylopectin structure. *Cereal Chemistry, 90,* 294-311.

Bertoft, E. (2015). Fine structure of amylopectin. *Starch: Metabolism and Structure*, Nakamura, Y. (Ed.). Springer. Japan. 3-40.

Bertoft, E., & Spoof, L. (1989). Fractional precipitation of amylopectin alpha-dextrins using methanol. *Carbohydrate Research, 189,* 169-180.

Bertoft, E., & Koch, K. (2000). Composition of chains in waxy-rice starch and its structural units. *Carbohydrate Polymers, 41,* 121-132.

Bertoft, E., Koch, K., & Åman, P. (2012a). Structure of building blocks in amylopectins. *Carbohydrate Research, 361*, 105-113.

Bertoft, E., Koch, K., & Åman, P. (2012b). Building block organisation of clusters in amylopectin from different structural types. *International Journal of Biological Macromolecules, 50*, 1212-1223.

Bertoft, E., Källman, A., Koch, K., Andersson, R., & Åman, P. (2011). The cluster structure of barley amylopectins of different genetic backgrounds. *International Journal of Biological Macromolecules, 49*, 441-453.

Bertoft, E., Laohaphatanalert, K., Piyachomkwan, K., & Sriroth, K. (2010). The fine structure of cassava starch amylopectin. part 2: Building block structure of clusters. *International Journal of Biological Macromolecules, 47*, 325-335.

Bertoft, E., Piyachomkwan, K., Chatakanonda, P., & Sriroth, K. (2008). Internal unit chain composition in amylopectins. *Carbohydrate Polymers, 74*, 527-543.

Bertoft, E., Zhu, Q., Andtfolk, H., & Jungner, M. (1999). Structural heterogeneity in waxy-rice starch. *Carbohydrate Polymers, 38*, 349-359.

Bijttebier, A., Goesaert, H., & Delcour, J. A. (2010). Hydrolysis of amylopectin by amylolytic enzymes: Structural analysis of the residual amylopectin population. *Carbohydrate Research, 345*, 235-242.

Biliaderis, C., Grant, D., & Vose, J. (1981). Structural characterization of legume starches. II. studies on acid-treated starches. *Cereal Chem, 58*, 502-507.

Blennow, A., Hansen, M., Schulz, A., Jørgensen, K., Donald, A. M., & Sanderson, J. (2003). The molecular deposition of transgenically modified starch in the starch granule as imaged by functional microscopy. *Journal of Structural Biology, 143*, 229-241.

Brückner, S. (2000). Estimation of the background in powder diffraction patterns through a robust smoothing procedure. *Journal of Applied Crystallography, 33*, 977-979.

Buttrose, M. S. (1960). Submicroscopic development and structure of starch granules in cereal endosperms. *Journal of ultrastructure research*, *4*, 231-257.

Carciofi, M., Shaik, S. S., Jensen, S. L., Blennow, A., Svensson, J. T., Vincze, É., & Hebelstrup, K. H. (2011). Hyperphosphorylation of cereal starch. *Journal of Cereal Science, 54,* 339-346.

Carciofi, M., Blennow, A., Jensen, S. L., Shaik, S. S., Henriksen, A., Buleon, A., Holm, P.B. Hebelstrup, K. H. (2012). Concerted suppression of all starch branching enzyme genes in barley produces amylose-only starch granules. *BMC Plant Biology, 12*, 223 doi: 10.1186/1471-2229-12-223

Chiba, S. (1988). Handbook of amylases and related enzymes. The Amylase Research Society of Japan. Oxford, 104-116.

Clarke, B. R., Denyer, K., Jenner, C. F., & Smith, A. M. (1999). The relationship between the rate of starch synthesis, the adenosine 5′-diphosphoglucose concentration and the amylose content of starch in developing pea embryos. *Planta, 209*, 324-329.

Commuri, P. D., & Keeling, P. L. (2001). Chain-length specificities of maize starch synthase I enzyme: Studies of glucan affinity and catalytic properties. *The Plant Journal, 25*, 475-486.

Comparot-Moss, S., & Denyer, K. (2009). The evolution of the starch biosynthetic pathway in cereals and other grasses. *Journal of Experimental Botany, 60*, 2481-2492.

Cooke, D., & Gidley, M. J. (1992). Loss of crystalline and molecular order during starch gelatinisation: Origin of the enthalpic transition. *Carbohydrate Research, 227*, 103-112.

Dubois, M., Gilles, K. A., Hamilton, J. K., Rebers, P., & Smith, F. (1956). Colorimetric method for determination of sugars and related substances. *Analytical Chemistry, 28*, 350-356.

Englyst, H., Wiggins, H., & Cummings, J. (1982). Determination of the non-starch polysaccharides in plant foods by gas-liquid chromatography of constituent sugars as alditol acetates. *Analyst, 107*, 307-318.

Fredriksson, H., Silverio, J., Andersson, R., Eliasson, A., & Åman, P. (1998). The influence of amylose and amylopectin characteristics on gelatinization and retrogradation properties of different starches. *Carbohydrate Polymers, 35*, 119-134.

Frey-Wyssling, V. A., & Buttrose, M. S. (1961). Makromolekulare feinstlamellen in den körnern der kartoffelstärke. *Die Makromolekulare Chemie, 44*, 173-178.

Frost, K., Kaminski, D., Kirwan, G., Lascaris, E., & Shanks, R. (2009). Crystallinity and structure of starch using wide angle X-ray scattering. *Carbohydrate Polymers, 78*, 543-548.

Geigenberger, P., & Stitt, M. (2000). Diurnal changes in sucrose, nucleotides, starch synthesis and AGPS transcript in growing potato tubers that are suppressed by decreased expression of sucrose phosphate synthase. *The Plant Journal, 23*, 795-806.

Gérard, C., Colonna, P., Buléon, A., & Planchot, V. (2002). Order in maize mutant starches revealed by mild acid hydrolysis. *Carbohydrate Polymers, 48*, 131-141.

Gidley, M. J., & Bulpin, P. V. (1987). Crystallisation of malto-oligosaccharides as models of the crystalline forms of starch: Minimum chain-length requirement for the formation of double helices. *Carbohydrate Research, 161*, 291-300.

Glaring, M. A., Koch, C. B., & Blennow, A. (2006). Genotype-specific spatial distribution of starch molecules in the starch granule: A combined CLSM and SEM approach. *Biomacromolecules, 7*, 2310-2320.

Goldstein, A., Nantanga, K. K. M., & Seetharaman, K. (2010). Review: Molecular interactions in starch-water systems: Effect of increasing starch concentration. *Cereal Chemistry, 87*, 370-375.

Gomand, S., Lamberts, L., Derde, L., Goesaert, H., Vandeputte, G., Goderis, B. Delcour, J. (2010a). Structural properties and gelatinisation characteristics of potato and cassava starches and mutants thereof. *Food Hydrocolloids, 24*, 307-317.

Gomand, S., Lamberts, L., Visser, R., & Delcour, J. (2010b). Physicochemical properties of potato and cassava starches and their mutants in relation to their structural properties. *Food Hydrocolloids, 24,* 424-433.

Hanashiro, I. (2015). Fine structure of amylose. *Starch: Metabolism and Structure*. Nakamura, Y. (Ed.).Springer. Japan, 41-60

Hermansson, A., & Svegmark, K. (1996). Developments in the understanding of starch functionality. *Trends in Food Science & Technology, 7*, 345-353.

Hoover, R., & Manuel, H. (1996). The effect of heat–moisture treatment on the structure and physicochemical properties of normal maize, waxy maize, dull waxy maize and amylomaize V starches. *Journal of Cereal Science, 23,* 153-162.

Horsley, R., Franckowiak, J., & Schwarz, P. (2009). Barley. *Cereals*. Carena, M.J. (Ed.). Springer. New York. 227-250.

Imberty, A., Búleon, A., Tran, V., & Pérez, S. (1991). Recent advances in knowledge of starch structure. *Starch/Stärke , 43,* 375-384.

Jacobs, H., Eerlingen, R. C., Rouseu, N., Colonna, P., & Delcour, J. A. (1998). Acid hydrolysis of native and annealed wheat, potato and pea starches—DSC melting features and chain length distributions of lintnerised starches. *Carbohydrate Research, 308*, 359-371.

James, M. G., Denyer, K., & Myers, A. M. (2003). Starch synthesis in the cereal endosperm. *Current Opinion in Plant Biology, 6*, 215-222.

Jane, J., & Shen, J. J. (1993). Internal structure of the potato starch granule revealed by chemical gelatinization. *Carbohydrate Research, 247,* 279-290.

Jane, J., Wong, K., & McPherson, A. E. (1997). Branch-structure difference in starches of A- and B-type X-ray patterns revealed by their naegeli dextrins. *Carbohydrate Research, 300*, 219-227.

Jane, J., Ao, Z., Duvick, S. A., Wiklund, M., Yoo, S., Wong, K., & Gardner, C. (2003). Structures of amylopectin and starch granules: How are they synthesized? *Journal of Applied Glycoscience, 50*, 167-172.

Jayakody, L., & Hoover, R. (2002). The effect of lintnerization on cereal starch granules. *Food Research International, 35*, 665-680.

Jenkins, P., & Donald, A. (1995). The influence of amylose on starch granule structure. *International Journal of Biological Macromolecules, 17*, 315-321.

Jiang, H., Srichuwong, S., Campbell, M., & Jane, J. (2010). Characterization of maize amylose-extender (ae) mutant starches. part III: Structures and properties of the naegeli dextrins. *Carbohydrate Polymers, 81,* 885-891.

Kainuma, K., & French, D. (1971). Naegeli amylodextrin and its relationship to starch granule structure. I. preparation and properties of amylodextrins from various starch types. *Biopolymers, 10*, 1673-1680.

Kalinga, D. N., Waduge, R., Liu, Q., Yada, R. Y., Bertoft, E., & Seetharaman, K. (2013). On the differences in the granular architecture and starch structure between pericarp and endosperm wheat starches. *Starch/Stärke , 65*, 791-800.

Kalinga, D. N., Bertoft, E., Tetlow, I., & Seetharaman, K. (2014). Structure of clusters and building blocks in amylopectin from developing wheat endosperm. *Carbohydrate Polymers, 112*, 325-333.

Kalt-Torres, W., Kerr, P. S., Usuda, H., & Huber, S. C. (1987). Diurnal changes in maize leaf photosynthesis : I. carbon exchange rate, assimilate export rate, and enzyme activities. *Plant Physiology, 83*, 283-288.

Kim, H., & Huber, K. C. (2010). Physicochemical properties and amylopectin fine structures of A-and B-type granules of waxy and normal soft wheat starch. *Journal of Cereal Science, 51*, 256-264.

Kling, J., & Hayes, P. (2004). Barley. *Encyclopedia of grain science. vol. 1*. Wrigley, C., Corke, H., Walker, C. (Eds.). Academic Press. New York. 27-37.

Klucinec, J. D., & Thompson, D. B. (1998). Fractionation of high-amylose maize starches by differential alcohol precipitation and chromatography of the fractions. *Cereal Chemistry, 75*, 887-896.

Koch, K., Andersson, R., & Åman, P. (1998). Quantitative analysis of amylopectin unit chains by means of high-performance anion-exchange chromatography with pulsed amperometric detection. *Journal of Chromatography A, 800*, 199-206.

Kong, X., Corke, H., & Bertoft, E. (2009). Fine structure characterization of amylopectins from grain amaranth starch. *Carbohydrate Research, 34*, 1701-1708.

Kozlov, S. S., Blennow, A., Krivandin, A. V., & Yuryev, V. P. (2007). Structural and thermodynamic properties of starches extracted from GBSS and GWD suppressed potato lines. *International Journal of Biological Macromolecules, 40*, 449-460

Laohaphatanaleart, K., Piyachomkwan, K., Sriroth, K., & Bertoft, E. (2010). The fine structure of cassava starch amylopectin: Part 1: Organization of clusters. *International Journal of Biological Macromolecules, 47*, 317-324.

Li, L., Jiang, H., Campbell, M., Blanco, M., & Jane, J. (2008). Characterization of maize amylose-extender (ae) mutant starches. part I: Relationship between resistant starch contents and molecular structures. *Carbohydrate Polymers, 74*, 396-404.

Lintner, C. (1886). Studien über diastase. *Journal Für Praktische Chemie, 34*, 378-394.

Lopez-Rubio, A., Flanagan, B. M., Gilbert, E. P., & Gidley, M. J. (2008). A novel approach for calculating starch crystallinity and its correlation with double helix content: A combined XRD and NMR study. *Biopolymers, 89*, 761-768.

Meyer A (1895) Untersuchungen über die Stärkekörner. Fischer, Jena, Germany.

Montgomery, E. M., & Senti, F. (1958). Separation of amylose from amylopectin of starch by an extraction-sedimentation procedure. *Journal of Polymer Science, 28*, 1-9.

Morell, M. K., Blennow, A., Kosar-Hashemi, B., & Samuel, M. S. (1997). Differential expression and properties of starch branching enzyme isoforms in developing wheat endosperm. *Plant Physiology, 113*, 201-208.

Morell, M. K., Kosar-Hashemi, B., Cmiel, M., Samuel, M. S., Chandler, P., Rahman, S.Li, Z. (2003). Barley sex6 mutants lack starch synthase IIa activity and contain a starch with novel properties. *The Plant Journal, 34*, 173-185.

Morrison, W. R., Tester, R. F., Gidley, M. J., & Karkalas, J. (1993). Resistance to acid hydrolysis of lipid-complexed amylose and lipid-free amylose in lintnerised waxy and non-waxy barley starches. *Carbohydrate Research, 245*, 289-302.

Mutisya, J., Sun, C., Rosenquist, S., Baguma, Y., & Jansson, C. (2009). Diurnal oscillation of SBE expression in sorghum endosperm. *Journal of Plant Physiology, 166*, 428-434.

Nägeli, W. (1874). Beiträge zur näheren kenntniss der stärkegruppe. *Justus Liebigs Annalen Der Chemie, 173*, 218-227.

Nakazawa, Y., & Wang, Y. (2003). Acid hydrolysis of native and annealed starches and branch-structure of their naegeli dextrins. *Carbohydrate Research, 338*, 2871-2882.

Peat, S., Whelan, W., & Thomas, G. (1952). Evidence of multiple branching in waxy maize starch. *Journal of the Chemical Society*, 4546-4548.

Pérez, S., & Bertoft, E. (2010). The molecular structures of starch components and their contribution to the architecture of starch granules: A comprehensive review. *Starch/Stärke, 62*, 389-420.

Pilling, E., & Smith, A. M. (2003). Growth ring formation in the starch granules of potato tubers. *Plant Physiology, 132,* 365-371.

Putaux, J., Molina-Boisseau, S., Momaur, T., & Dufresne, A. (2003). Platelet nanocrystals resulting from the disruption of waxy maize starch granules by acid hydrolysis. *Biomacromolecules, 4*, 1198-1202.

Rabinowitch, E. & Govindjee (1969). Taking photosynthesis apart. 1. The light and the dark stage. *Photosynthesis.* John Wiley & Sons, Inc. New York, 56-66.

Regina, A., Berbezy, P., Kosar-Hashemi, B., Li, S., Cmiel, M., Larroque, O., Bird, A., Swain, S., Cavanagh, C., Jobling, S. A. (2015). A genetic strategy generating wheat with very high amylose content. *Plant Biotechnology Journal,* doi*: 10.1111/pbi.12345*

Robin, J. (1974). Lintnerized starches. Gel filtration and enzymatic studies of insoluble residues from prolonged acid treatment of potato starch. *Cereal Chemistry, 51*, 389-406.

Sargeant, J. (1982). Determination of amylose: Amylopectin ratios of starches. *Starch/Stärke , 34*, 89-92.

Shi, Y., & Seib, P. A. (1992). The structure of four waxy starches related to gelatinization and retrogradation. *Carbohydrate Research, 227*, 131-145.

Shi, Y., Seib, P., & Bernardin, J. (1994). Effects of temperature during grain-filling on starches from six wheat cultivar. *Cereal Chemistry, 71*, 369-383.

Slade, L., & Levine, H. (1988). Non-equilibrium melting of native granular starch: Part I. temperature location of the glass transition associated with gelatinization of A-type cereal starches. *Carbohydrate Polymers, 8*, 183-208.

Smith, A. M. (2012). Starch in the arabidopsis plant. *Starch/Stärke , 64*, 421-434.

Smith, S. M., Fulton, D. C., Chia, T., Thorneycroft, D., Chapple, A., Dunstan, H., Smith, A. M. (2004). Diurnal changes in the transcriptome encoding enzymes of starch metabolism provide evidence for both transcriptional and posttranscriptional regulation of starch metabolism in Arabidopsis leaves. *Plant Physiology, 136*, 2687-2699.

Song, Y., & Jane, J. (2000). Characterization of barley starches of waxy, normal, and high amylose varieties. *Carbohydrate Polymers, 41*, 365-377.

Srichuwong, S., Isono, N., Mishima, T., & Hisamatsu, M. (2005). Structure of lintnerized starch is related to X-ray diffraction pattern and susceptibility to acid and enzyme hydrolysis of starch granules. *International Journal of Biological Macromolecules, 37*, 115-121.

Stark, J., & Yin, X. (1986). The effect of physical damage on large and small barley starch granules. *Starch/Stärke , 38*, 369-374.

Stitt, M., & Zeeman, S. C. (2012). Starch turnover: Pathways, regulation and role in growth. *Current Opinion in Plant Biology, 15*, 282-292.

Streb, S., & Zeeman, S. C. (2012). Starch Metabolism in Arabidopsis. *The Arabidopsis Book / American Society of Plant Biologists, 10*, e0160. doi:10.1199/tab.0160

Svensson, E., & Eliasson, A. (1995). Crystalline changes in native wheat and potato starches at intermediate water levels during gelatinization. *Carbohydrate Polymers, 26*, 171-176.

Takeda, Y., Guan, H., & Preiss, J. (1993). Branching of amylose by the branching isoenzymes of maize endosperm. *Carbohydrate Research, 240*, 253-263.

Takeda, Y., Hizukuri, S., Takeda, C., & Suzuki, A. (1987). Structures of branched molecules of amyloses of various origins, and molar fractions of branched and unbranched molecules. *Carbohydrate Research, 165*, 139-145.

Tang, H., Ando, H., Watanabe, K., Takeda, Y., & Mitsunaga, T. (2001). Fine structures of amylose and amylopectin from large, medium, and small waxy barley starch granules. *Cereal Chemistry, 78*, 111-115.

Tester, R. F. (1997). Influence of growth conditions on barley starch properties. *International Journal of Biological Macromolecules, 21*, 37-45.

Tester, R. F., & Morrison, W. R. (1990). Swelling and gelatinization of cereal starches. I. effects of amylopectin, amylose, and lipids. *Cereal Chemistry, 67*, 551-557.

Tester, R., South, J., Morrison, W., & Ellis, R. (1991). The effects of ambient temperature during the grain-filling period on the composition and properties of starch from four barley genotypes. *Journal of Cereal Science, 13*, 113-127.

Tester, R., Debon, S., Qi, X., Sommerville, M., Yousuf, R., & Yusuph, M. (2001). Amylopectin crystallisation in starch. *Special Publication-Royal Society of Chemistry, 271*, 97-102.

Tetlow, I. J. (2011). Starch biosynthesis in developing seeds. *Seed Science Research, 21*, 5-32.

Trathnigg, B. (2000). Size-exclusion chromatography of polymers. *Encyclopedia of Analytical Chemistry.* Meyers, R.A. (Ed.), John Wiley & Sons Ltd. Chichester, 8008-8034.

Umeki, K., & Kainuma, K. (1981). Fine structure of nägeli amylodextrin obtained by acid treatment of defatted waxy-maize starch—Structural evidence to support the double-helix hypothesis. *Carbohydrate Research, 96*, 143-159.

Vamadevan, V., & Bertoft, E. (2015). Structure-function relationships of starch components. *Starch/Stärke , 67*, 55-68.

Vamadevan, V., Bertoft, E., & Seetharaman, K. (2013). On the importance of organization of glucan chains on thermal properties of starch. *Carbohydrate Polymers, 92*, 1653-1659.

Van De Sande-Bakhuyzen, H.L. (1925). The structure of starch grains from wheat grown under constant conditions. *Experimental Biology and Medicine, 23*, 302-305.

Van den Koornhuyse, N., Libessart, N., Delrue, B., Zabawinski, C., Decq, A., Iglesias, A., & Ball, S. (1996). Control of starch composition and structure through substrate supply in the monocellular alga Chlamydomonas reinhardtii. *Journal of Biological Chemistry, 271*, 16281-16287.

Vandeputte, G., Vermeylen, R., Geeroms, J., & Delcour, J. (2003). Rice starches. I. structural aspects provide insight into crystallinity characteristics and gelatinisation behaviour of granular starch. *Journal of Cereal Science, 38*, 43-52.

Vasanthan, T., & Hoover, R. (2009). Barley starch: production, properties, modification and uses. *Starch: Chemistry and Technology. Third Edition.:* BeMiller, J., Whistler, R. (Eds.). Elsevier. Burlington, 601-628.

Vrinten, P. L., & Nakamura, T. (2000). Wheat granule-bound starch synthase I and II are encoded by separate genes that are expressed in different tissues. *Plant Physiology, 122,* 255-264.

Waduge, R., Hoover, R., Vasanthan, T., Gao, J., & Li, J. (2006). Effect of annealing on the structure and physicochemical properties of barley starches of varying amylose content. *Food Research International, 39,* 59-77.

Wang, S., Blazek, J., Gilbert, E., & Copeland, L. (2012). New insights on the mechanism of acid degradation of pea starch. *Carbohydrate Polymers, 87,* 1941-1949.

Wang, S., & Copeland, L. (2015). Effect of acid hydrolysis on starch structure and functionality: A review. *Critical Reviews in Food Science and Nutrition, 55*, 1081-1097.

Watanabe, T., & French, D. (1980). Structural features of naegeli amylodextrin as indicated by enzymic degradation. *Carbohydrate Research, 84*, 115-123.

Whatley, F. R., Tagawa, K., & Arnon, D. I. (1963). Separation of the light and dark reactions in electron transfer during photosynthesis. *Proceedings of the National Academy of Sciences of the United States of America, 49,* 266-270.

Wikman, J., Blennow, A., & Bertoft, E. (2013). Effect of amylose deposition on potato tuber starch granule architecture and dynamics as studied by lintnerization. *Biopolymers, 99,* 73-83.

Yamaguchi, M., Kainuma, K., & French, D. (1979). Electron microscopic observations of waxy maize starch. *Journal of Ultrastructure Research, 69,* 249-261.

Zhang, X., Szydlowski, N., Delvalle, D., D'Hulst, C., James, M. G., & Myers, A. M. (2008). Overlapping functions of the starch synthases SSII and SSIII in amylopectin biosynthesis in Arabidopsis. *BMC Plant Biology, 8,* 96

Zhu, F., Bertoft, E., & Seetharaman, K. (2013). Composition of clusters and building blocks in amylopectins from maize mutants deficient in starch synthase III. *Journal of Agricultural and Food Chemistry, 61,* 12345-12355.

Zhu, F., Bertoft, E., Szydlowski, N., d'Hulst, C., & Seetharaman, K. (2015). Branching patterns in leaf starches from arabidopsis mutants deficient in diverse starch synthases. *Carbohydrate Research, 401,* 96-108.